Mathematical Modeling of Phosphorylation in Circadian Clocks from Cyanobacteria to Mammals

by

Yining Lu

A dissertation submitted in partial fulfillment
of the requirements for the degree of
Doctor of Philosophy
(Applied and Interdsciplinary Mathematics)
in The University of Michigan
2018

Doctoral Committee:

Professor Daniel B. Forger, Co-Chair
Associate Professor David K. Lubensky, Co-Chair
Associate Professor Silas Alben
Associate Professor Victoria Booth
Assistant Professor Qiong Yang

Yining Lu

yininglu@umich.edu

ORCID iD: 0000-0002-8662-090X

ACKNOWLEDGEMENTS

I have been extremely fortunate to be able to study at the University of Michigan. I have received tremendous help and advice from faculty, fellow graduate students, as well as staff at Michigan.

First, I would like to thank my advisor Prof. Daniel Forger for his mentoring throughout my program. Danny has taught me how to look for interesting problems, conduct research, work with collaborators and write up manuscripts. He has always been encouraging and inspiring during our meetings. Without his help, I would never have been able to make a smooth transition into the field of mathematical biology. I am also grateful for my co-advisor Prof. David Lubensky. David has provided great advice on mathematical modeling as well as feedback on our manuscripts. I would also like to thank Prof. Silas Alben, Prof. Victoria Booth and Prof. Qiong Yang for serving on my committee and providing valuable feedback on my thesis. The staff members at the graduate math office have also been really helpful. I would never have been able to navigate through graduate school without their help with logistics and administrative tasks.

Outside the University of Michigan, I owe many thanks to our collaborators from different institutions around the globe. I am especially grateful for Prof. David Virshup's lab at Duke-NUS medical school and Prof. Carrie Partch's lab at UC Santa Cruz for their help in understanding the system of mammalian circadian clocks. Prof. Jae Kyoung Kim at KAIST has also taught me a lot about mathematical modeling and simulations. I would like to thank Prof. Michael Rust at the University of Chicago for his generous advice on our manuscript and for sharing his insights on the

cyanobacterial circadian clocks.

Finally, I would like to express my gratitude to all my friends in Ann Arbor for being supportive and encouraging during these years. Without them, I would not have been able to enjoy my life here at Ann Arbor throughout many winters and summers.

PREFACE

Part of Chapter III is taken from the previously published paper: Narasimamurthy, Rajesh, Sabrina R. Hunt, Yining Lu, Jean-Michel Fustin, Hitoshi Okamura, Carrie L. Partch, Daniel B. Forger, Jae Kyoung Kim, and David M. Virshup. "CK1/ protein kinase primes the PER2 circadian phosphoswitch." Proceedings of the National Academy of Sciences (2018)

TABLE OF CONTENTS

LIST OF FIGURES

Figure

LIST OF TABLES

Table

ABSTRACT

Endogenous circadian clocks (period around 24 h) are self-sustained biological oscillators that are present in many species. This rhythmic behavior is crucial for reliable regulation of biological activities. Disruption of circadian rhythms can decrease fitness and survival of both prokaryotes and eukaryotes. A common theme among the mechanisms of biological clocks is protein phosphorylation, a key regulator of the clock's period. This dissertation focuses on the mathematical modeling of protein phosphorylation and investigates the connections and distinctions among various systems of circadian clocks from cyanobacteria to mammals. First, we study the simplest circadian clock in cyanobacteria where three key clock proteins KaiA, KaiB, KaiC have been identified. Oscillations in KaiC phosphorylation level are present without any transcription or translation. KaiA activates the phosphorylation of KaiC while KaiB attenuates this process by restricting the activity of KaiA. Here we propose a mathematical model for the post-translational cyanobacterial clock and show that the sequestration mechanism in cyanobacteria involving KaiA, KaiB and KaiC is mathematically equivalent to the transcription regulation in mammalian circadian timekeeping involving the corresponding activators and repressors. We also find that an additional negative feedback loop keeps the molar ratio of clock proteins in balance and increases the robustness of the circadian clocks, which is another similarity shared between cyanobacteria and mammals. Therefore, similar dynamical principles regulating molecular timekeeping may have emerged in cyanobacteria and mammals through convergent evolution. Second, we focus on the sequential phosphorylation process of the key clock protein PERIOD 2 (PER2) in mammalian clocks. Mutation of a specific phosphorylation site on PER2 can shorten the period of circadian clocks,

thus causing Familial advanced sleep phase (FASP). It is known that members of the casein kinase 1 (CK1) family are more efficient in phosphorylating the downstream sites of PER2 when the FASP site is already phosphorylated, yet the priming kinase targeting the FASP site has not been identified. Here, we incorporate into our mathematical model the new experimental result that the CK1 is indeed the kinase that works on both the priming FASP site and the downstream phosphorylation sites of PER2. Our modeling result suggests a robust yet fragile design of PER2 phosphorylation: the period of the circadian clock is robust to environmental variations but can be sensitive to regulatory changes in the tail behavior of CK1. Taken together, this presents a new mechanism for regulation of circadian period that is surprisingly divergent from that used in flies, where a separate priming kinase has been identified. Finally, we take a step further and study a much more general model of the multisite phosphorylation process of proteins. One observation that motivates our study is that individual phosphorylation events (minutes) are typically much quicker than circadian timescales (hours), yet the changes in protein phosphorylation can affect the period of circadian clocks. Another motivation is that many interval timers are related to protein phosphorylation where a certain biological process can be paused for a fixed amount of time before it resumes. In our model, we show how kinases and phosphatases can work together to create an interval timer with a timescale much longer than individual phosphorylation events. We also show that product inhibition through sequestration on the kinase can be indispensable in sustaining the circadian rhythms.

CHAPTER I

Introduction

Endogenous circadian clocks (period $\sim$ 24 h) are self-sustained biological oscillators that are present in many species including cyanobacteria, fungi, algae, plants, flies, birds and human (Bell-Pedersen et al. 2005). This rhythmic behavior is vital for reliable regulation of biological activities and daily events: for example, *Drosophila* eggs hatch only in the morning, *Neurospora*, a mold begins producing spores only in the evening. In plants, rhythmic events include leaf movement, stomata opening, and the expression of many genes. In mammals, body temperature, blood pressure, sleep/wake cycle and even hormone secretion can also be regulated by circadian rhythms (Schibler and Sassone-Corsi 2002). In humans, disruption of circadian rhythms due to causes such as shift work and jet lag might increase the risk of depression, cancer and diabetes (Lie et al. 2006, Sahar and Sassone-Corsi 2009). Disregulation of circadian rhythms can clearly decrease fitness and survival of both prokaryotes and eukaryotes (Ouyang et al. 1998, DeCoursey and Krulas 1998). On one hand, circadian rhythms can be entrained or reset by external signals such as light and metabolism (food intake). One the other hand, these self-sustained rhythms can function even in the absence of external stimuli and maintain the 24h period over a temperature range that is physiologically relevant (Hastings and Sweeney 1957). These properties of circadian rhythms have provided the foundation for mathematical modeling and inspired many researchers to work collaboratively in the field (Rust

et al. 2007, Van Zon et al. 2007, Forger et al. 2007, Gonze 2011, Kim and Forger 2012, Zhou et al. 2015, Narasimamurthy et al. 2018). Since the 1980s, the molecular biology revolution has led to the identification of many genes and proteins constituting the biochemical networks for circadian rhythms (Dunlap 1999, Sancar 2008). There are also many design principles for mathematical modeling as well as guidelines for data analysis (Novák and Tyson 2008, Forger 2011). However, despite tremendous amount of experimental and modeling work, our understanding of the circadian rhythms is still far from complete.

There are without doubt many complex biological networks and reactions responsible for constructing circadian rhythms, but a common theme among these different biological systems is protein phosphorylation. Protein phosphorylation is a post-translational modification of proteins where a covalently bound phosphate group is added to an amino acid residue (serine, threonine, and tyrosine in eukaryotes, and histidine in prokaryotes and plants) with the help of a protein kinase. Phosphorylation sometimes alters the structural conformation of a protein, causing it to become activated, deactivated, or modifying its function. Many publications have acknowledged the significance of protein phosphorylation in circadian rhythms from cyanobacteria to mammals. Protein phosphorylation is the key regulator of the period of circadian rhythms found in almost all organisms. In *Drosophila* and mammals, casein kinase 1 (CK1) sequentially phosphorylates several sites on the PERIOD (PER) proteins. CK1's combined action with phosphatases determines the circadian period (Lee et al. 2011a). A similar mechanism exists in *Neurospora* and even cyanobacteria (*Synechococcus elongatus*) through protein phosphorylation (Tomita et al. 2005, Rust et al. 2011, Van Zon et al. 2007, Nishiwaki and Kondo 2012).

Studies in *Drosophila* have provided some of the most important breakthroughs to help researchers understand the molecular basis of circadian clocks with the *period (per)* gene being the first identified clock gene (Konopka and Benzer 1971). A

groundbreaking result in Hardin et al. (1990) shows that the *per* mRNA levels can be regulated by PER protein activity in a negative feedback loop. This breakthrough has led to the current standard view of the transcriptional translational feedback loop as a central part in the circadian pacemakers (Glossop et al. 1999). In fact, for many animal clocks, PER expression oscillates at both the mRNA and protein levels. PER can be targeted for rapid degradation by the ubiquitin/proteasome pathway (Edery et al. 1994, Lee et al. 2001). The first clock relevant kinase DOUBLETIME (DBT) was identified in *Drosophila* (Kloss et al. 1998, Price et al. 1998) and CK1δ/ϵ for PER2 phosphorylation was identified in the mammalian circadian clock (Eide et al. 2005, Harms et al. 2004). On one hand, the phosphorylation process of PER2 can be influenced by metabolic and environmental stimuli (Badura et al. 2007, Gallego and Virshup 2007). On the other hand, PER phosphorylation plays a critical part in the temperature compensation of the circadian clocks (Shinohara et al. 2017a, Isojima et al. 2009). Mutations related to PER2 phosphorylation have been shown to disrupt the circadian period of *Drosophila* (Kloss et al. 1998, Price et al. 1998), mouse (Meng et al. 2008) and even humans (Xu et al. 2007, Lowrey et al. 2000, Toh et al. 2001). Phosphorylation also plays an indispensable role in the synchronization of the *Drosophila* clock to the daily light-dark cycles through the interactions between TIMELESS (TIM) and PER (Price et al. 1995, Naidoo et al. 1999, Ashmore and Sehgal 2003).

In fungal clocks, the clock gene *frequency* (*frq*) is a central piece in the negative feedback loop responsible for maintaining the circadian rhythms for *Neurospora crassa* (Dunlap 1999). In *Neurospora*, circadian rhythms have been seen in both the abundance and the phosphorylation level of frequency (FRQ) proteins (Garceau et al. 1997) and mutations in phosphorylation sites of the key clock proteins including FRQ can affect the period length of the internal clock (Liu et al. 2000). Similar to PER in mammalian clocks, the phosphorylation process of FRQ is mediated by

several kinases and phosphatases (Dunlap 2006). Just like PER is targeted for rapid degradation, FRQ is targeted for degradation through the activity of SCF-ubiquitin ligase-recruiting protein FWD-1 (Heintzen and Liu 2007).

In the cyanobacteria *Synechococcus elongatus*, unlike the transcription-translation oscillator model that explains the circadian rhythms in most organisms, early experiments show that even when metabolic activity including total RNA and protein synthesis is suppressed under constant dark conditions for a few days, circadian rhythms remain unchanged (Xu et al. 2000). Three key proteins KaiA, KaiB and KaiC are identified as componets of the circadian clock, where KaiC protein plays a central role. Groundbreaking results from Tomita et al. (2005) shows clear evidence of temperature-compensated, robust circadian rhythms of KaiC phosphorylation without transcription or translation. Moreover, this post-translational oscillation of the KaiC phosphorylation is successfully constructed *in vitro* by Nakajima et al. (2005) with temperature compensation. The post-translational process of KaiC phosphorylation also plays an important role in the transcriptional translational feedback loop. When KaiC phosphorylation reaches its peak, SasA and RpaA work together through interactions with KaiC phosphorylation activities to regulate the transctiption factors (Gutu and OShea 2013, Tseng et al. 2017, Takai et al. 2006).

Phosphorylation again plays a significant role in the mechanisms of the plant circadian clock. The clock-associated protein Circadian Clock Associated 1 (CCA1) and the Late Elongated Hypocotyl (LHY) proteins have been shown to be closely associated with clock function in *Arabidopsis thaliana* (Wang and Tobin 1998, Fowler et al. 1999). Both CCA1 and LHY have robust circadian oscillations in transcript as well as protein levels under continuous light and control their own gene expression levels through negative feedback loops. Casein Kinase 2 (CK2) can modulate CCA1 activity either by direct interaction or phosphorylation and is also able to interact with and phosphorylate LHY *in vitro* (Sugano et al. 1998, 1999). It was later confirmed that

CCA1 phosphorylation by CK2 is indispensable for the central oscillator to function normally (Daniel et al. 2004). Another important element of the *Arabidopsis* clock is TOC1/PRR3, the phosphorylation of which may enhance the amplitude of the circadian rhythms through inhibition of ZEITLUPE (ZTL) targeted degradation of TOC1 (Más et al. 2003, Fujiwara et al. 2008). PRR5 is shown to regulate phosphorylation, nuclear import and subnuclear localization of TOC1 in the *Arabidopsis* circadian clock (Wang et al. 2010).

As we can see, there are many similarities among the *Drosophila*, mammalian and fungal clocks. The plant clocks, on the other hand are extremely complicated and quite different, which we will leave as future work. As a result, we focus our investigation on the cyanobacterial and the mammalian circadian clocks and especially the phosphorylation activity of the corresponding key clock proteins. We are interested in using the tool of mathematical modeling to look at these systems of circadian clocks and provide insights into future experimental studies.

In chapter II, we study the cyanobacterial circadian clocks, which is perhaps the simplest circadian clock one can find. The temperature-compensated oscillation of KaiC phosphorylation has been shown to be present *in vivo* as well as reconstituted *in vitro* (Xu et al. 2000, Nakajima et al. 2005, Tomita et al. 2005). KaiA activates the phosphorylation of KaiC while KaiB attenuates KaiC phosphorylation by restricting the activity of KaiA (Iwasaki et al. 2002, Kageyama et al. 2003, Kitayama et al. 2003, Rust et al. 2007, Nishiwaki et al. 2007). First, we established a detailed mathematical model that can reproduce many existing experimental results including temperature compensation and the robustness of circadian clocks under ATP variations. Then we propose a simplified mathematical model and show that the sequestration mechanism in cyanobacteria involving KaiA, KaiB and KaiC is mathematically equivalent to the transcription regulation in the mammalian timekeeping mechanism involving BMAL1/CLOCK and the PERIOD proteins. In both systems, we find through

mathematical analysis that, a tight binding between the activator and the repressor is required for the sequestration mechanism to work at its most power. Additional simulations show that the transcriptional regulation of the KaiABC system increases the robustness of the circadian oscillations by keeping the molar ratio of clock proteins in balance, just as it does in a secondary loop in the mammalian circadian timekeeping system. Surprisingly, although these two clocks are very different in biochemical mechanisms, they are functionally equivalent. We believe this could be a common dynamical principle of circadian timekeeping in many different organisms.

In chapter III, we further investigate the PER2 phosphorylation of the mammalian circadian clocks. Mutations related to PER2 phosphorylation have been shown to disrupt the circadian period of *Drosophila*, mouse and even humans (Kloss et al. 1998, Price et al. 1998, Meng et al. 2008, Xu et al. 2007, Lowrey et al. 2000). A mutation of S662 (S662G) in human PER2 (S659 in mouse) can speed up the degradation of PER2 and shorten the period of circadian clocks, thus causing Familial advanced sleep phase (FASP) (Toh et al. 2001). Another key phosphorylation region of PER2 (S477-S479 in mPER2) has been identified to be indispensable for $\beta-$TrcP-dependent degradation of PER2. It is known that the members of the casein kinase 1 (CK1) family preferentially phosphorylate primed sites where a phosphorylated residue drives the recognition of a downstream serine in the +3 position (Flotow et al. 1990). Multiple studies and recent reviews have concluded that an additional but currently unidentified priming kinase is required to phosphorylate the FASP site before the downstream serines can be phosphorylated by CK1δ and/or CK1ϵ (Isojima et al. 2009, Toh et al. 2001, Xu et al. 2007, Shanware et al. 2011). While the Nemo-like kinase has been recently identified by Chiu et al. (2011) as a priming kinase for *Drosophila* PER, the mammalian priming kinase responsible for the phosphorylation of S659 in mPER2 remains unknown. Together with our collaborators, we find that CK1δ/ϵ itself is indeed the priming kinase. Using an NMR-based assay that quantitatively probes phospho-

rylation with site-specific resolution, we demonstrate that the phosphorylation of S659 on mPER2 by CK1δ/ϵ is necessary and sufficient for the rapid phosphorylation of downstream consensus sites. Interestingly, the previously proposed phosphoswitch model in Zhou et al. (2015) continues to present features of the model including the PER2 degradation pattern when CK1δ/ϵ is introduced as the priming kinase. Our modeling work suggests a robust yet fragile design to PER phosphorylation that allows the period of the circadian clock to be robust to environmental variations but also allows for regulatory changes in the CK1 carboxyl terminus to have a large effect on circadian period. This model makes the prediction that the CK1 tail preferentially controls phosphorylation on the FASP site, a prediction that is experimentally verified. Taken together, this presents a new mechanism for regulation of circadian period that is surprisingly divergent from that used in *Drosophila*.

In chapter IV, we take a step further and investigate in general the multisite phosphorylation process of proteins to understand the role of protein phosphorylation in the circadian clocks. Individual phosphorylation events are typically much quicker than circadian timescales. Additionally, in the *Drosophila* circadian clock, multisite phosphorylation can lead to an interval timer gating protein nuclear entry (Meyer et al. 2006, Saez and Young 1996). In mammals, a similar interval timer was discovered gating PERIOD2 degradation (Zhou et al. 2015). Based on these studies, we would like to answer several of the most important questions in circadian research with mathematical modeling: How could timescales on the orders of hours emerge from phosphorylation events that are likely orders of magnitude faster, especially as kinases are tightly bound to their products? How could changes in PER protein affect timescales of minutes, as well as a circadian timescale? Why would kinases and phosphatases both be bound to PER? Is the fact that PER has large disordered regions important to these phenomena? In this chapter, we show how kinases and phosphatases can work together to create an interval timer with a timescale much

longer than individual phosphorylation events. The proposed mechanism is based on phosphate groups being rapidly shuttled on and off a protein, multiple conformational changes to a protein allowing additional sites to be phosphorylated and at least in PER2, an initial phosphoswitch determining protein fate. We also find that, product inhibition through sequestration on the kinase can play a crucial role in sustaining the circadian rhythms, which resonates with our work in chapter II.

In chapter V, we summarize the importance and contributions of our work on the mathematical modeling of phosphorylations in circadian clocks. We also conclude with future directions for both theoretical and experimental research to expand this topic.

CHAPTER II

Circadian rhythms in divergent species evolved convergently

2.1 Abstract

Circadian clocks are vital to many organisms and adapt to environmental signals and pressures. One of the simplest circadian clocks exists in cyanobacteria (*Synechococcus elongatus*), where three key clock proteins KaiA, KaiB and KaiC constitute a post-translational oscillator (Ishiura et al. 1998, Nishiwaki et al. 2000, Xu et al. 2000, Tomita et al. 2005). Temperature-compensated oscillation of KaiC phosphorylation was shown to be present in vivo as well as reconstituted in vitro (Tomita et al. 2005, Nakajima et al. 2005). KaiA activates the phosphorylation of KaiC while KaiB attenuates this process by restricting the activity of KaiA (Iwasaki et al. 2002, Kageyama et al. 2003, Kitayama et al. 2003, Rust et al. 2007, Nishiwaki et al. 2007). Here, we propose a mathematical model for the post-translational cyanobacterial clock and show that the sequestration mechanism in cyanobacteria involving KaiA, KaiB and KaiC is mathematically equivalent to the transcription regulation in mammalian circadian timekeeping involving BMAL1/CLOCK and PER1-2/CRY1-2. We also show that, similar to what is found in the mammalian circadian clock, an additional negative feedback loop keeps the molar ratio of the clock proteins in balance to increase

the robustness of circadian oscillations. Convergent evolution is observed in many organisms at all levels of biological complexity and leads to similar dynamical principles occurring in species with very different biological mechanisms (Brazhnik and Tyson 2006). Our work suggests further that even though prokaryotes and eukaryotes are phylogenetically unrelated and different in many ways, similar dynamical principles regulating molecular timekeeping may have emerged through convergent evolution. This work also raises questions about what common evolutionary pressures could yield such similar dynamical mechanisms with such dissimilar components.

2.2 Introduction

Endogenous circadian clocks are self-sustained biological oscillators present in many species, the period of which are roughly 24 hours. This rhythmic behavior is vital in order for organisms to have reliable regulation of biological activities. Cyanobacteria are the simplest organisms in which a stable circadian rhythm can be found. It has been discovered that there are three key clock proteins in cyanobacteria, KaiA, KaiB and KaiC (Ishiura et al. 1998). In higher organisms including most prokaryotes, the negative feedback loop regulating gene expression is widely accepted as the main drive for circadian rhythms. On the other hand, early experiments from Xu et al. (2003) together with the ground breaking results in Tomita et al. (2005) show clear evidence of temperature-compensated, robust circadian rhythms of KaiC phosphorylation without transcription or translation. Self-sustainable oscillation of KaiC phosphorylation is shown to be present *in vivo* (Tomita et al. 2005) as well as reconstituted *in vitro* (Nakajima et al. 2005). KaiC forms a hexameric ring both in vivo and in vitro, KaiA dimers activate the phosphorylation of KaiC in addition to its autophosphorylation while KaiB tetramers or dimers attenuates the KaiC phosphorylation by restricting the activity of KaiA (Iwasaki et al. 2002, Kageyama et al. 2003, Kitayama et al. 2003). Two indispensable phosphorylation sites, Ser-431 (S431) and Thr-432 (T432)

have been identified (Nishiwaki et al. 2004, Xu et al. 2004) and the KaiC phosphorylation cycle proceeds in an ordered pattern (Rust et al. 2007, Nishiwaki et al. 2007, Phong et al. 2013). The KaiC protein monomer has two distinctly functioning domains, an ATP binding site with high affinity in the N-terminal domain (CI) and another ATP binding site in the C-terminal domain (CII) with low affinity (Hayashi et al. 2004). Structural analysis by Kim et al. (2008) proposes a dynamic balance between different states of the C-terminal (A-loop) that regulates the KaiABC syetem. Monomer exchange was proposed by Emberly and Wingreen (2006) as an innovating mechanism to produce synchronized oscillations, which is further investigated in Ito et al. (2007). However, this model requires the fully phosphorylated KaiC hexamers to form higher order clusters, a hypothesis questioned in recent experiment Kageyama et al. (2006). An allosteric model adopting similar assumption is proposed in Van Zon et al. (2007), where KaiC hexamers go through a conformational transition at highly phosphorylated or unphosphorylated states. A cyclic behavior in the phosphorylation process therefore stems from differentiating binding affinities of KaiC with ATP, KaiA and KaiB. Unphosphorylated KaiC prefers to stay active and highly phosphorylated KaiC prefers to stay inactive. In addition, active KaiC is more stable than inactive KaiC, leading to a uni-directional bias in conversion rates similar to the first design principle in Jolley et al. (2012). Each KaiC monomer can be phosphorylated or unphosphorylated independent of its active/inactive state. THe phosphorylation level of each KaiC hexamer is then modeled through the number of phosphorylated monomers present within each complex. Sequestration of KaiA through tight binding with the KaiBC complexes has been proposed to be the key process that enables sustainable circadian rhythms in cyanobacteria. Modeling work has utilized different mechanisms based on the sequestration building negative feedback that can produce either a relaxation oscillator coupled with positive feedback (Phong et al. 2013, Rust et al. 2007) or a delayed oscillator (Clodong et al. 2007, Van Zon et al. 2007).

2.3 Detailed Mathematical Modeling of the Cyanobacterial Clock

Our mathematical model of the KaiABC system (Fig 2.1) relies on a detailed sequestration mechanism of KaiA through KaiBC proteins revealed recently by crystal structural analysis of protein complexes in the KaiABC system (Tseng et al. 2017): Once the S431 site is phosphorylated (resulting KaiC-ST and KaiC-S), KaiC undergoes a conformational change from a pre-hydrolysis state to a post-hydrolysis state creating a hub. KaiB undergoes a fold-change transition into an active state that is captured by the post-hydrolysis KaiC (Chang et al. 2015). We consider a model with KaiC proteins in four different states: the unphosphorylated KaiC (denoted by U), the S431 phosphorylated KaiC (denoted by S), the T432 phosphorylated KaiC (denoted by T), S431 and T432 phosphorylated KaiC (denoted by ST). The notations for KaiBC complexes follow in the natural way and KaiA acts as an enzyme to enhance the KaiC phosphorylation. The corresponding mass action dynamics are described by Equations (2.12-2.19). Experiments suggest that KaiB interacts with KaiC in different phosphorylation states with different binding affinities and that phosphorylation on Ser431 is necessary for KaiC to bind with KaiB (Lin et al. 2014, Rust et al. 2007), we propose in our models that KaiB binding only happens when S431 site is phosphorylated in KaiC. The sequestration mechanism of KaiA works in the following way: when the S431 site is being phosphorylated on the KaiC protein, the KaiB complex is bound the N-terminal (CI) of KaiC and recruits KaiA proteins to prevent KaiC activation on the C-terminal (CII). In other words, free KaiA proteins are depleted by KaiBC complexes (See Equation 2.21). Simulations suggest that the model can oscillate for a wide range of reaction rates. Analyzing the temporal profiles of KaiABC oscillator, we can see that the fraction of phosphorylated KaiC oscillates with a roughly 24h period (Fig. 2.2B). Phase analysis of the profiles suggests that the

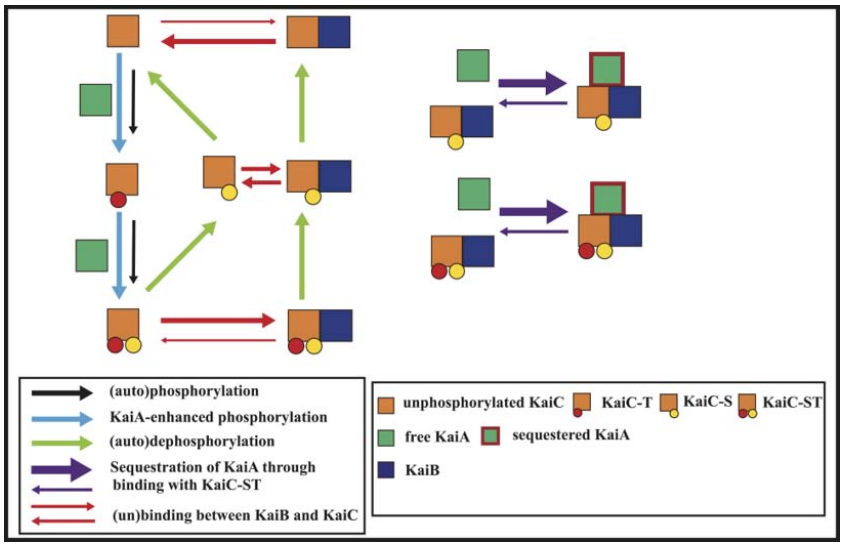

Figure 2.1: The schematic for the detailed cyanobacterial clock model. Squares are KaiABC proteins in different states, small circles indicate the phosphatase groups on the corresponding sites. Arrows indicate reactions among proteins, the width of which shows the relative strength. The KaiBC complexes (KaiBC-S and KaiBC-ST) sequester KaiA through tight binding.

dynamics are indeed what we expected: unphosphorylated KaiC (U) is first activated by KaiA; the activated KaiC first phosphorylates on the T432 site, becoming state T, and then slowly phosphorylates the S431 site, becoming ST; the total phosphorylation level of KaiC increases accordingly during this phase. Meanwhile, KaiB starts to bind with the phosphorylated KaiC and the resulting KaiBC complexes in turn sequester KaiA through tight binding. Once enough free KaiA proteins are depleted from the system, phosphorylation stops and dephosphorylation becomes dominant, leading the system back to a highly unphosphorylated state. Stochastic simulations (Fig. 2.11) and bifurcation analysis (Fig. 2.10) of our model presents a similar results as Van Zon et al. (2007) where the relative ratio of KaiA, KaiB with respect to KaiC plays an important role in the circadian clock. Our model captures the core mechanism necessary for reproducing interesting results both qualitatively and quantitatively including temperature compensation. The parameters for the simulations are described in Table 2.2 and 2.1. Asymmetric circadian rhythms consistent with the

previous experiment results in Rust et al. (2007) can also be observed in our system where KaiC proteins spend less time in phosphorylation compared to dephosphorylation (Fig. 2.2 A-B). Compared with the circadian data from Phong et al. (2013), our model shows a robust period around 24h with less than a 5% change in circadian period under different ATP/ADP ratios (Fig. 2.2 C-F). The CI domain of KaiC is responsible for binding with KaiB during night and thus sequestration of KaiA. Our model produces simulation results confirming the importance of the CI domain of KaiC in the cyanobacterial system (Fig. 2.2 G-H).

2.4 A Simple Mechanism Revealing Convergent Evolution

We propose then a simplified model of the cyanobacterial clock where only the KaiA and the KaiC proteins are explicitly included (Fig. 2.3). In our core model, the KaiA-enhanced phosphorylation process on the T site is much faster than the autophosphorylation on S site. The tight binding between KaiA and the unphosphorylated KaiC ensures that phosphorylation can proceed rapidly even with a small amount of free KaiA. As the phosphorylation process proceeds, the KaiC proteins become phosphorylated on S431 and start to sequester the KaiA proteins through tight binding. Our model shares similarities with many other existing models including Rust et al. (2007) and Van Zon et al. (2007) (See discussion for details). We can observe in the simulations of our detailed model that KaiA is indeed mainly sequestered by KaiC phosphorylated on S431 with help of KaiB (Fig 2.1).

Previous experiments (Lee et al. 2001, 2011a,b) and modeling works (Kim and Forger 2012) have provided much evidence to support a protein sequestration scheme over the hill-type oscillators for mammalian circadian clocks (See Kim (2016) for detailed comparisons). Here we compare our core mechanism for the cyanobacterial

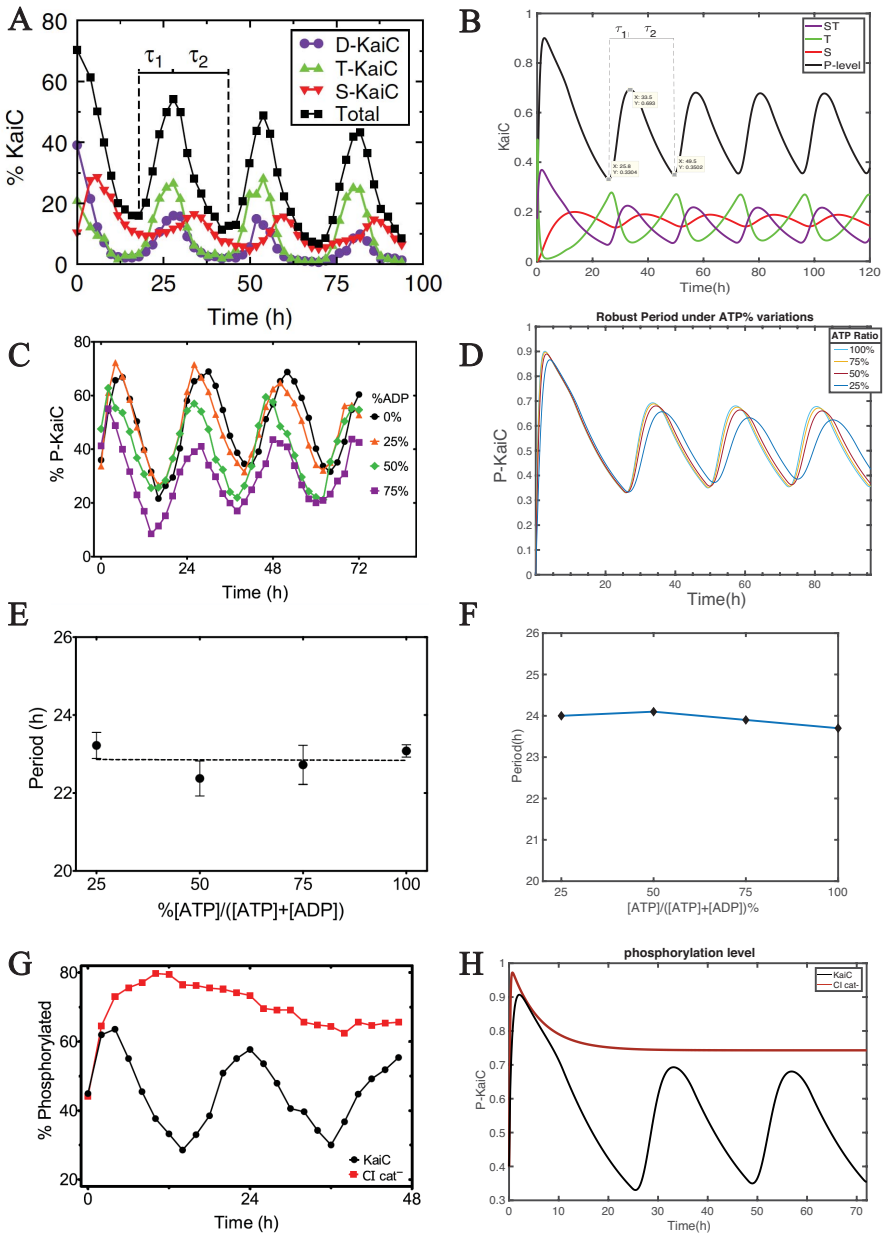

Figure 2.2: Comparing simulations of detailed model with experiments. (A-B) Comparison with experimental data from Rust et al. (2007). In both results, $\tau_1 \approx 9.5h$ is the phosphorylation phase duration and $\tau_1 \approx 18.5h$ is the dephosphorylation phase duration. (C-F) Comparison with circadian data from Phong et al. (2013), our model shows a robust period around 24 h under different ATP/ADP ratios (Equations 2.22-2.23). (G-H) Comparison with Phong et al. (2013), where we confirmed the importance of CI domain insustaining oscillations. We simulate the model with weak KaiB-KaiC binding representing the KaiC muted in the CI domain (CI cat-) and the oscillation is abolished

circadian clock with a protein sequestration model from Kim and Forger (2012) for the mammalian circadian clock. The system of equations for the cyanobacterial system is written in Equations (2.1-2.4) where the total amount of KaiC protein in the system is denote by C_T and the free amount of KaiA denoted by $[A]$ is computed under equilibrium assumptions similar to that in Kim and Forger (2012) (See Equation 2.25-2.28 for details). In fact, we tested two models, one where KaiA only facilitates the phosphorylation from U to T (Fig. 2.3), and another where KaiA facilites both the U to T phosphorylation and the T to ST phosphorylation (Fig. 2.4). The difference between these models depends on whether we use the term $k_2[T]$ or $k_2[A][T]$. Both models can oscillate for a wide range of parameters and show similar results including molar ratio balance as well as the effects of binding affinity between KaiA and KaiC-S. Here we focus our analysis on the model with $k_2[T]$ for which we can show a straightforward comparison with the mammalian clocks.

$$\frac{\mathrm{d}[T]}{\mathrm{d}t} = k_1[A](C_T - [T] - [ST] - [S]) - k_2[T] \tag{2.1}$$

$$\frac{\mathrm{d}[ST]}{\mathrm{d}t} = k_2[T] - k_3[ST] \tag{2.2}$$

$$\frac{\mathrm{d}[S]}{\mathrm{d}t} = k_3[ST] - k_4[S] \tag{2.3}$$

$$[A] = \left(A_T - [S] - K_d + \sqrt{(A_T - [S] - K_d)^2 + 4K_dA_T}\right)/2 \tag{2.4}$$

Equations (2.5 - 2.8) proposed by Kim and Forger (2012) describe a mechanism between the activator BMAL1/CLOCK (denoted by A) and the repressor PER1-2/CRY1-2 (denoted by P) in the mammalian circadian clock. Comparing these two system of equations, we can draw a connection where the activator BMAL1/CLOCK corresponds to KaiA in our system and the repressor PER1-2/CRY1-2 corresponds

to KaiC-S.

$$\frac{\mathrm{d}[M]}{\mathrm{d}t} = \alpha_1 f(P, A_T, K_d) - \beta_1[M] \tag{2.5}$$

$$\frac{\mathrm{d}[P_c]}{\mathrm{d}t} = \alpha_2[M] - \beta_2[P_c] \tag{2.6}$$

$$\frac{\mathrm{d}[P]}{\mathrm{d}t} = \alpha_3[P_c] - \beta_3[P] \tag{2.7}$$

$$f(P, A_T, K_d) = \left(A_T - [P] - K_d + \sqrt{(A_T - [P] - K_d)^2 + 4K_d A_T}\right)/(2A_T) \tag{2.8}$$

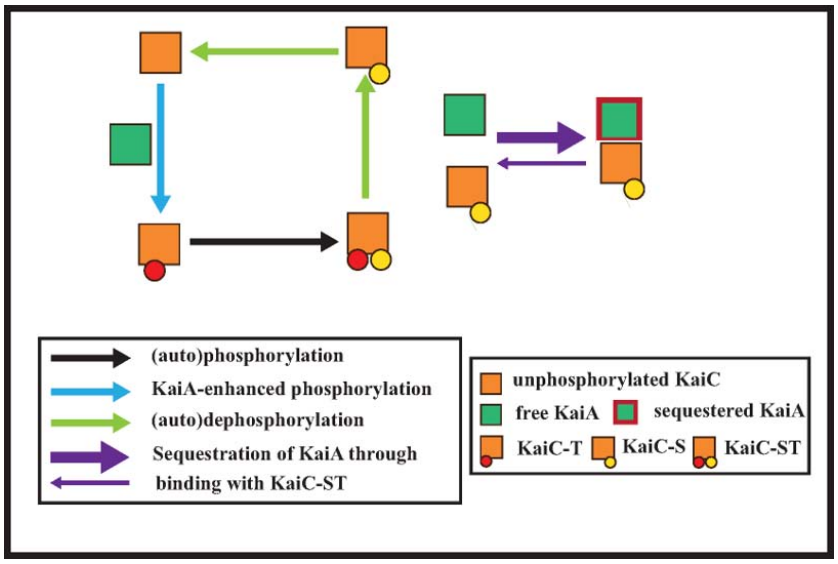

Figure 2.3: The schematic for the core cyanobacterial clock model. Squares are KaiA and KaiC proteins in different states, small circles indicate the phosphatase groups on the corresponding sites. Arrows indicate reactions among proteins, the width of which shows the relative strength. KaiA only enhances the phosphorylation from U to T. KaiC-S sequesters KaiA through tight binding.

Our simulations demonstrate that in this simple model, KaiA sequestration through tight binding with KaiC-S is indispensable for generating oscillations. For each different value of the dissociation constant K_d, we simulate our model for a total of 10^5 randomly generated parameter sets. We plot the fraction of simulations with oscillations against the value of K_d on a log-log plot (Fig. 2.5). These results show that the system is more likely to generate stable oscillations when there is stronger KaiA

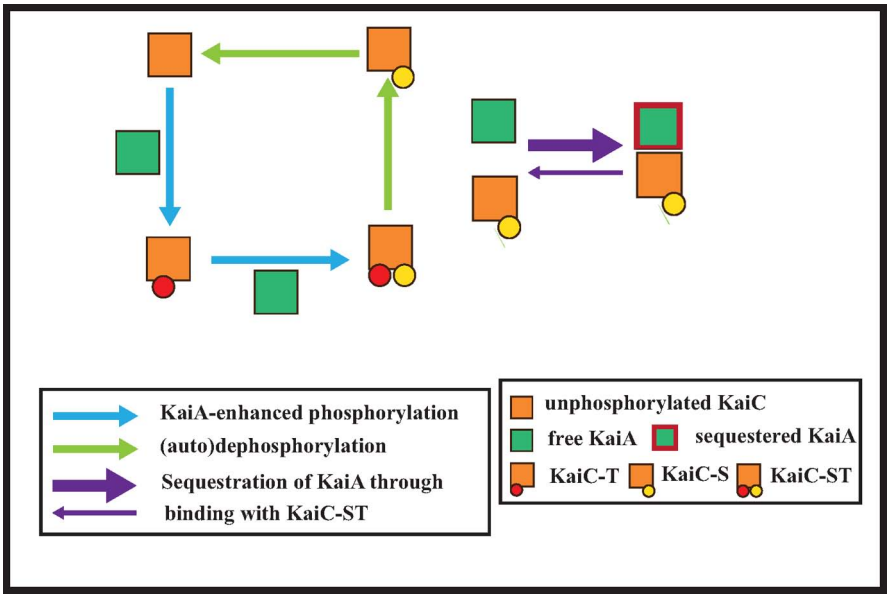

Figure 2.4: The schematic for the alternative core mechanism. Squares are KaiA and KaiC proteins in different states, small circles indicate the phosphatase groups on the corresponding sites. Arrows indicate reactions among proteins, the width of which shows the relative strength. KaiA facilitates both U to T and T to ST transition. KaiC-S sequesters KaiA through tight binding.

sequestration (smaller K_d), which is consistent with the results in mammalian clocks (Kim and Forger 2012, Lee et al. 2011b).

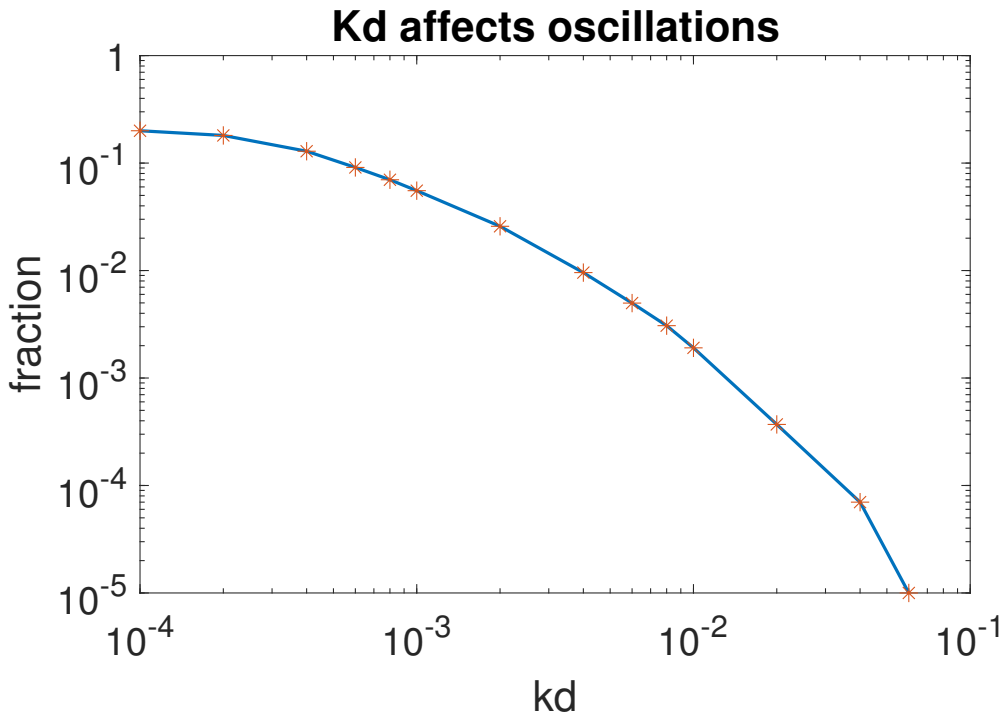

Figure 2.5: Simulation of the core model with different values of binding affinity K_d. The core model can generate oscillations for a higher fraction of parameter sets as K_d decreases from 10^{-1} to 10^{-4}. The parameter sets are plotted as sample points (indicated by *) with a fitted curve on a log log plot.

Additional theoretical analysis in section 2.6.2 and simulations confirm that a necessary condition for oscillations to occur in our model is

$$C_T - (1 + r)A_T > \epsilon \tag{2.9}$$

where r is a constant of order 1 related to the rates of phosphorylation and dephosphorylation and ϵ is a constant of small positive value. Detailed analysis along with definition of these constants can be found in 2.6.2 (Supplement Information). Consistent with existing experimental and modeling results from Kageyama et al. (2006), Van Zon et al. (2007), our simulations suggest that a balanced molar ratio between

the KaiA and KaiC abundance is crucial for generating sustainable oscillations. The observation that the KaiB abundance does not affect circadian rhythms in the same way as KaiA does is also consistent with the model design. In our simulations, we choose parameter values such that $r = 2$ and $\epsilon \ll 1$. The condition in equation (2.9) then turns into a linear criterion:

$$C_T - 3A_T > 0 \tag{2.10}$$

Simulation results verify that parameters violating this condition rarely generate oscillations (Fig. 2.6). Similarly in mammalian circadian clocks, sustainable oscillations require that the repressors and activators interact through tight binding and remain in a balanced molar ratio (Kim and Forger 2012, Lee et al. 2011b). We also find that an

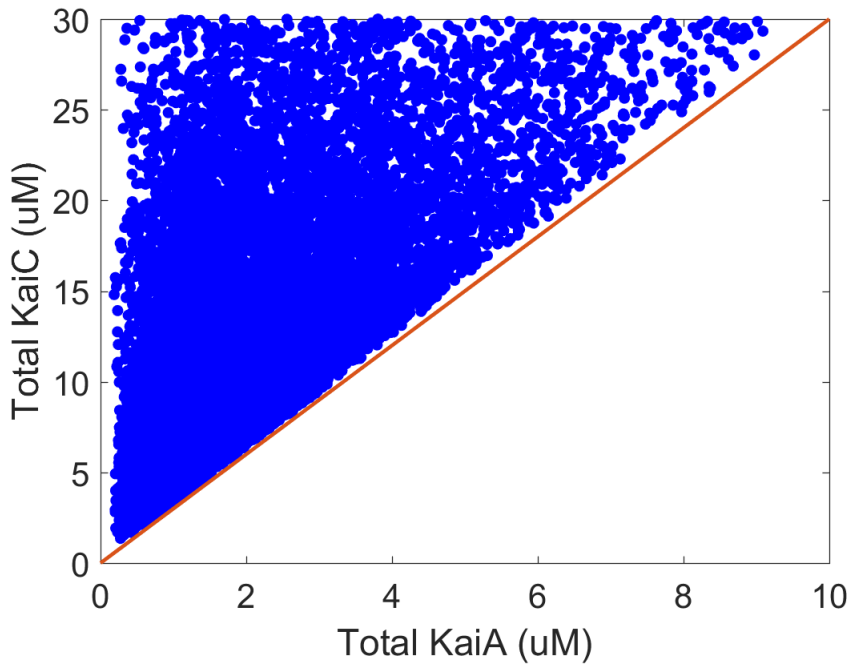

Figure 2.6: Simulations for molar ratio condition. Any parameter set that generates oscillations is located below the line $C_T = 3A_T$,verifying the balanced molar ratio condition

additional transcription translational feedback loop (TTFL) plays a significant role in

sustaining robust circadian oscillations. Besides the KaiABC system, SasA and CikA proteins are two important histidine kinases to regulate the output signaling from the post translational oscillator to the transcriptional activity, which is important when we study the *in vivo* oscillator. The integrated roles of SasA, CikA and RpaA together with KaiABC in the cyanobacterial circadian clock have been summarized recently in Swan et al. (2018). When KaiC phosphorylation reaches its peak, SasA binds to CI domain of the ST-phosphorylated KaiC (Gutu and OShea 2013, Tseng et al. 2017), autophosphorylates and transfers the phosphate group to RpaA, thus turning on the transcription factor (Takai et al. 2006). During the dephosphorylation phase, KaiB kicks off SasA from S-phosphorylated to form the KaiBC complex. CikA is then recruited by the KaiBC complex, dephosphorylates RpaA and thus inhibiting the transcription. In other words, transcription of the *kaiBC* gene is activated when most of the KaiC proteins are at their peak phosphorylation level and inhibited when KaiC proteins are mostly in the S state. As a result, we model the TTFL as an inhibition scheme where KaiC-S acts like an inhibitor of the *kaiBC* gene (Fig. 2.7). In this way, we can capture the dynamics without involving complicated biochemistry or introducing additional components into our core model. This extended wild type model is then compared with a post translational regulation (PTR) model with constitutive transcription rate (Fig. 2.8). We simulate both models over 22500 randomly generated parameter sets varying transcription rates K_s and KaiA concentrations A_T.

The wild type model can produce circadian oscillations under a wide range of parameters (98.44%, see Fig. 2.9 A) while the PTR model without the additional feedback loop can only produce oscillations under a condition similar to the balanced molar ratio criterion we developed above (72.41%, see Fig. 2.9 B). What's more, the wild type model can show oscillations with more robust period compared to the PTR model.

We calculate the period of each oscillation by first applying Fast Fourier Transform

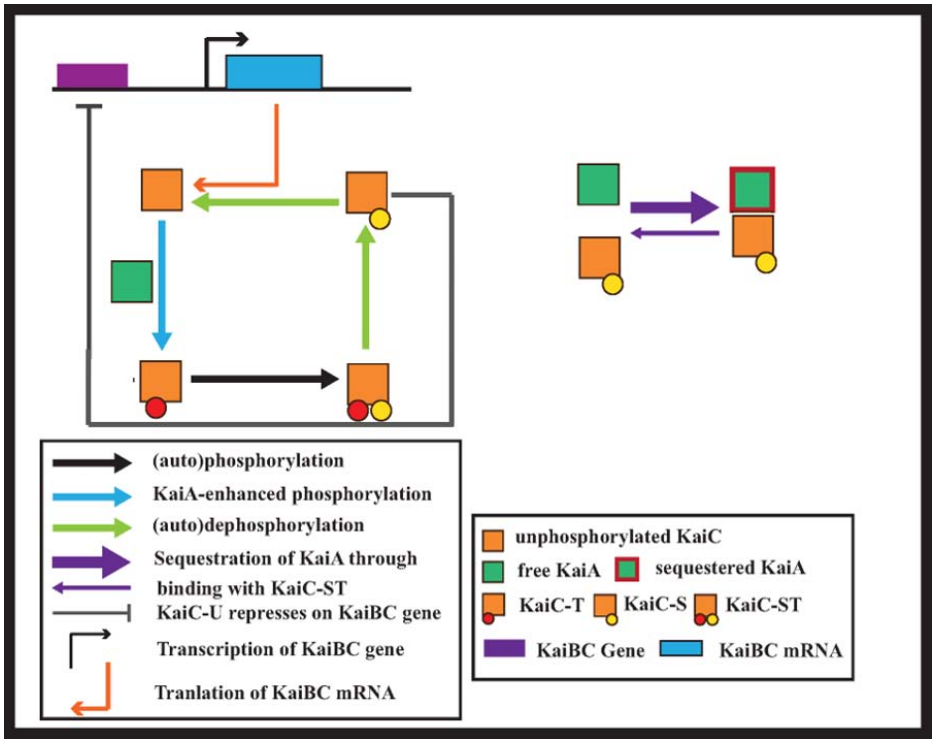

Figure 2.7: Schematic of the wild type TTFL model. Extension of the core mechanism with both a post-translational regulation and a negative feedback of KaiC-S on its own gene.

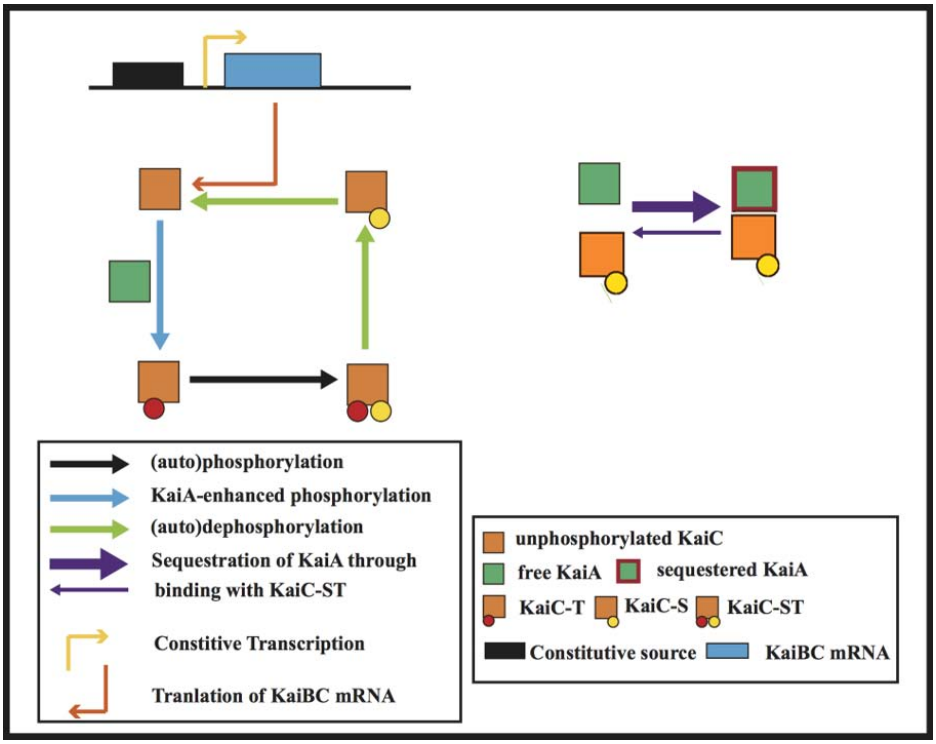

Figure 2.8: Schematic of the PTR model. Extension of the core mechanism: post-translational regulation with a constitutive source of transcription.

(FFT) on the time course and then identifying the strongest frequency in the spectrum. Here we present the FFT analysis for one parameter set in both the wild type (Fig. 2.9 C) and the post-translational regulation model (Fig. 2.9 D). See Equation (2.45-2.56) of section 2.6.3 for detailed equations and parameters of the two models compared here.

Our analysis and simulations altogether suggest that the TTFL as an additional negative feedback loop in the cyanobacterial clocks can help sustain the required molar ratio balance through a homeostatic mechanism, which resonates with the mammalian clock (Kim and Forger 2012, Lee et al. 2011b).

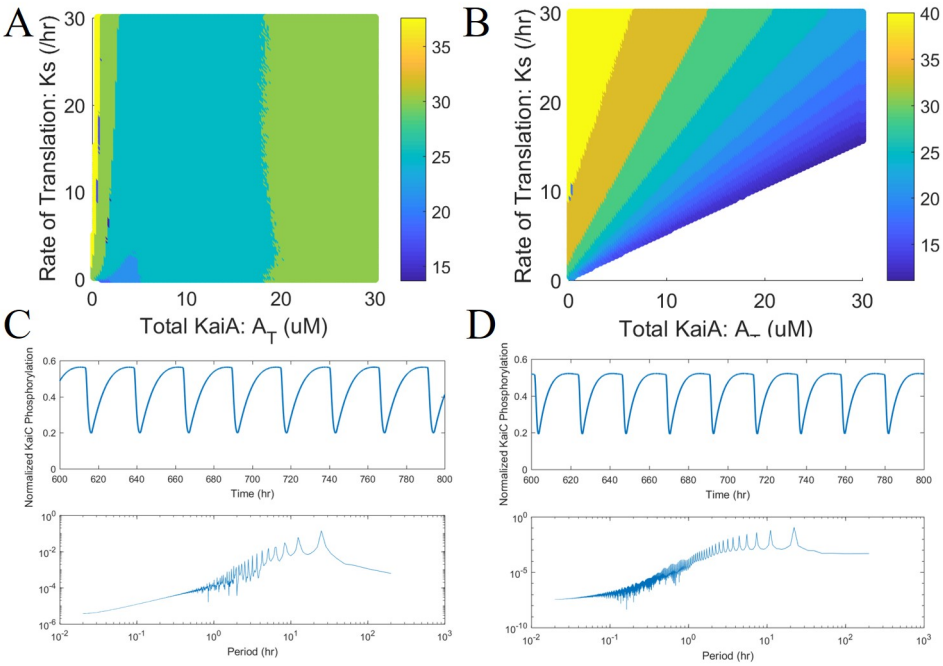

Figure 2.9: Simulation of TTFL versus PTR model. For (A) the wild type model and (B) the post translational regulation model, each oscillation is plotted as a point with a scaled color representing the period length. Sample oscillations and FFT analysis of the signals for the (C) TTFL model and (D) the PTR model with $A_T = 5.034\mu M$ and $K_s = 10.07/hr$. See Table 2.2B for detailed description of the parameters.

2.5 Discussion

We studied a model for the cyanobacterial circadian clock based the following mechanism: KaiA is required for the phosphorylation on KaiC on the T site. When the subsequent S site of KaiC is phosphorylated, KaiC binds to KaiB and gets activated. The "activated" KaiC can then bind and inactivate KaiA, with the help of KaiB. We assume that KaiC (when bound to KaiB) is very efficient in inhibiting KaiA, such that practically all KaiA is sequestered even in the presence of a small amount of KaiC with the S site phosphorylated. After the phosphorylation is completed and KaiC gets dephosphorylated on the S site, there is eventually not enough KaiC to sequester all KaiA and some KaiA is released. The free KaiA then efficiently phosphorylates unphosphorylated KaiC, starting the cycle again. The mammalian clock works via a similar mechanism when viewed through this lens. BMAL1/CLOCK activates the PER1-2/CRY1-2 proteins transcriptionally in a way that is functionally similar to KaiA activating KaiC on the T site. Subsequently the PER1$-$2/CRY1-2 proteins are phosphorylated, which causes them to sequester and inactivate the BMAL1/CLOCK complex. This is similar to the KaiC phosphorylation on the S site which allows KaiC to sequester and inactivate KaiA. In the mammalian system, the PER1-2/CRY1-2 proteins degrade until there is not enough to sequester the BMAL1/CLOCK complex, which allows BMAL1/CLOCK to produce more PER1-2/CRY1-2. Similarly, as KaiC is dephosphorylated below a certain threshold, it releases KaiA which then produced KaiC phosphorylated on the T site. Despite huge differences between the cyanobacterial and the mammalian clock systems, it is surprising that the core mechanisms of both systems share similar conditions for generating stable oscillations.

These similarities extend well beyond the fact that they are both negative feedback loops with delay. For example, in the mammalian clock, if BMAL1/CLOCK does bind directly to DNA, the cyanobacterial and the mammalian clocks will not have the same dynamics. For these reasons, we propose that similar evolutionary pressures may have

caused these clocks in divergent species to have evolved convergently. Future work should determine specifically how these evolutionary pressures may have caused the dynamical structures we observe.

Our model can reproduce experimental data including the time courses and the various effects of molar ratio among KaiABC proteins on the clock. Several works have addressed the role of TTFL in cyanobacteria as making the circadian clock more robust to biomedical noises in growing cells (Zwicker et al. 2010, Teng et al. 2013). Our analysis and simulations, on the other hand, have shown that the TTFL as an additional negative feedback loop can sustain the required molar ratio balance through a homeostatic mechanism, thus making the original oscillator more robust to all perturbations of this nature.

Different models have been built upon the sequestration mechanisms including relaxation oscillators (Phong et al. 2013, Rust et al. 2007) and delayed oscillators (Clodong et al. 2007, Van Zon et al. 2007). Our model is different from the existing models with delayed oscillation including that in Van Zon et al. (2007) because we distinguish KaiC protein by the number of phosphorylated sites instead of the number of phosphorylated sub-units in a hexamer. While adopting the widely accepted ordered phosphorylation feature of KaiC and the sequestration scheme in Rust et al. (2007), we do not assume quasi-steady-state (QSS) to apply Michaelis-Menten dynamics. The model in Rust et al. (2007) requires that KaiA inhibits the dephosphorylation process from KaiC-ST to KaiC-S, while KaiA is sequestered by KaiC-S efficiently through the help of KaiB. In this way, KaiC-S indirectly facilitates itself, forming a positive feedback loop in the system. Our model, however, does not need this positive feedback loop since KaiA only enhances the phosphorylation in the initial step while activating KaiC. The model of Jolley et al. (2012) requires similar assumptions as us by considering two distinct phosphorylation sites on the substrate to design a multisite phosphorylation oscillator. On the other hand, differences between the models

can be observed in many aspects - their model relies on a separate phosphatase for the dephosphorylation process and the fact that kinase activity is involved in phosphorylating on the two sites, both of which are not necessary in our model. Their work is significant in that they proposed two simple design principles that can be applied in building general PTO (post-translational oscillator) while our model specifically draws a connection between the similar sequestration mechanisms in the Kai ABC system and the BMAL1/CLOCK feedback loop revealing convergent evolution on a high level.

We hope our analysis guides further experiments to reveal the mechanisms of cyanobacterial circadian rhythms, as well as how researchers can understand the dynamical principles of timekeeping across species on all levels.

2.6 Supplement Information

2.6.1 Detailed Mathematical Model

To describe the full model, all the reactions are listed in Equation (2.11). Consistent with the main text, we consider KaiC proteins in four different states: unphosphorylated KaiC (denoted by U), S431 phosphorylated KaiC (denoted by S), T432 phosphorylated KaiC (denoted by T), double phosphorylated KaiC (denoted by ST). The notations for KaiBC complexes follow as $\mathrm{B}\cdot\mathrm{U}$, $\mathrm{B}\cdot\mathrm{S}$, $\mathrm{B}\cdot\mathrm{T}$ and $\mathrm{B}\cdot\mathrm{ST}$. See Table 2.2A for detailed description of the parameters.

The reactions in the detailed model are:

$$\begin{gathered}
\mathrm{U}+\mathrm{A}\xrightarrow{k_1^{\mathrm{f}}}\mathrm{AU}, \quad \mathrm{U}\xleftarrow{k_1^{\mathrm{b}}}\mathrm{AU}\xrightarrow{k_{\mathrm{cat}}}\mathrm{T} \\
\mathrm{T}+\mathrm{A}\xrightarrow{k_2^{\mathrm{f}}}\mathrm{AT}, \quad \mathrm{T}\xleftarrow{k_2^{\mathrm{b}}}\mathrm{AT}\xrightarrow{k_{\mathrm{cat}}}\mathrm{ST} \\
\mathrm{U}\xrightarrow{k_{\mathrm{ps}}}\mathrm{T}\xrightarrow{k_{\mathrm{ps}}}\mathrm{ST} \\
\mathrm{U}+\mathrm{B}\underset{k_1^{\mathrm{off}}}{\overset{k_1^{\mathrm{on}}}{\rightleftarrows}}\mathrm{B}\cdot\mathrm{U}, \quad \mathrm{S}+\mathrm{B}\underset{k_2^{\mathrm{off}}}{\overset{k_2^{\mathrm{on}}}{\rightleftarrows}}\mathrm{B}\cdot\mathrm{S}, \quad \mathrm{ST}+\mathrm{B}\underset{k_3^{\mathrm{off}}}{\overset{k_3^{\mathrm{on}}}{\rightleftarrows}}\mathrm{B}\cdot\mathrm{ST} \\
\mathrm{B}\cdot\mathrm{ST}\xrightarrow{k_{\mathrm{dps}}}\mathrm{B}\cdot\mathrm{S}\xrightarrow{k_{\mathrm{dps}}}\mathrm{B}\cdot\mathrm{U} \\
\mathrm{ST}\xrightarrow{k_{\mathrm{dps}}}\mathrm{S}\xrightarrow{k_{\mathrm{dps}}}\mathrm{U}
\end{gathered} \tag{2.11}$$

The corresponding mass action equations are as follows:

$$\frac{d[U]}{dt} = k_1^{\mathrm{b}}[AU] - k_1^{\mathrm{f}}[A][U] + k_1^{\mathrm{off}}[BU] - k_1^{\mathrm{on}}[U][B] - k_{\mathrm{ps}}[U] + k_{\mathrm{dps}}[S] \tag{2.12}$$

$$\frac{d[AU]}{dt} = k_1^{\mathrm{f}}[A][U] - (k_{\mathrm{cat}} + k_1^{\mathrm{b}})[AU] \tag{2.13}$$

$$\frac{d[T]}{dt} = k_{\mathrm{cat}}[AU] + k_2^{\mathrm{b}}[A][T] + k_{\mathrm{ps}}([U] - [T]) - k_2^{\mathrm{f}}[A][T] + k_{\mathrm{dps}}([ST] - [T]) \tag{2.14}$$

$$\frac{d[AT]}{dt} = k_{\mathrm{cat}}[A][T] - k_2^{\mathrm{b}}[AT] \tag{2.15}$$

$$\frac{d[ST]}{dt} = k_{\mathrm{ps}}[T] + k_3^{\mathrm{off}}[BST] - k_3^{\mathrm{on}}[ST][B] + k_{\mathrm{f}}[AT] - k_{\mathrm{dps}}[ST] \tag{2.16}$$

$$\frac{d[BST]}{dt} = -k_{\mathrm{dps}}[BST] - k_3^{\mathrm{off}}[BST] + k_3^{\mathrm{on}}[ST][B] \tag{2.17}$$

$$\frac{d[BS]}{dt} = k_{\mathrm{dps}}[BST] - k_2^{\mathrm{off}}[BS] + k_2^{\mathrm{on}}[S][B] \tag{2.18}$$

$$\frac{d[BU]}{dt} = k_{\mathrm{dps}}[BS] - k_1^{\mathrm{off}}[BU] + k_1^{\mathrm{on}}[U][B] \tag{2.19}$$

KaiA can be sequestered by the KaiBC complex when the S site is phosphorylated on KaiC (BS and BST), where $n = 2$ indicates the strength of sequestration.

$$[B] = [B]_T - [UB] - [BS] - [BST] \tag{2.20}$$

$$[A] = \max\{0, [A]_T - n \cdot ([BST] + [BS]) - ([AU] + [AT])\} \quad n = 2 \tag{2.21}$$

To study the stability of our model under ATP variations, we adopt the competitive inhibition among ATP, ADP and KaiC in Phong et al. (2013)

$$k_{ps} = \frac{[ATP]}{[ATP] + K_I[ADP]} k_{ps}^0 \tag{2.22}$$

$$k_{cat} = \frac{[ATP]}{[ATP] + K_I[ADP]} k_{cat}^0 \tag{2.23}$$

where k_{ps}^0 and k_{cat} are the constant rates under 100% ATP and K_I is the strength of inhibition from ADP. Simulation of the model under different [ATP]/([ATP]+[ADP]) ratios show that the cyanobacterial circadian clock is robust against ATP variations (Fig. 3 in main text), which is consistent with previous experimental result Phong et al. (2013).

A bifurcation diagram is generated for our model using XPP-AUTO (Fig. 2.10). Our bifurcation diagram presents similar property as that in Van Zon et al. (2007). Oscillations occur when the ratio between concentration of KaiA and KaiC is within a bounded range while the relative concentration of KaiB does not have much effect on whether there are oscillations or not in the system .

We have also simulated our model with the Gillespie algorithm (kinetic Monte Carlo). Keeping the KaiC total concentration a constant $C_T = 1\mu M$, the number of KaiC molecules is directly related to the total volume in our simulation. We simulate the discrete model for different V and compare the corresponding phophorylation levels of KaiC(Fig.2.11). We notice that when the number of molecules is low ($V = 10, 20, 50$), the trajectory does show randomness without any sustained oscillations. As the number of KaiC molecules increases, the corresponding oscillations become more stable. When the number of molecules V becomes large enough, the general shape of the profile stays almost the same even if the number is doubled from $V = 5000$ to $V = 10000$. The amplitude of the oscillations from stochastic simulation

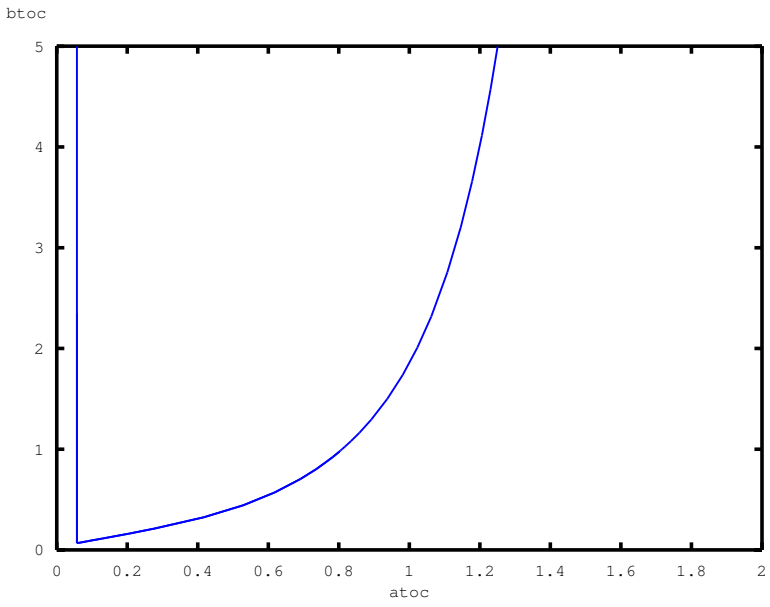

Figure 2.10: Two parameter bifurcation diagram of the KaiC system. atoc is the fraction of KaiA concentration to KaiC concentration. btoc is the fraction of KaiB concentration to KaiC concentration. Points within the region enclosed by the blue curve give initial distributions that can produce oscillations while we expect no oscillations outside this region.

approaches that from the deterministic model as the number of molecules increases. Besides, the phase difference between the stochastic and deterministic simulations decreases significantly as the number of molecules increases. We therefore predict that in order to observe stable and synchronized oscillations, the total amount of KaiC proteins must be above a certain threshold.

An important feature of circadian clocks, which is also true for most biological clocks, is their ability to remain at an almost unchanged period while environmental temperature can vary. This feature is known as temperature compensation, meaning that the effect of changes in temperature is compensated through an endogenous mechanism controlling the clock. A natural question to ask then is how this temperature-compensation is realized in circadian clocks, enabling the robust regulation of biological behavior essential to the survival of most organisms. Different theories have been proposed to explain the mechanism Hastings and Sweeney (1957), Lakin-Thomas et al. (1991).

Here we show that our model generates oscillations that can be temperature compensated through a mechanism combining both theories in Ruoff (2004) and Lakin-Thomas et al. (1991). To investigate the effects of varying reaction rates, we varied KaiA binding rates, KaiB binding rates as well as the KaiA-activated phosphorylation rate while keeping the rates of autokinase/phosphatase unchanged. In other words, we constrain the slow (de)phosphorylation rates to be rather temperature-insensitive while allowing binding rates to vary. This assumption is supported by the experiments from Tomita et al. (2005), where they demonstrated that KaiC alone when incubated with ATP presents temperature-compensated autokinase/phosphatase activities.

We find that varying KaiB binding rates almost does not affect the period at all, possibly since these reactions are already fast enough and the period depend rather weakly on these rates. On the other hand, KaiA binding rates are much slower, which can have a more significant effect on the period. We indeed find that KaiA binding

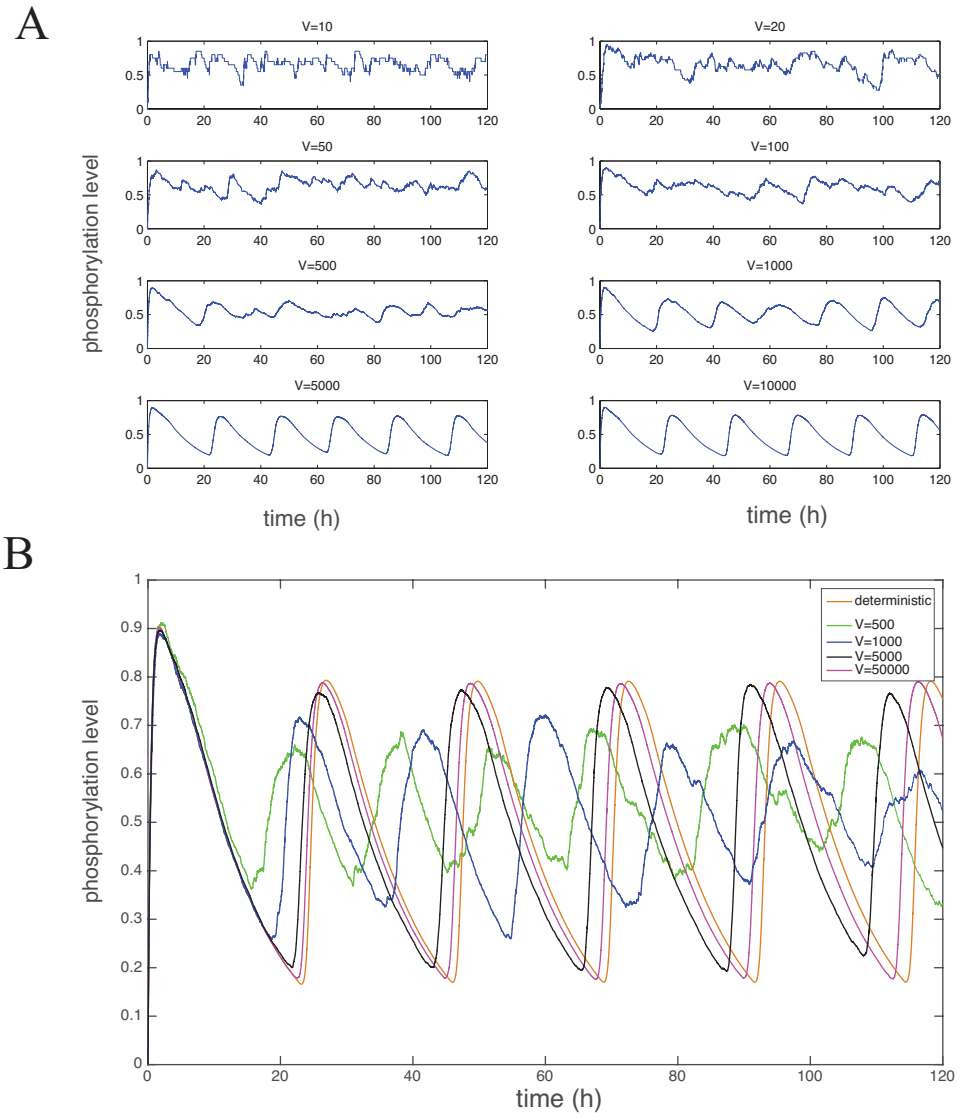

Figure 2.11: Stochastic simulations of the detailed model. (A) Trajectories from stochastic simulations for various total number of KaiC molecules are compared side by side. The horizontal axis of all plots are 'time(h)' while the vertical axis shows the relative phophorylation level of KaiC protein. V = 10,20,50,100,500,1000,5000,10000. (b) Trajectories from stochastic simulations for various total number of KaiC molecules are compared with the deterministic simulation from the continuous model. $V = 500, 1000, 5000, 50000$

can in fact serve as a temperature compensation element (Table 2.1A).

A

	k_{ps}	k_i^f	k_i^b	k_{cat}	$k_i^{\text{on}}(k_i^{\text{off}})$	k_{dps}	Period (h)
T_0	1	1	1	1	1	1	23.54
T_1	1	2	6	2	2	1	23.54
T_2	1	4	27.5	5	5	1	23.53
T_3	1.2	4	25	6	8	1	22.69

B

	k_1(/hr)	k_2(/hr)	k_3(/μMhr)	k_4(/μMhr)	k_5(/μMhr)	k_6(/μMhr)
Original	6.4201	0.1538	2.3317	0.1942	0.3641	1.1485
Increased	6.4201*2	0.1538*3.5	2.3317*2	0.1942*3	0.3641*1.5	1.1485*2
Effect	+	-	+	=	+	-

Table 2.1: (A) Reaction rates are balanced at each hypothetical temperature to achieve temperature compensation. The notation of reaction rates are the same as that in Equation (2.12 - 2.19). T_0 is the reference temperature (parameters are described in Table 2.2A), T_1 and T_1 are two increased temperatures with a temperature-insensitive auto-phosphorylation rate. T_3 is a temperature at which the auto-phosphorylation rate also increases. (B) The first two rows show the parameters we use for the corresponding simulations. The last row shows how increasing each reaction rates affects the dephosphorylation process. '+' : the process is faster when the rate increases; '-': the process is slower when the rate increases; '=': the process remains almost the same when the rate increases.

Here we model the dephosphorylation process as a detailed mechanism inspired by previous experimental results. A transient increase in the ATP level during the dephosphorylation process of KaiC KaiC was previously discovered (Nishiwaki and Kondo 2012, Nishiwaki-Ohkawa et al. 2014). They propose that KaiC transfers a phosphoryl group to ADP during the dephosphorylation process. Such exchange of ADP with ATP in the CII ATPase domain is also shown to be regulated by the level of KaiA and KaiB Nishiwaki-Ohkawa et al. (2014). In particular, the phosphoryl group is not directly removed from the phosphorylation site, instead, KaiC binds with ADP and the phosphoryl group is transferred. The ATP that is produced then goes through hydrolysis to provide energy in the system. This mechanism may explain the temperature compensation of the dephosphorylation process of KaiC. Here we

present a model for the KaiC dephosphorylation based on these observations:

$$\begin{aligned} \mathrm{ATP} &\underset{k_2}{\overset{k_1}{\rightleftarrows}} \mathrm{ADP} \cdot \mathrm{Pi} \\ \mathrm{ST} + \mathrm{ADP} &\underset{k_4}{\overset{k_3}{\rightleftarrows}} \mathrm{S} + \mathrm{ATP} \\ \mathrm{S} + \mathrm{ADP} &\underset{k_6}{\overset{k_5}{\rightleftarrows}} \mathrm{U} + \mathrm{ATP} \end{aligned} \tag{2.24}$$

In our simulations, we first choose a parameter set that shows similar quantitative behavior as that in Nishiwaki and Kondo (2012). The initial conditions for the simulations are:

$$[ATP/ADP]_{total} = 0.5106\mu M,\ [ATP] = 0.0344 * [ATP/ADP]_{total},$$

$$[C]_{total} = 1.5\mu M,\ [U] = 0.2 * [C]_{total},\ [S] = 0.5 * [C]_{total},\ [ST] = 0.3 * [C]_{total}$$

Indeed, our model is consistent with the experimental result where a transient increase in the ATP level is observed during the KaiC dephosphorylation process Nishiwaki and Kondo (2012) (Fig. 2.12). Then we vary the reaction rates individually to find out how each of them affects the dephosphorylation process (Table 2.1B). In the end, we find a balance among all rate changes such that temperature compensation can be achieved (Fig. 2.12).

In conclusion, we propose the following mechanism for temperature compensation in Cyanobacterial circadian rhythm:

1. The dephosphorylation rate is temperature compensated itself without engaging KaiA or KaiB. We have also demonstrated how this can be realized through the balance of several decomposed reactions.

2. The (auto)phosphorylation rate has very low sensitivity to temperature: when temperature increases, the (auto)phosphorylation rate is first temperature-compensated and once the temperature enters a certain region, the reaction speeds up slowly.

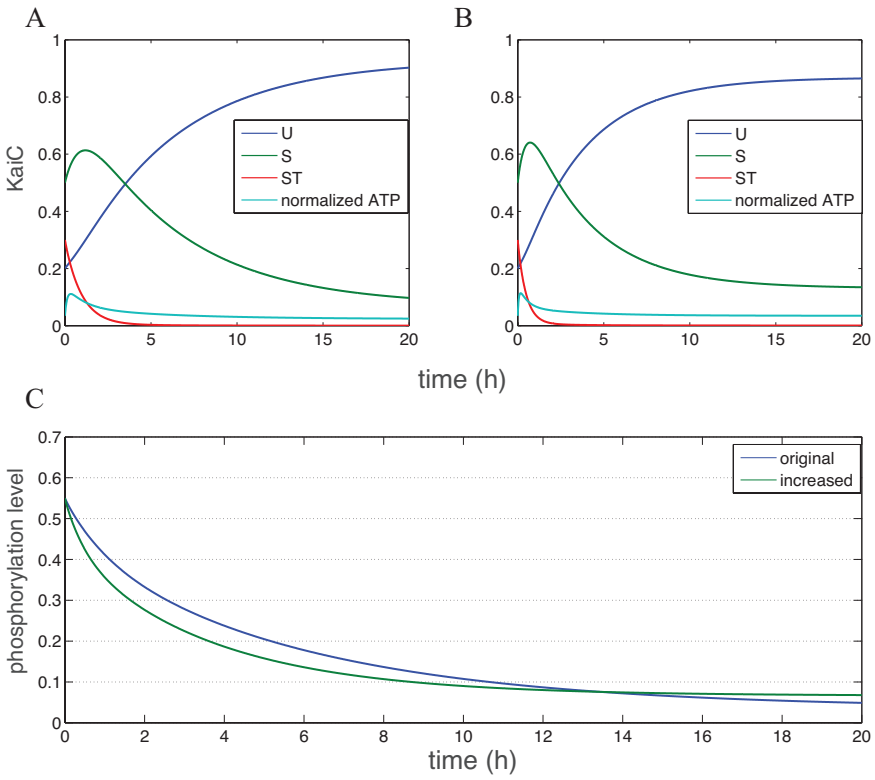

Figure 2.12: Temperature compensation of the KaiC auto-dephosphorylation process. KaiC dephosphorylation files at a low temperature (A) and a high temperature (B) with the same initial conditions. All concentrations are normalized. The parameters corresponding to the original and increased temperature are in Table 2.1B. (C) The phosphorylation levels of KaiC at two different temperatures. Although the curves do not overlap completely, the differences between them are small enough compare to the rate changes.

3. The unbinding rate of KaiA to KaiC is rather sensitive to the temperature and serves as the main temperature compensation element. It counteracts the period shortening effect from increased phosphorylation rates.

4. KaiC (un)binds with KaiB fast enough so that even when the rates are increased several folds, there is no significant effect on the period.

2.6.2 Linear Stability Analysis of the core model

Here we present a linear stability analysis of the simplified model. We continue to use $[T], [ST], [S]$ as the state variables for KaiC concentrations and $[A]$ the concentration of KaiA. Constants C_T and A_T indicate the total amount of the KaiC and KaiA proteins respectively and K_d is the dissociation constant in the sequestration of KaiA through KaiC-S. We assume that sequestration happens on a faster timescale, thus reaching equilibrium quickly. Due to the different time scales and the fact that the binding of KaiA does not impact other reactions of S, we can solve for the concentration of free KaiA.

$$[A][S_{\text{free}}] = K_d[AS] \tag{2.25}$$

$$\implies (A_T - [AS])([S] - [AS]) = K_d[AS] \tag{2.26}$$

$$\implies [AS] = \left(A_T + [S] + K_d - \sqrt{(A_T + [S] + K_d)^2 - 4A_T[S]}\right)/2 \tag{2.27}$$

$$\implies [A] = A_T - [AS] = \left(A_T - [S] - K_d + \sqrt{(A_T - [S] - K_d)^2 + 4K_dA_T}\right)/2 \tag{2.28}$$

The system of equations describing the mechanism in Fig 2.1 can therefore be written as follows. Here we reduce the number of variables by applying the following conservation law

$$[U] = C_T - [T] - [ST] - [S]$$

.

$$\frac{\mathrm{d}[T]}{\mathrm{d}t} = k_1[A](C_T - [T] - [ST] - [S]) - k_2[T] \tag{2.29}$$

$$\frac{\mathrm{d}[ST]}{\mathrm{d}t} = k_2[T] - k_3[ST] \tag{2.30}$$

$$\frac{\mathrm{d}[S]}{\mathrm{d}t} = k_3[ST] - k_4[S] \tag{2.31}$$

$$[A] = \left(A_T - [S] - K_d + \sqrt{(A_T - [S] - K_d)^2 + 4K_dA_T}\right)/2 \tag{2.32}$$

Our simulations show that the value of K_d has to be small enough for the system to generate sustainable oscillations. Therefore when $K_d \ll A_T$, we can take limit as $K_d \to 0$ in $[A]$ to get an approximation expression $[A] = \max\{A_T - [S], 0\}$. The system is then simplified to:

$$\frac{\mathrm{d}[T]}{\mathrm{d}t} = k_1(A_T - [S])(C_T - [\mathrm{T}] - [\mathrm{ST}] - [\mathrm{S}]) - k_2[\mathrm{T}] \tag{2.33}$$

$$\frac{\mathrm{d}[ST]}{\mathrm{d}t} = k_2[T] - k_3[ST] \tag{2.34}$$

$$\frac{\mathrm{d}[S]}{\mathrm{d}t} = k_3[ST] - k_4[S] \tag{2.35}$$

Solving the system for the equilibrium solutions, we obtain $[ST] = \frac{k_4}{k_3}[S], [T] = \frac{k_4}{k_2}[S]$ from Equation (2.34) and Equation (2.35). With all other variables plugged in, Equation (2.33) can be reduced to a quadratic in terms of $[S]$.

$$k_1(A_T - [S])(C_T - (1 + \frac{k_4}{k_2} + \frac{k_4}{k_3})[S]) - k_4[S] = 0$$

In addition, we assume $k_4 \ll k_1$ since KaiA-enhanced phosphorylation is much faster then (auto)phosphorylation. Hence we can drop the last term $k_4[S]$ in the quadratic

equation by dividing k_1 through all terms and find two steady state solutions:

$$(A_T - [S])(C_T - (1 + \frac{k_4}{k_2} + \frac{k_4}{k_3})[S]) - \frac{k_4}{k_1}[S] = 0 \tag{2.36}$$

$$\implies (A_T - [S])(C_T - (\frac{k_4}{k_2} + \frac{k_4}{k_3})[S]) = 0 \tag{2.37}$$

$$\implies [S]^* = A_T, \quad [S]^* = \frac{C_T}{1+r}, \quad \text{where} \quad r = \frac{k_4}{k_2} + \frac{k_4}{k_3} \tag{2.38}$$

- First, we compute the Jacobian at the equilibrium $[S]^* = A_T$

$$J_1 = \begin{pmatrix} -k_2 & 0 & -k_1(C_T - (1+r)A_T) \\ k_2 & -k_3 & 0 \\ 0 & k_3 & -k_4 \end{pmatrix} \tag{2.39}$$

  The corresponding characteristic function is then:

$$f_1(\lambda) = (\lambda + k_2)(\lambda + k_3)(\lambda + k_4) + k_1 k_2 k_3 (C_T - (1+r)A_T)$$

  We conclude from the secant condition that oscillations occur when

$$\frac{k_1 k_2 k_3 (C_T - (1+r)A_T)}{k_2 k_3 k_4} \geq (\sec(\frac{\pi}{3}))^3$$

$$C_T - (1+r)A_T \geq \frac{8k_4}{k_1} \tag{2.40}$$

  In the main text, the condition is written as $C_T - (1+r)A_T \geq \epsilon$ where $r = \frac{k_4}{k_2} + \frac{k_4}{k_3}$ and $\epsilon = \frac{8k_4}{k_1}$. To verify our analysis, we simulate the model for $k_2 = k_3 = k_4 = 0.1$ and compare our results with $C_T - 3A_T > \frac{0.8}{k_1}$.

- To analyze the Jacobian matrix at the other equilibrium $[S]^* = \frac{C_T}{3}$ without introducing too much computational details, we further assume that $k_2 = k_3 = k_4$ which means the autodephosphorylation and the autphosphorylation of KaiC are on the same time scale. The Jacobian at $[S]^* = \frac{C_T}{3}$ can be then simplified

$$J_2 = \begin{pmatrix} -k_1(A_T - \frac{C_T}{3}) - k_2 & -k_1(A_T - \frac{C_T}{3}) & -k_1(A_T - \frac{C_T}{3}) \\ k_2 & -k_2 & 0 \\ 0 & k_2 & -k_2 \end{pmatrix} \tag{2.41}$$

The characteristic function of 2.41 is a cubic function:

$$\begin{aligned} f_2(\lambda) &= (b + k_2 + \lambda)(k_2 + \lambda)^2 + bk_2(k_2 + \lambda) + bk_2^2 \\ &= (\lambda + k_2)^3 + b(k_2 + \lambda)^2 + bk_2(k_2 + \lambda) + bk_2^2 \\ &= \lambda^3 + (3k_2 + b)\lambda^2 + (3k_2^2 + 3bk_2)\lambda + k_2^3 + 3bk_2^2 \end{aligned} \tag{2.42}$$

where $b = k_1(A_T - \frac{C_T}{3}) > 0$.

The Routh-Hurwitz Stability Criterion tells us that a necessary condition for a cubic function $h(x) = x^3 + a_2x^2 + a_1x + a_0$ to be stable (all of its roots have negative real part) is $a_0 > 0, a_2 > 0, a_2a_1 > a_0$.

Applying this to our cubic function above, we already have $a_0 > 0, a_2 > 0$ and we compute the third one accordingly:

$$\begin{aligned} a_1a_2 - a_0 &= (3k_2 + b)(3k_2^2 + 3bk_2) - k_2^3 + 3bk_2^2 \\ &= (3k_2 + b)(3k_2 + 3b) - k_2^2 + 3bk_2 \\ &= 8k_2^2 + 9bk_2 + 3b^2 \\ &> 0 \qquad\qquad \forall\ b, k_2 > 0 \end{aligned} \tag{2.43}$$

Therefore we know that all three roots of the characteristic function always have nagative roots, meaning the steady state is stable and there is no oscillations around that point.

To conclude, we have found a necessary condition for the system to generate

oscillation which is also verified by simulation in the main text.

$$C_T - (1+r)A_T \geq \frac{8k_4}{k_1} \tag{2.44}$$

2.6.3 Transcriptional Translational Feedback Loop versus Post Translational Regulation

As explained in the main text, we investigated the role of the transcriptional translational feedback loop (TTFL) as an additional negative feedback loop in the KaiC system. We simulated a modified system with an additional TTFL and another post translational regulatory system with a constitutive source of transcription.

The corresponding equations with transcription, translation and degradation activities for both systems are listed here (See Table 2.2B for detailed description of parameters and the range for parameter perturbation).

TTFL

$$\frac{\mathrm{d}[M]}{\mathrm{d}t} = V_{\mathrm{trsp}}\frac{100}{1+[S]^4} - V_m[M] \tag{2.45}$$

$$\frac{\mathrm{d}[U]}{\mathrm{d}t} = K_s[M] - k_1[A][U] + k_4[S] - V_d[U] \tag{2.46}$$

$$\frac{\mathrm{d}[T]}{\mathrm{d}t} = k_1[A][U] - k_2[T] - V_d[T] \tag{2.47}$$

$$\frac{\mathrm{d}[ST]}{\mathrm{d}t} = k_2[T] - k_3[ST] - V_d[ST] \tag{2.48}$$

$$\frac{\mathrm{d}[S]}{\mathrm{d}t} = k_3[ST] - k_4[S] - V_d[S] \tag{2.49}$$

$$[A] = \left(A_T - [S] - K_d + \sqrt{(A_T - [S] - K_d)^2 + 4K_dA_T}\right)/2 \tag{2.50}$$

PTR

$$\frac{\mathrm{d}[M]}{\mathrm{d}t} = V_{\mathrm{trsp}} - V_m[M] \tag{2.51}$$

$$\frac{\mathrm{d}[U]}{\mathrm{d}t} = K_s[M] - k_1[A][U] + k_4[S] - V_d[U] \tag{2.52}$$

$$\frac{\mathrm{d}[T]}{\mathrm{d}t} = k_1[A][U] - k_2[T] - V_d[T] \tag{2.53}$$

$$\frac{\mathrm{d}[ST]}{\mathrm{d}t} = k_2[T] - k_3[ST] - V_d[ST] \tag{2.54}$$

$$\frac{\mathrm{d}[S]}{\mathrm{d}t} = k_3[ST] - k_4[S] - V_d[S] \tag{2.55}$$

$$[A] = \left(A_T - [S] - K_d + \sqrt{(A_T - [S] - K_d)^2 + 4K_dA_T}\right)/2 \tag{2.56}$$

A

Description	Symbol	Value
Binding rates between KaiA and unphosphorylated KaiC (U)	k_1^{f}	20.73 /μMhr
Binding rates between KaiA and T-phosphorylated KaiC (T)	k_2^{f}	87.59 /μMhr
Unbinding rates between KaiA and unphosphorylated KaiC (U)	k_1^{b}	3.338 /hr
Unbinding rates between KaiA and T-phosphorylated KaiC (T)	k_2^{b}	6.113 /hr
Binding rates between KaiB and unphosphorylated KaiC (U)	k_1^{on}	11.50 /μMhr
Binding rates between KaiB and KaiC-S	k_2^{on}	66.79 /μMhr
Binding rates between KaiA and doubly-phosphorylated KaiC (ST)	k_3^{on}	7.18 /μMhr
Uninding rates between KaiB and unphosphorylated KaiC (U)	k_1^{off}	10.72 /hr
Uninding rates between KaiB and KaiC-S	k_2^{off}	12.32 /hr
Uninding rates between KaiA and doubly-phosphorylated KaiC (ST)	k_3^{off}	13.59 /hr
KaiA-enhanced phosphorylation for KaiC	k_{cat}	28.15 /hr
Auto-phosphorylation rate for KaiC (U,T)	k_{ps}	0.0384 /hr
Auto-dephosphorylation rate for KaiC (T,S,ST,BS,BST)	k_{dps}	0.1270 /hr
Total KaiC concentration	C_{T}	1 μM
Total KaiA concentration	A_{T}	1.0401 μM
Total KaiB concentration	B_{T}	1.3468 μM

B

Description	Symbol	Value
Phosphorylation rate from T to ST	k_2	0.1 /hr
Dephosphorylation rate from ST to S	k_3	0.1 /hr
Dephosphorylation rate from S to U	k_4	0.1 /hr
Transcription rate (consititutive)	V_{trsp}	0.05 /hr
Degradation rate for KaiC	V_d	0.05 /hr
Degradation rate for mRNA	V_m	0.1 /hr
Parameters perturbed for robustness	**Symbol**	**Range**
KaiA-enhanced phosphorylation rate of unphosphorylated U to T	k_1	$0.1 \sim 25/\mu$Mhr
Dissociation between KaiA and S	K_d	$10^{-4} \sim 10^{-1}/\mu$M
Total KaiC concentration	C_{T}	$0.01 \sim 30$ μM
Total KaiA concentration	A_{T}	$0.01 \sim 10$ μM
Translation rate	K_s	$0.01 \sim 10/hr$

Table 2.2: Description for parameters used in simulations for (A) detailed mathematical model and (B) the core model

CHAPTER III

CK1δ/ϵ protein kinases prime the PER2 circadian phosphoswitch

3.1 Abstract

Multisite phosphorylation of the PER2 protein is the key step that determines the period of the mammalian circadian clock. Previous studies concluded that an unidentified kinase is required to prime PER2 for subsequent phosphorylation by casein kinase 1 (CK1), an essential clock component that is conserved from algae to humans. These subsequent phosphorylations stabilize PER2, delay its degradation and lengthen the period of the circadian clock. A comprehensive biochemical and biophysical analysis of mouse PER2 (mPER2) priming phosphorylation has shown that CK1δ/ϵ are indeed the priming kinases. We find that both CK1ϵ and a newly characterized CK1δ2 splice variant more efficiently prime mPER2 for downstream phosphorylation in cells than the well-studied splice variant CK1δ1. While CK1 phosphorylation of PER2 was previously shown to be robust to changes in the cellular environment, our revised phosphoswitch mathematical model of circadian rhythms shows that the CK1 carboxyl terminal tail can allow the period of the clock to be sensitive to cellular signaling. Additional simulations provide the prediction that the extreme carboxyl terminus of CK1 might have been a key regulator of circadian timing.

3.2 Introduction

Many key features in circadian rhythms have been discovered by extensive research including self-sustained oscillations without external stimuli, regulation by metabolic signals, and temperature compensated response to environmental changes (Pattanayak et al. 2015, Bass and Takahashi 2010, Hastings and Sweeney 1957). The PERIOD (PER) proteins play a crucial role in regulating the circadian rhythms. PER was originally discovered in *Drosophila* as an important regulator (Konopka and Benzer 1971) whose mutation could lead to disrupted period. This key finding has inspired many researchers to study the mechanism of PER proteins and its significance in circadian time keeping. In all metazoan clocks, PER2 expression oscillates at both the mRNA and protein levels and the multisite phosphorylation of PER regulates its accumulation through β-TrCP-dependent proteasomal degradation (Lee et al. 2001, Edery et al. 1994). On one hand, this phosphorylation process of PER2 can be influenced by metabolic and environmental stimuli (Badura et al. 2007, Gallego and Virshup 2007). On the other hand, PER phosphorylation plays a critical part in the temperature compensation of the circadian clocks (Shinohara et al. 2017a, Isojima et al. 2009).

Mutations related to PER2 phosphorylation have been shown to disrupt the circadian period of *Drosophila*, mouse and even humans (Kloss et al. 1998, Price et al. 1998, Meng et al. 2008, Xu et al. 2007, Lowrey et al. 2000). In particular, a mutation of S662 (S662G) in human PER2 (S659 in mouse) can speed up the degradation of PER2 and shorten the period of circadian clocks, thus causing Familial advanced sleep phase (FASP) (Toh et al. 2001). Another key phosphorylation region of PER2 (S477-S479 in mPER2) has been identified to be indispensable for β-TrCP-dependent degradation of PER2. In the casein kinase 1 (CK1) family, several kinases (CK1δ/ϵ) can phosphorylate PER2 at both the FASP site and the β-TrCP binding region, yet it remains unclear how PER2 phosphorylation interact with other parts of the system to

regulate circadian time keeping. A phosphoswitch mathematical model was proposed by Zhou et al. (2015) where CK1δ/ϵ work together with an unknown priming kinase to regulate the stability of PER2. This phosphoswitch model not only explained the three-stage temporal profile of PER2 degradation but also provided a mechanism for temperature compensation.

It is known that the members of the CK1 family preferentially phosphorylate primed sites where a phosphorylated residue drives recognition of a downstream serine in the +3 position (Flotow et al. 1990). Multiple studies and recent reviews have concluded that an additional but currently unidentified priming kinase is required to phosphorylate the FASP site before the downstream serines can be phosphorylated by CK1δ and/or CK1ϵ (Isojima et al. 2009, Toh et al. 2001, Xu et al. 2007, Shanware et al. 2011). While the Nemo-like kinase has been recently identified by Chiu et al. (2011) as a priming kinase for *Drosophila* PER, the mammalian priming kinase responsible for phosphorylation of S659 in mPER2 remains unknown. The priming phosphorylation on FASP site along with the downstream serine phosphorylations can act as a delay element creating a plateau in the PER2 degradation process. As the temperature increases, the phosphorylation at the FASP site increases much faster compared to the β-TrCP site, thus effectively lengthening the period and compensating the clock (Zhou et al. 2015).

Together with our collaborators, we find that CK1δ/ϵ itself is the priming kinase. Using an NMR-based assay that quantitatively probes phosphorylation with site-specific resolution, we demonstrate that phosphorylation of mPER2 S659 by CK1δ/ϵ is necessary and sufficient for the rapid phosphorylation of downstream consensus sites. In cells, CK1ϵ and a newly discovered splice variant of CK1δ (CK1δ2) that resembles CK1ϵ at the extreme carboxyl terminus are more efficient priming kinases than CK1δ1. Interestingly, the previously proposed phosphoswitch model can recapitulate salient features of the model including the PER2 degradation pattern when

CK1 δ/ϵ is introduced as the priming kinase (Zhou et al. 2015). Our modeling work suggests a robust yet fragile design to PER phosphorylation that allows the period of the circadian clock to be robust to environmental variations, e.g., changes in temperature, but also allows for regulatory changes in the CK1 carboxyl terminus to have a large effect on circadian period. This model makes the prediction that the CK1 tail preferentially controls phosphorylation on the FASP site, a prediction that is experimentally verified. Taken together, this presents a new mechanism for regulation of circadian period that is surprisingly divergent from that used in *Drosophila*.

3.3 Experimental Evidence Identifies the Priming Kinase

3.3.1 CK1δ Protein is Sufficient to Phosphorylate S659 of mPER2

As illustrated in Fig. 3.1A, phosphorylation of the FASP serine cluster of mPER2 by CK1 follows a progressive after upstream phosphorylation of the priming site (S659 on mPER2) by an unidentified kinase. Experiments with a synthesized peptide of the mPER2 FASP region and limiting concentration of CK1$\delta\Delta$C [a constitutively active form of recombinant CK1δ lacking its carboxyl-terminal autoregulatory domain]. As predicted, efficient downstream phosphorylation of a primed FASP peptide phosphorylated on S658 (pS659) can be observed. Moreover, the unprimed wild-type peptide (FASP-WT), despite its significant lower efficienty, can also be phosphorylated in the presence of CK1$\delta\Delta$C (Fig. 3.1B). Increasing the kinase concentration by only 10-fold led to an increased efficiency of phopshorylation on FASP-WT, but not the S659 mutant (Fig. 3.1C). These results suggest that CK1$\delta\Delta$C can act as a priming kinase when its local concentration is increased to a level better mimicking the *in*

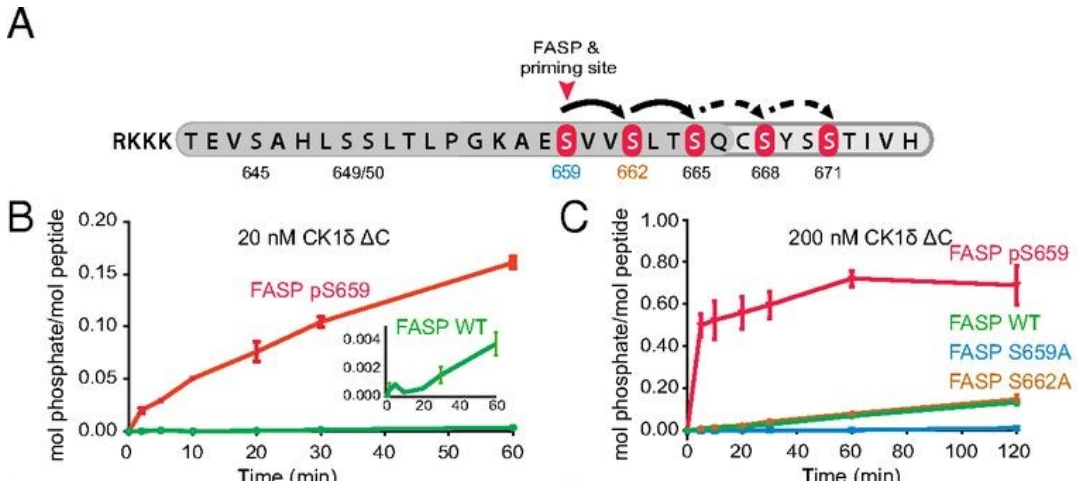

Figure 3.1: Processive phosphorylation of the mPER2 FASP region is dependent on S659 phosphorylation. (A) Schematic diagram of the FASP serine cluster phosphorylation in a synthetic peptide. Time course of representative peptide phosphorylation assays with 20 nM (B) or 200 nM (C) CK1$\delta\Delta$C. (Narasimamurthy et al. 2018)

vivo enviroment.

Additional experiment was conducted to test whether CK1δ1 could phosphorylate the FASP priming site of mPER2 in full-length protein. Indeed, addition of increasing amounts of recombinant CK1δ1 protein was sufficient to increase the phosphorylation of S659 in full-length mPER2 (Fig. 3.3). As seen in Fig. 3.2, mutation of the priming site (S659) abolished the phosphorylation of S662, confirming the progressive nature of FASP phosphorylation in cells.

3.3.2 CK1δ/ϵ is the Priming Kinase in Cells

So far, it has been established that CK1δ1 could phosphorylate the priming site in the peptide and in the immunopurified protein, and it remains to test whether CK1δ1 could phosphorylate the mPER2 priming site in intact cells.

We conclude that CK1δ and CK1ϵ are both necessary and sufficient to phosphorylate the mPER2 FASP priming and downstream sites in vitro and in cells

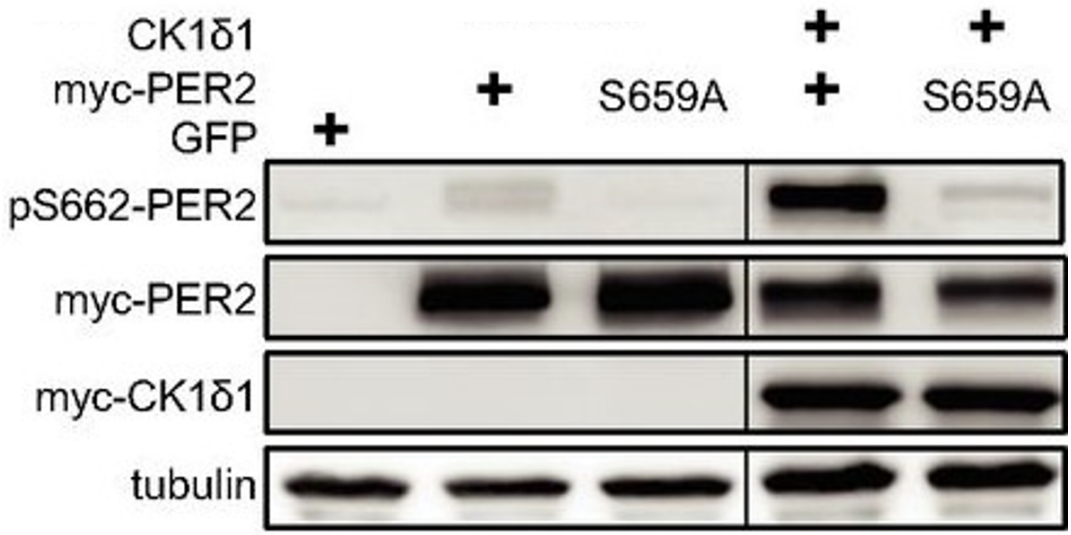

Figure 3.2: Phosphorylation of S662 is dependent on the S659 site.

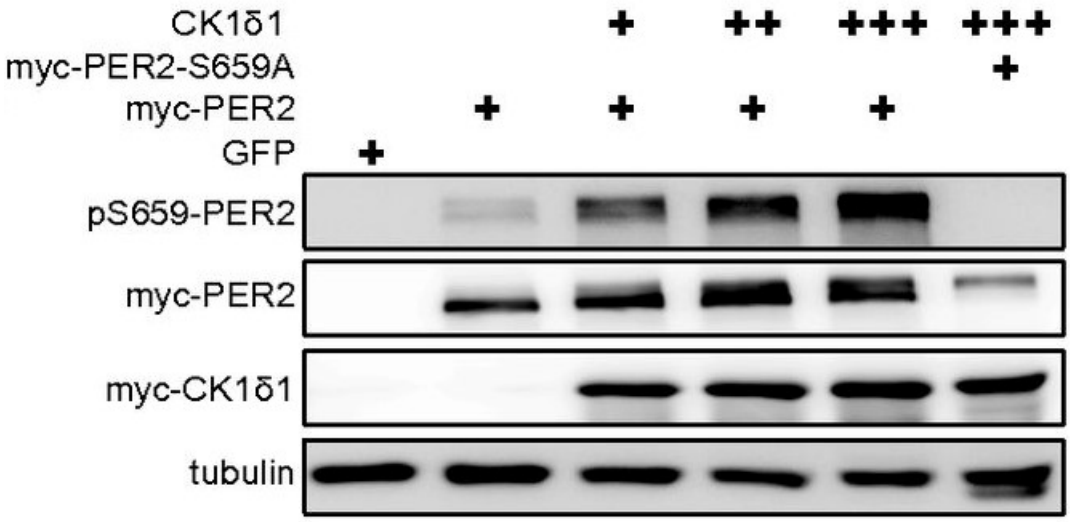

Figure 3.3: Phosphorylation of the priming site by CK1δ1. CK1δ1 phosphorylates mPER2 in cells. mPER2 expression plasmid (1 g) was cotransfected with 10 ng (+), 25 ng (++), and 50 ng (+++) of CK1δ1 expression plasmid. (Narasimamurthy et al. 2018)

3.4 Revising the Phosphoswitch Mathematical Model

3.4.1 Simulations Confirm the Role of the CK1δ/ϵ Carboxyl Terminus in Temperature Compensation

Preliminary experimental data suggests that the CK1 catalyzed phosphorylation rate for the priming site (S659 of mPER2) strongly depends on the presence of CK1 tail (carboxyl terminus), which is not the case for the β-TrCP binding site (Fig. 3.4). In addition, the CK1 full length proteins tends to be fully (auto)phosphorylated at the tail within 30 mins. This suggests that the activity of CK1 is inhibited via autophosphorylation of the carboxy-terminal residue and CK1 can actively regulate the priming phosphorylation. Further experimental data shows that truncation of CK1δ1 at amino acid 400, removing the last 16 residues, can increase the activity of the kinase on the priming site to a level similar to that of CK1δ2 and CK1ϵ (Fig. 3.5 B and C).

Here, we study a preliminary model where CKU (CK1 with unphosphorylated tail) phosphorylates PER2 on the priming FASP site much faster than CKP (CK1 with fully phosphorylated tail) without affecting the β-TrCP binding. CK1 acts as the priming kinase and acts differently at the two PER2 sites depending on the tail status. After investigating the system, we find that increasing the dephosphorylation of CK1 tail can shorten the period, which acts in balance with other cellular processes including the phosphorylation of PER on the FASP downstream sites (Fig. 3.6). We propose a temperature mechanism as follows: although CK1 global activity is temperature compensated, there is a separate mechanism regulating CK1 through its tail. As temperature increases, CK1 tail dephosphorylation is faster, driving more CK1 into the unphosphorylated state, which in turn, slows down the clock. These preliminary together with experimental data suggest a previously unappreciated role for the extreme carboxyl terminus of CK1 in influencing the activity of the kinase.

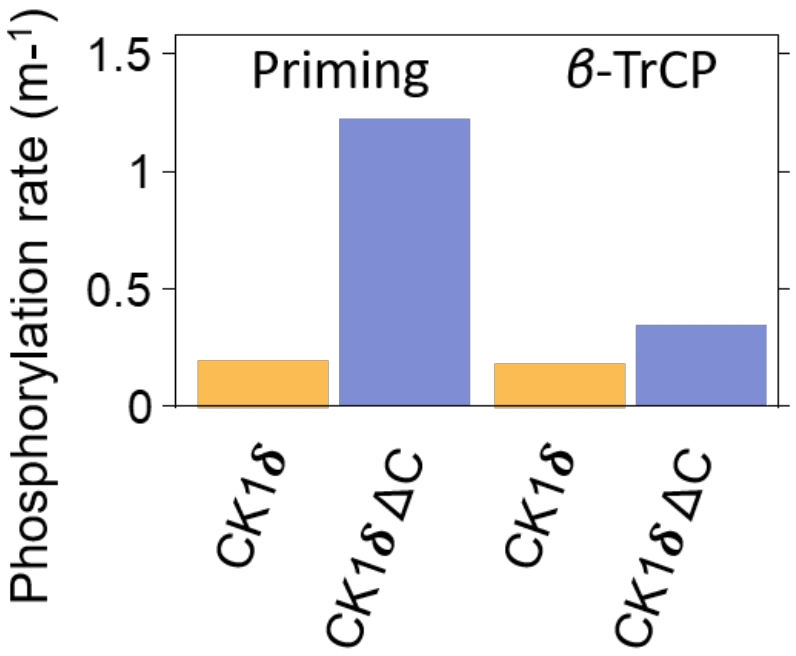

Figure 3.4: Differentiated sensitivity of PER2 phosphorylation sites to CK1 tail. The priming phosphorylation rate increases up to 6-fold when the tail is truncated from CK1 (CK1$\delta\Delta$C), while the phosphorylation rate of the β-TrCP binding only increased by 1.4-fold.

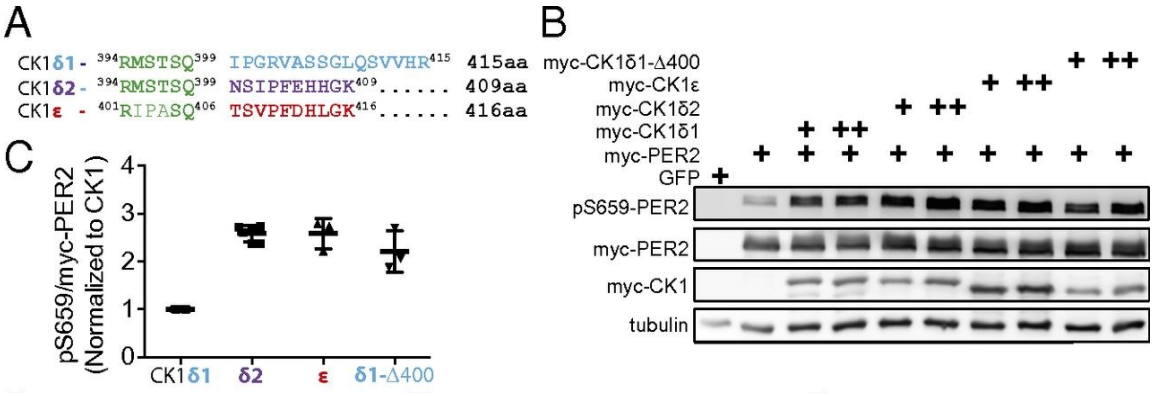

Figure 3.5: The extreme carboxyl terminus of CK1 regulates priming phosphorylation. (A) Alignment of the carboxyl termini of CK1δ1, CK1δ2, and CK1ϵ (B) CK1δ2 and CK1ϵ are more active than CK1δ1 as PER2 priming kinase. mPer2 plasmid (1 μg) was cotransfected with 5 ng (+) and 10 ng (++) of the indicated CK1 isoforms, and lysates were probed with indicated antibodies. (C) Analysis of the priming kinase activity of CK1 isoforms. The ratio of pS659 to myc-PER2 was calculated after normalization to CK1 expression, and the value of CK11 was taken as 1 to express fold change. (Narasimamurthy et al. 2018)

3.4.2 A Robust Yet Fragile Mechanism Regulates the Temperature Compensation

With the identification of CK1 as the priming kinase, we asked if the phosphoswitch model was still predictive and accurate. We modified our previous phosphoswitch model by incorporating the new finding that CK1δ1/δ2/ϵ functions as the priming kinase but with different kinetic activities. This revised model continues to accurately simulate the three stage kinetics of PER2 degradation containing a plateau (Fig. 3.7), consistent with the result in Zhou et al. (2015).

Furthermore, the model successfully reproduces the negligible period change of CK1ϵ-/- mutant mice (Etchegaray et al. 2010), the longer period of CK1δ-/- mutant mice (Etchegaray et al. 2010, Lee et al. 2009), and the shorter period of FASP humans and mice (Toh et al. 2001, Xu et al. 2007)(Fig. 3.8). Our results are also consistent with Fustin et al. (2018) where they find that over expression of CK1δ2, a kinase

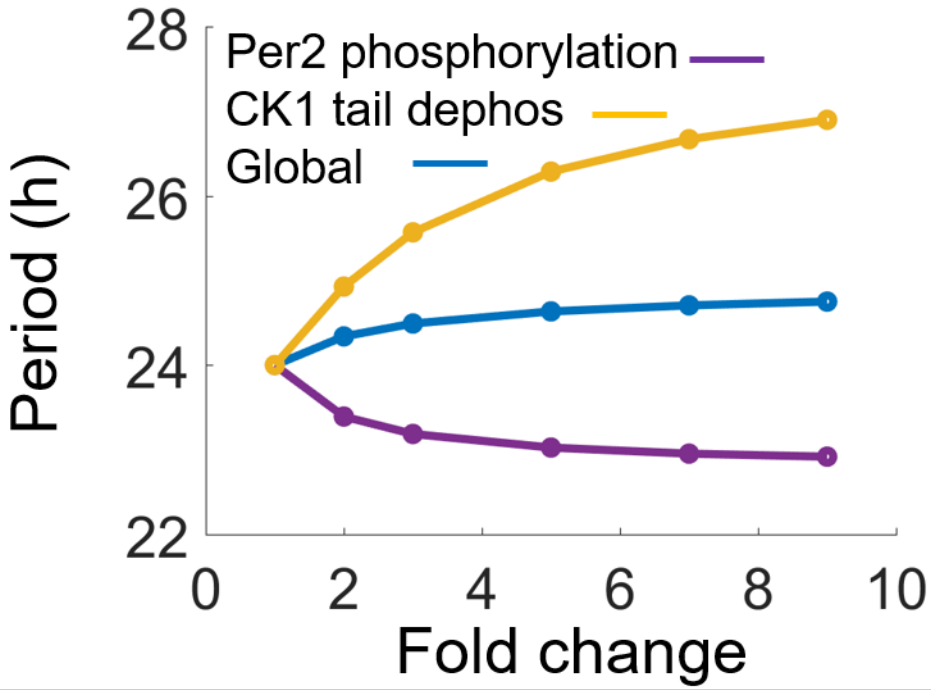

Figure 3.6: Effects of different reactions on PER2 period. Period shortens as the phosphorylation rate of PER2 on the FASP downstream sites increases, lengthens as the dephosphorylation on CK1 tail increases and remains almost unchanged when global activity changes in the system.

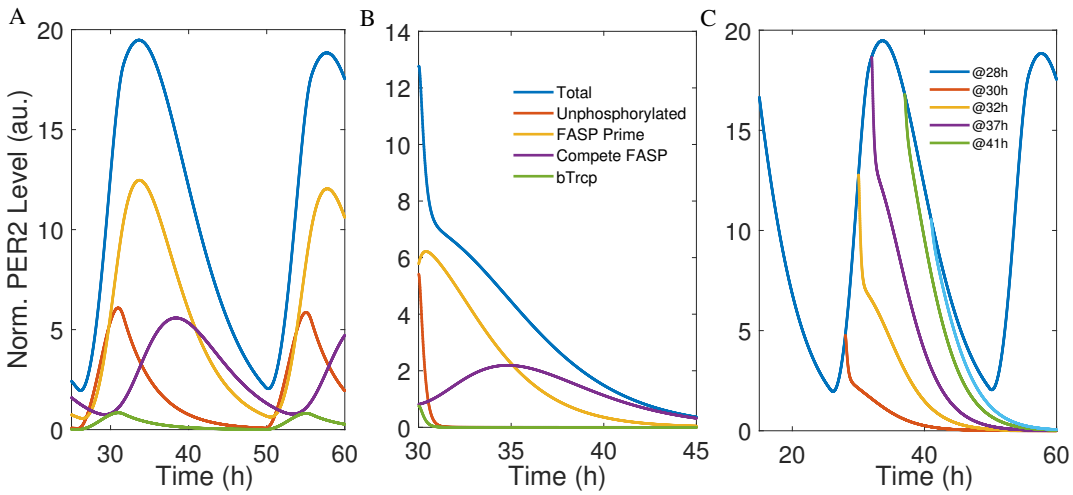

Figure 3.7: Reproducing the circadian rhythms and three stage degradation. (A) Circadian rhythms and (B) degradation profiles of PER2,PER2 unphosphorylated, PER2 phosphorylated on FASP prime site, PER2 phosphorylated completely at FASP, PER2 phophosrylated at β-TrCP binding site. (C) Various degradation profiles of PER2 when protein translation is inhibited by cycloheximide (CHX).

more active on the FASP site, leads to a lengthened period period in cells (Fig. 3.9).

It is proposed by Shinohara et al. (2017b) that CK1 phosphorylation of PER2 is temperature compensated *in vitro* by balancing the higher dissociation constant and higher phosphorylation rate at higher temperatures. Our model shows simulation results consistent this temperature compensation mechanism. Increasing phosphorylation activity at the priming site alone lengthens the period, which acts in balance with the effect of other cellular processes. When the dissociation constant of CK1 and phosphorylation rates for both the priming site, downstream sites and the β-TrCP site of PER2 increase together, the period is nearly constant in the model (Fig. 3.10).

3.5 Conclusion

Regulation of PER2 abundance controls circadian timing, yet understanding the phosphorylation of the key control point has been elusive. Here, we show by multiple

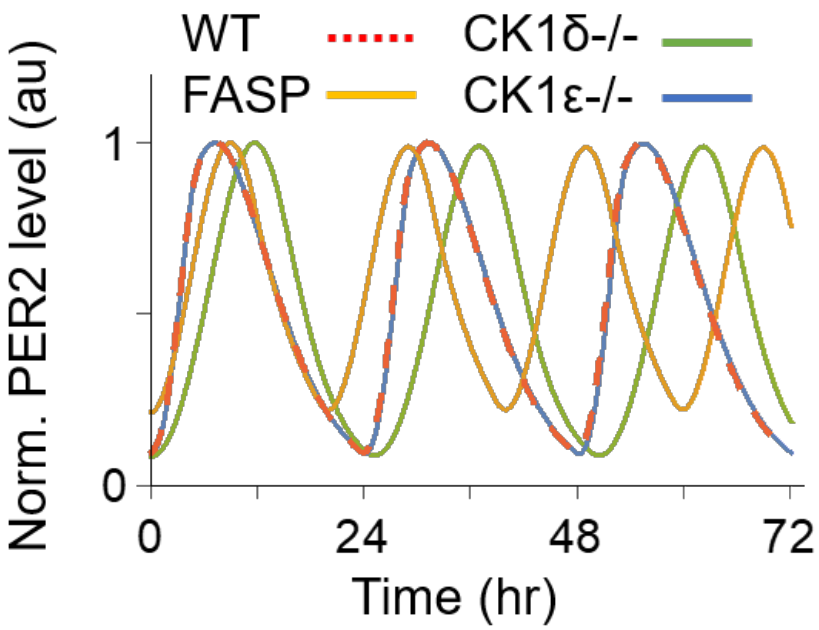

Figure 3.8: Simulation results consistent with various CK1 mutation phenotypes findings.

approaches that CK1δ/ϵ can function as the PER2 priming kinase, resolving a long-standing question in circadian biology.

Additionally, we find that CK1δ1 and CK1ϵ differ significantly in their ability to phosphorylate the priming site. CK1δ2, which has residues at the extreme carboxyl terminus more closely resembling CK1ϵ, displays increased priming kinase activity like CK1ϵ (Fustin et al. 2018). These studies highlight the role of the δ/ϵ carboxyl terminus to regulate priming activities as well as the circadian clock. Because CK1δ/ϵ is also regulated by phosphorylation and dephosphorylation of the carboxyl terminus, this also suggests a mechanism for cellular signaling pathways to regulate PER2 priming rates. Inspired by these results, we first propose a preliminary model with CK1 tail phopshorylation acting as the main regulator of the priming phosphorylation. Simulations of our model confirm the indispensable role of CK1 carboxyl terminus in regulating the temperature compensation and proposed that the phosphorylation of CK1 tail is the key regulator of the circadian time keeping.

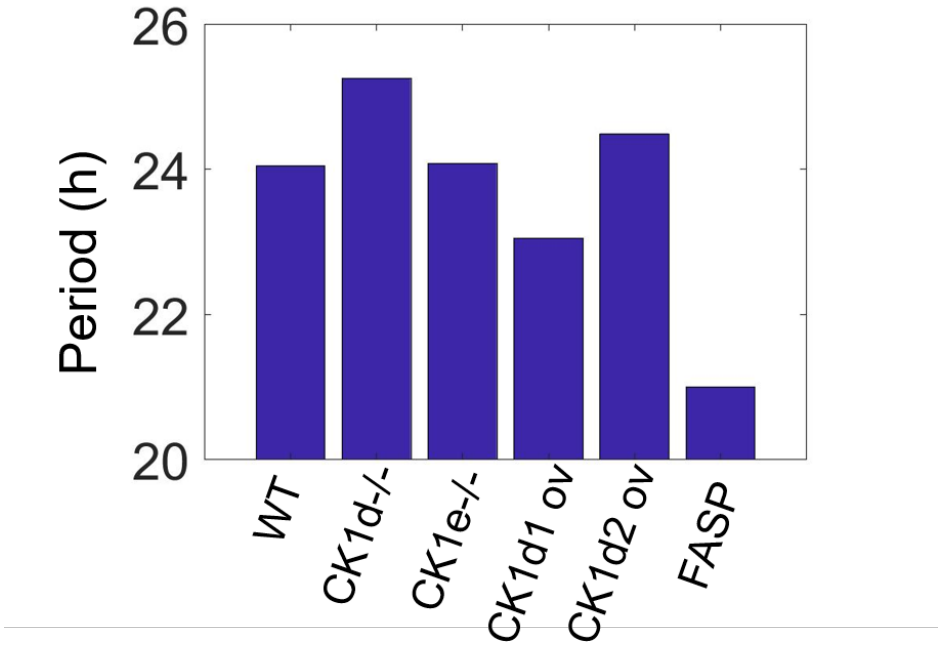

Figure 3.9: Effect of various mutations on the PER2 circadian period. Wild type (WT) shows a circadian period around 24h. CK1 δ-/- shows a lengthened period, over expression of CK1δ1 shows a shortened period and CK1 δ2-/- CK1 ϵ-/- mutations shows negligible change on the period.

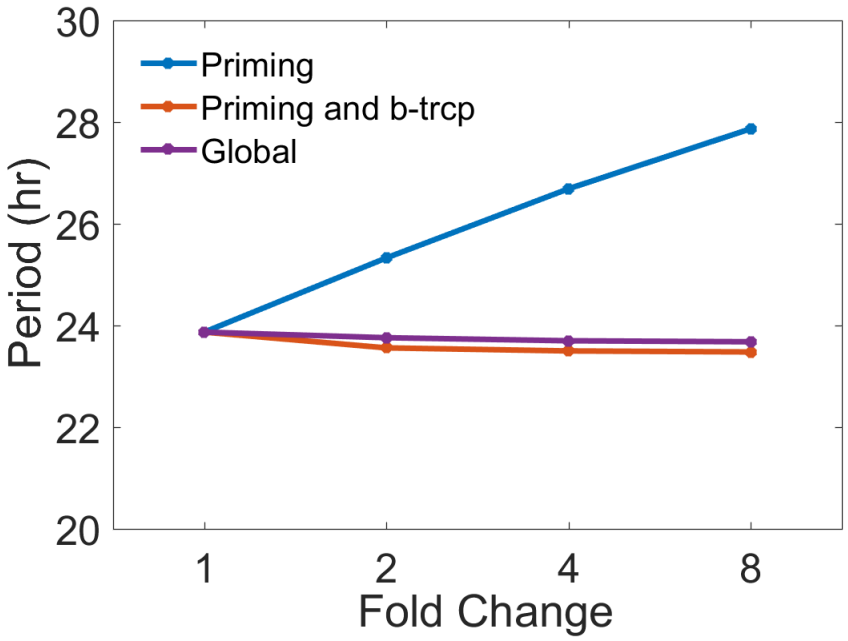

Figure 3.10: Temperature compensation in the revised phosphoswitch model. Period is robust to global changes in CK1 phosphorylation activity but sensitive to isolated change of the phosphorylation rate on the priming site. Period is robust to the simultaneous change of CK1 phosphorylation rate and dissociation constant (global activity). Here, CK1 phosphorylation rate and dissociation constant for both the priming and the β-TrCP sites are changed in the same magnitude

We then propose a revised phosphoswitch model incorporating the fact that CK1 $\delta 1$/CK1$\delta 2$/CK1ϵ is the priming kinase with differentiated kinetics. We successfully recover the three-stage degradation of PER2 as well as the temperature compensation feature of the circadian clocks. We also confirm that while CK1 is itself temperature compensated, the system can be sensitive to the changes in the CK1 carboxyl terminus, which regulates the clock in reaction to temperature changes and cellular signals.

3.6 Supplement Information

Here we list the differential equations to describe the preliminary model with CK1 regulating the phosphoswitch through its tail phosphorylation.

$$\frac{d[m]}{dt} = a_0 \frac{AC_t - [R] - K_d + \sqrt{(AC_t - [R] - K_d)^2 + 4K_d AC_t}}{2AC_t} - d_0[m]$$

$$\frac{d[P_0]}{dt} = a_t[m] - P_0(kcf_u[CK_u] + kcf_p[CK_p]) + K_{cb}([P_0CK_p] + [P_0CK_u])$$
$$+ kdp[P_1PP] + kdp_0[P_bPP] - b_0[P_0]$$

$$\frac{d[P_0CK_u]}{dt} = kcf_u[P_0][CK_u] - (K_{cb} + kpu + kp_0 + b_0)[P_0CK_u] - kck_{ps}[P_0CK_u]$$
$$+ kck_{dps}[P_0CK_p]$$

$$\frac{d[P_0CK_p]}{dt} = kcf_p[P_0][CK_p] - (K_{cb} + K_{pp} + kp_0 + b_0)[P_0CK_p] + kck_{ps}[P_0CK_u]$$
$$- kck_{dps}[P_0CK_p]$$

$$\frac{d[P_t]}{dt} = kp_0(P_0CK_u + P_0CK_p) - kppf[P_t][PP] + kppb[P_tPP] - P_t(ub + b_0)$$

$$\frac{d[P_tPP]}{dt} = kppf[P_t][PP] - [P_tPP](kppb + ub + b_0 + kdp_0)$$

$$\frac{d[P_1]}{dt} = (kpu[P_0CK_u] + kpp[P_0CK_p]) - kppf[P_1][PP] + kppb[P_1PP] - b_0[P_1]$$
$$- kcf[P_1]([CK_u] + [CK_p]) + kpb_1([P_1CK_u] + [P_1CK_p]) + kdp[P_2PP]$$

$$\frac{d[P_1PP]}{dt} = kppf * [P_1][PP] - (kppb + b_0 + kdp)[P_1PP]$$

$$\frac{[P_1CK_u]}{dt} = -kck_{ps}[P_1CK_u] + kck_{dps}[P_1CK_p] + kcf[P_1][CK_u]$$
$$- (kpb_1 + b_0 + kpp)[P_1CK_u]$$

$$\frac{[P_1CK_p]}{dt} = -kck_{dps}[P_1CK_p] + kck_{ps} * p1cku + kcf[P_1][CK_p]$$
$$- (kpb1 + b0 + kpp)[P_1CK_p]$$

$$\frac{d[P_2PP]}{dt} = kppf[P_2][PP] - (kppb + b_0 + kdp)P_2PP$$

$$\frac{d[P_2]}{dt} = kpp([P_1CK_p] + [P_1CK_u]) - kppf[P_2][PP] + kppb[P_2PP] - b_0[P_2]$$
$$- kcf[P_2]([CK_u] + [CK_p]) + kpb_1([P_2CK_u] + [P_2CK_p]) + kdp[P_3PP]$$
$$\frac{d[P_2CK_u]}{dt} = kck_{dps}[P_2CK_p] - kck_{ps}[P_2CK_u] - (kpb_1 + b_0 + kpp)[P_2CK_u]$$
$$+ kcf[P_2][CK_u]$$
$$\frac{d[P_2CK_p]}{dt} = -kck_{dps}[P_2CK_p] + kck_{ps}[P_2CK_u] - (kpb_1 + b_0 + kpp)[P_2CK_p]$$
$$+ kcf[P_2][CK_p]$$
$$\frac{d[P_3]}{dt} = kpp[P_2CK_p] + kpp[P_2CK_u] - kppf[P_3][PP] + kppb[P_3PP] - b_0[P_3]$$
$$- kcf[P_3]([CK_u] + [CK_p]) + kpb_2([P_3CK_p] + [P_3CK_u]) + kdp[P_4PP]$$
$$\frac{d[P_3PP]}{dt} = kppf[P_3][PP] - [P_3PP](kppb + b_0 + kdp)$$
$$\frac{d[P_3CK_u]}{dt} = -kckp[P_3CK_u] + kck_{dps}[P_3CK_p] + kcf[P_3][CK_u]$$
$$- (kpb_2 + b_0 + kpu)[P_3CK_u]$$
$$\frac{d[P_3CK_p]}{dt} = kckp[P_3CK_u] - kck_{dps}[P_3CK_p] + kcf[P_3][CK_p]$$
$$- (kpb_2 + b_0 + kpu)[P_3CK_p]$$
$$\frac{d[P_4]}{dt} = kpp[P_3CK_p] + kpu[P_3CK_u] - kppf[P_4][PP] + kppb[P_4PP]$$
$$- kcf[P_4]([CK_u] + [CK_p]) + kpb_2([P_4CK_u] + [P_4CK_p]) - bh[P_4]$$
$$\frac{d[P_4CK_u]}{dt} = kck_{dps}[P_4CK_p] - kck_{ps}[P_4CK_u] + kcf[P_4][CK_u] - (kpb_2 + bh)[P_4CK_u]$$
$$\frac{d[P_4CK_p]}{dt} = kck_{ps}[P_4CK_u] - kck_{dps}[P_4CK_p] + kcf[P_4][CK_p] - (kpb_2 + bh)[P_4CK_p]$$
$$\frac{d[P_4PP]}{dt} = kppf[P_4][PP] - [P_4PP](kppb + bh + kdp)$$
$$\frac{d[P_{ub}]}{dt} = ub([P_t] + [P_tPP]) - bt[P_{ub}]$$

$$\begin{aligned}\frac{d[CK_u]}{dt} &= -kcf([P_0]+[P_1]+[P_2]+[P_3]+[P_4])[CK_u] + kcb[P_0CK_u] \\ &+ kpb_1([P_1CK_u]+[P_2CK_u]) + kpb_2([P_3CK_u]+[P_4CK_u]) \\ &- kck_{ps}[CK_u] + kck_{dps}[CK_p] + (b_0+kpu+kp_0)[P_0CK_u] \\ &+ (b_0+kpu)([P_1CK_u]+[P_2CK_u]+[P_3CK_u]) + bh[P_4CK_u]\end{aligned}$$

The auxiliary variables are explained in the next few equations.

$$\begin{aligned}[R] &= [P_4]+[P_4PP]+[P_4CK_u]+[P_4CK_p] \\ [CK_p] &= CK_t - ([P_0CK_u]+[P_0CK_p]+[P_1CK_u]+[P_1CK_p]+[P_2CK_u] \\ &+ [P_2CK_p]+[P_3CK_u]+[P_3CK_p]+[P_4CK_u]+[P_4CK_p]) - [CK_u] \\ [PP] &= PP_t - ([P_tPP]+[P_1PP]+[P_2PP]+[P_3PP]+[P_4PP])\end{aligned}$$

(A) Variables of the model

Description	Symbol
The concentration of CK1 with unphosphorylated tail	$[CK_u]$
The concentration of CK1 with phosphorylated tail	$[CK_p]$
The concentration of Per2 mRNA	$[m]$
The concentration of unphosphorylated PER2	$[P_0]$
The concentration of unphosphorylated PER2 bound to CK1	$[P_0CK_u]/[P_0CK_p]$
The concentration of PER2 phosphorylated at β-TrCP binding site	$[P_t]$
The concentration of PER2 phosphorylated at β-TrCP site bound to phosphatase	$[P_tPP]$
The concentration of PER2 phosphorylated at ith FASP site ($i = 1, 2, 3, 4$)	$[P_i]$
The concentration of PER2 phosphorylated at ith FASP site bound to phosphatase ($i = 1, 2, 3, 4$)	$[P_iPP]$
The concentration of PER2 phosphorylated at ith FASP site bound to CK1 ($i = 1, 2, 3, 4$)	$[P_iCK_u]/[P_iCK_p]$
The concentration of ubiquitinated PER2	$[P_{ub}]$
The concentration of phosphatase	$[PP]$

(B) Parameters of the model

Description	Symbol	Value
Phosphorylation rate of CK1 tail	kck_{ps}	0.1 /hr
Dephophosrylation of CK1 tail	kck_{dps}	0.1 /hr
Transcription rate constant for *Per2* mRNA	a_0	59.5 nM/hr
Degradation rate constant for *Per2* mRNA	d_0	0.242 /hr
Translation rate constant for PER2	a_t	1 /hr
Dissociation constant between PER2 and BMAL1-CLOCK	K_d	$1.555 * 10^{-5}$nM
Binding rate constant for unphosphorylated CK1 to unphosphorylated PER2	$kcfu$	4.76 /nMhr
Binding rate constant for phosphorylated CK1 to unphosphorylated PER2	$kcfp$	0.476 /nMhr
Binding rate constant for CK1 to primed PER2	kcf	2.38 /nMhr
Unbinding rate constant between CK1 and unphosphorylated PER2	K_{cb}	$3.922 * 10^{-5}$/hr
Unbinding rate constant between CK1 and PER2 phosphorylated at 1st & 2nd FASP sites	kpb_1	1.14710^{-4}/hr
Unbinding rate constant between CK1 and PER2 phosphorylated at 3rd & 4th FASP sites	kpb_2	1.312^{-8}/hr
CK1 phosphorylation rate constant for β-TrCP binding site	kp_0	9.11 /hr
Priming phosphorylation rate constant for PER2 at FASP binding site by unphosphorylated CK1	kpu	6.033 /hr
Phosphorylation rate constant for PER2 at FASP binding site by phosphorylated CK1	kpp	0.694 /hr
Dephosphorylation rate constant for PER2 at FASP sites	kdp	9.608 /hr
Dephosphorylation rate constant for PER2 at β-TrCP binding site	kdp_0	28.166 /hr
Binding rate constant for phosphatase to PER2	$kppf$	7.31 nM/hr
Unbinding rate constant between phosphatase and PER2	$kppb$	0.0694 /hr
Degradation rate constant for ubiquitinated PER2	bt	73.157 /hr
Degradation rate constant for fully phosphorylated PER2 at FASP sites	bh	0.339 /hr
Degradation rate constant for PER2 and related complexes	b_0	$6.7 * 10^{-4}$ /hr
Ubiquitination rate constant for PER2 phosphorylated at β-TrCP binding site	ub	655.9 /hr
Total CK1 concentration	CK_t	146.245 nM
Total phosphatase concentration	PP_t	11.504 nM
Total activator (BMAL1-CLOCK) in nucleus concentration	AC_t	1.336 nM

Table 3.1: Description of the variables and parameters used for the preliminary simulation with CK1 tail regulation.

CHAPTER IV

How to time events with multi-site phosphorylations of proteins

4.1 Abstract

Multi-site protein phosphorylation has been shown to be a key part of all circadian clocks. Sequential phosphorylation facilitated by different kinases/phosphatases can be found in *Drosophila*, *Neurosphora*, mammals and even cyanobacteria. Individual phosphorylation events are typically much quicker than circadian timescales. Additionally, in the Drosophila circadian clock, multisite phosphorylation can lead to an interval timer gating protein nuclear entry (Meyer et al. 2006, Saez and Young 1996). In mammals, a similar interval timer was discovered gating PERIOD2 degradation (Zhou et al. 2015). Here, we show how kinases and phosphatases can work together to create an interval timer with a timescale much longer than individual phosphorylation events. The proposed mechanism is based on phosphate groups being rapidly shuttled on and off a protein, multiple conformational changes to a protein allowing additional sites to be phosphorylated and at least in PERIOD2, an initial phosphoswitch determining protein fate. We also find that, in the mammalian circadian clocks, product inhibition on the kinase through sequestration mechanism can play a crucial rule in sustaining the circadian clocks. This work puts surprising constraints on the mecha-

nisms of phosphorylation in circadian clocks and points to a possible universal design principle for circadian timekeeping.

4.2 Introduction

Protein phosphorylation is the key regulator of the period of circadian rhythms found in almost all organisms. In *Drosophila* and mammals, casein kinase 1 (CK1) sequentially phosphorylates several sites on the PERIOD (PER) proteins. The combined actions of CK1 and the phosphatases determines the circadian period (Lee et al. 2011a). A similar mechanism exists in *Neurospora* and even cyanobacteria (*Synechococcus elongatus*) through protein phosphorylation (Tomita et al. 2005, Rust et al. 2011, Van Zon et al. 2007, Nishiwaki and Kondo 2012). This biochemical motif is at the heart of several of the most important questions in circadian research: How could timescales on the order of hours emerge from phosphorylation events that are likely orders of magnitude faster, especially as kinases are tightly bound to their products? How could changes in PER affect timescales of minutes, as well as a circadian timescale? Why would kinases and phosphatases both be bound to PER? Is the fact that PER has large disordered regions important to these phenomena?

Results from two landmark studies on PER have yet to be fully understood. When the Young lab expressed PER and its partner TIM in Drosophila cells, they noted that the amount of time for these proteins to enter the nucleus was on the order of hours and always a near fixed amount of time (interval timer). Mammalian cells do not have this carefully gated nuclear entry (Smyllie et al. 2016), yet Kim and Forger (2012) show that once sequential phosphorylation of PER is triggered by phosphorylation at site 659, PER degradation is paused for a near fixed amount of time, thus creating a plateau in protein expression. A similar sequential phosphorylation motif is found in Drosophila. From these studies, another key question emerges from the circadian field: How can a molecular interval timer be built? Can an efficient interval timer be

built with just one molecule, or does it require the collective action of many? Recent studies in *Drosophila* and *Neurospora* suggest that widely separated phosphorylation sites on PER and FRQ interact in a temporal manner (Baker et al. 2009, Chiu et al. 2011, Garbe et al. 2013, Querfurth et al. 2011, Shanware et al. 2011), but how they combine to regulate circadian rhythms remains elusive.

Here, we describe a mechanism whereby the time needed for sequential protein phosphorylation grows exponentially rather than additively with the number of protein phosphorylation sites, creating long time intervals even though individual phosphorylation events are fast. Key to the mechanism is rapid shuttling of the phosphate group on and off the protein by the combined action of a kinase and phosphatase. We propose an additional mechanism where the time for this process to take becomes fixed (an interval timer). In this mechanism, after a site is phosphorylated, the kinase does not immediately move to the next phosphorylation site. Instead, several steps (which also occur on a fast timescale) are needed for the protein to reach the proper conformation and for the kinase and phosphatase to move to the next site. Phosphorylation on the original site is necessary to provide the energy for these conformational changes. We also find that product inhibition of the kinase can play an important role in the protein phosphorylation and degradation process. When applied to the mammalian circadian clocks, our simulations suggest that weakened product inhibition can lead to disrupted circadian rhythms. This or similar mechanisms could explain the long timescales and interval timer behavior that is required for proper functioning of circadian clocks.

4.3 Results

4.3.1 Sequential Model

Shown in Figure 4.1 is the standard model for sequential protein phosphorylation. The protein can be phosphorylated at any of the N sites, however, phosphorylation must occur sequentially, e.g., phosphorylation at site $X-1$ must occur before site X. After all sites have been phosphorylated, we assume that the protein can then be degraded. We call the rate of phosphorylation p and the rate of dephosphorylation q, with $k = q/p$ being the ratio of these two.

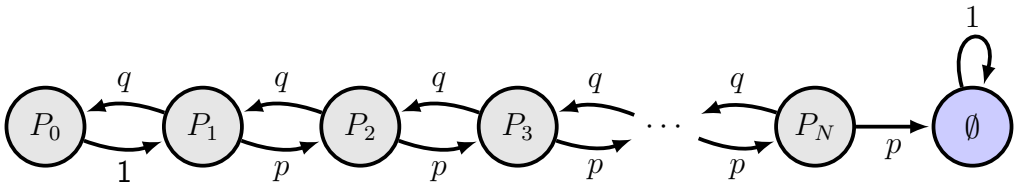

Figure 4.1: A general sequential multi-site phosphorylation model with N phosphorylation sites, e.g., FASP sites.

In Section 4.4.3, we calculate the average time to degradation where three cases are considered. In the case that $p > q$, we find that the time to degradation is $O(N)$, meaning that it grows linearly with the number of phosphorylation sites. This is intuitively correct, since if the protein was only phosphorylated ($q \sim 0$), then the time to degradation would be simply the sum of the time for each of the N phosphorylation events to occur. When $p \sim q$, and the time course of the kinase and phosphatase is similar, the time to degradation is $O(N^2)$ which grows quadratically (See. Table 4.1).

However, when $q > p$, the time to degradation is $O(k^N)$ giving exponential growth. This explains how much larger timescales can be generated from faster processes. For example, let $p = 1$ and $n = 5$. Figure 2 shows the expected time to degradation can get very large as k increases. This can be understood intuitively in the following way. Even if a protein is nearing full phosphorylation, high k value means stronger

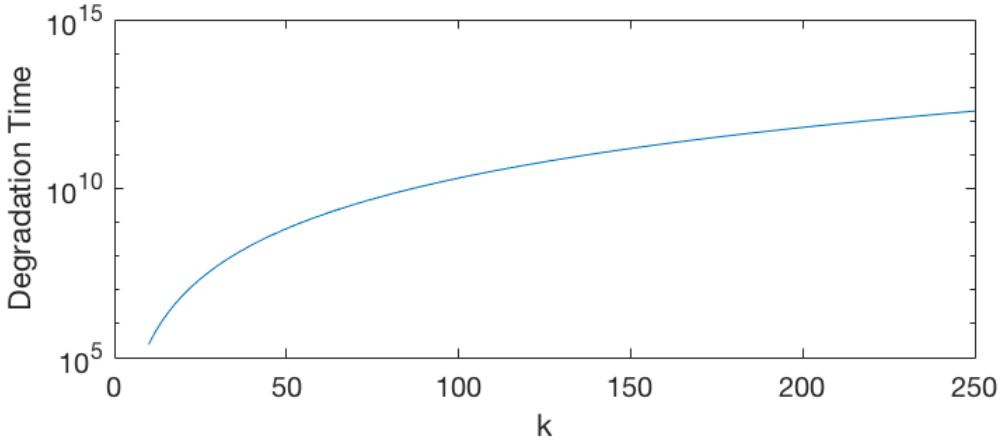

Figure 4.2: The expected protein degradation time as a function of k.

phophatase activity and dephosphorylation can quickly bring it back to the unphosphorylated state, losing the effects of all previous phosphorylations and increasing the wait time. In fact, the speed and rhythmicity of PER phosphorylation (therefore degradation) can be closely related to the period of the circadian clock. Our result is therefore consistent with Lee et al. (2011a) where they find that the period of the circadian oscillator can be significantly affected by the balance between the kinase and phosphatase activity.

An additional phosphorylation site in another region of PERIOD (459 in mPER2, x in Drosophila) also leads to degradation. We now consider the 459 (β-TrCP) site of PER2 and modified the model so that CK1 could phosphorylate the β-TrCP site in the same way it does the sequential phosphorylation. As shown in the supplement, this additional β-TrCP site act as a sink. When this happens the protein does not get delayed in the low phosphorylation states, instead it gets degraded, losing the long timescale. Based on this result, we would predict that even though there is only one binding site for CK1 to bind with PER2, the phosphorylation of each PER2 protein can only proceed either on the β-TrCP site or the FASP sequential phosphorylation sites. Narasimamurthy et al. (2018) provides experimental data supporting this claim.

4.3.2 Network model with conformational changes

There are two additional items that this model must address to fit data on the PER protein. First, if k is large, which is when the long timescales are generated, the remaining PER protein in the model will spend most of its time in the states of low phosphorylation regardless of the amount of time elapsed since it has been produced. However, the PER protein shows increasing phosphorylation levels over time Lee et al. (2001). Additionally, the degradation time course predicted by this model is the standard exponential decay one typically sees in biochemical reactions, which does not match what is seen experimentally Zhou et al. (2015).

To address these data, we considered not only the phosphorylation events, but also the subsequent conformational changes, changes to the kinase and phosphatase positioning etc. that occur due to phosphorylation. We first consider a standard model shown in Figure. 4.3 where a protein can undergo conformational changes at any time, and that phosphorylation events increase the likelihood of these changes. Once they are completed and the protein is fully phosphorylated, the protein can be degraded. However, we were able to show in Section 4.4.3 that this model could be reduced to the sequential model we previously derived. In other words, adding in conformational changes could increase the time needed for the protein to degrade, but would not affect the degradation time course, nor build an interval timer.

4.3.3 Interval Timer

Finally, we considered a model where conformation changes must instead happen before each new site is phosphorylated. The model is described in Figure 4.4 and has the following structure. The kinase and likely phosphatase are always centered around one site and the phosphate group is continually being added or removed. It is possible the kinase both adds and removes the phosphate group. This is consistent with cyanobacterial data from the Ueda lab. When the phosphate group is added,

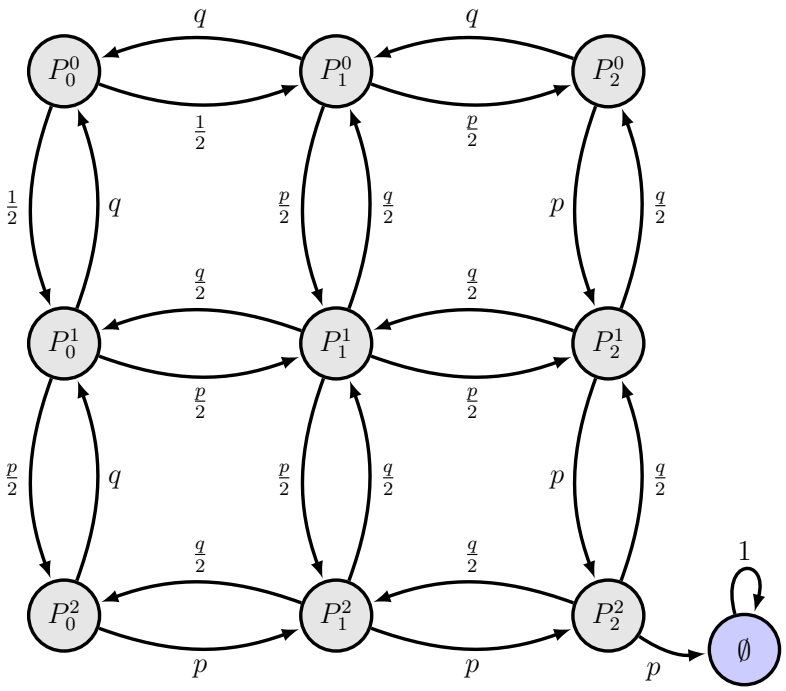

Figure 4.3: An example model for multi-site phosphorylation with 3 micro states and 2 phosphorylation sites.

it provides energy to enable conformational changes. We call these conformational changes microstates. The protein must progress through several microstates until the next phosphorylation occurs. The phosphate group could also be removed, at which time the protein will remain in its current microstate and not progress to the next microstate until the phosphate group is added back. Such a model was simulated with the Gillespie method, which also accounts for the randomness of molecular events.

In this system, four types of reactions can happen. First, a phosphate group can be temporarily added to an unoccupied site of a protein molecule given that all previous sites on that protein have been properly phosphorylated, e.g., $P_1^* \xrightarrow{K_1} P_2^0$ or $P_1^* \xrightarrow{K_1} P_2^5$. Second, when a phosphate group is already added temporarily to a protein, that protein molecule can acquire the necessary amount of energy to go though one additional step of conformational change, e.g., $P_2^5 \xrightarrow{K_3} P_2^6$. Third, a temporarily added phosphate group can be removed by phosphatases from a protein and that protein molecule will remain in its current conformation, e.g., $P_2^6 \xrightarrow{K_2} P_1^*$.

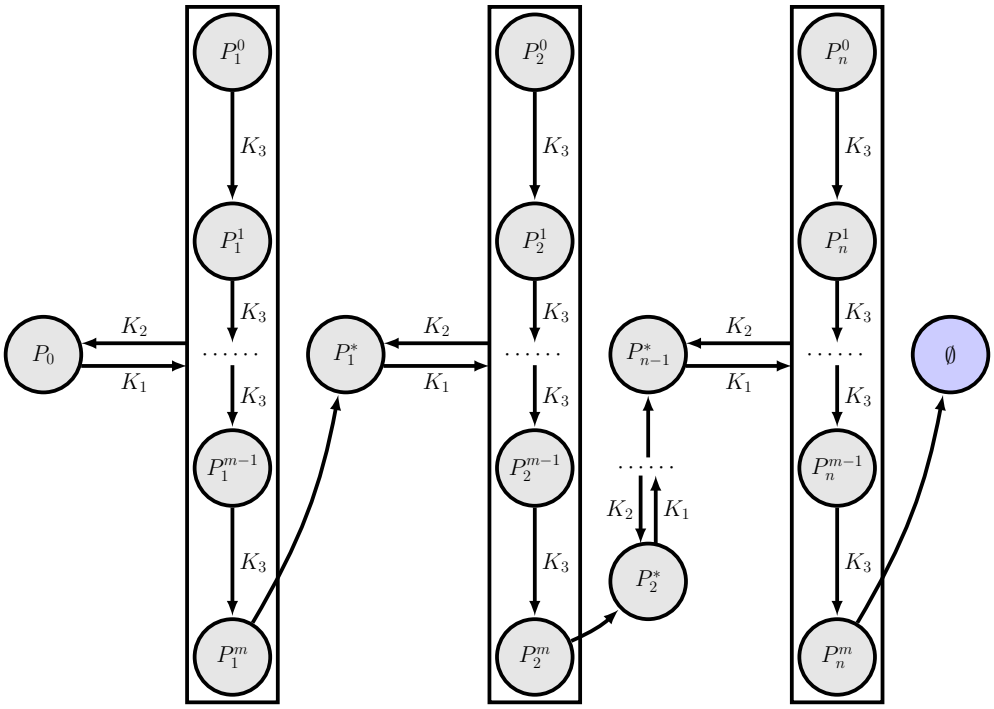

Figure 4.4: General model for the interval timer with m microstates (conformational states) and n phosphorylation sites

Finally, when a protein molecule has temporarily acquired phosphate groups on a specific site for many times and has proceeded to the final stage of the conformational change, it will tightly bind with the next phosphate group added to that site, thus being properly phosphorylated, e.g., $P_1^m \xrightarrow{K_3} P_1^*$ or $P_2^m \xrightarrow{K_3} P_2^*$.

Surprisingly, this model gave interval timers in almost all cases (See Figure 3). It also allows for progressively increasing phosphorylation levels. Thus, it matches the two additional behaviors we set out to match. Figure 3 shows that even with just one phosphorylation level, progressing from 1 to 10 microstates gives an interval timer. This interval timer becomes more robust as further microstates are added (Figure 4.5) or additional progressive phosphorylations occur (Figure 4.6).

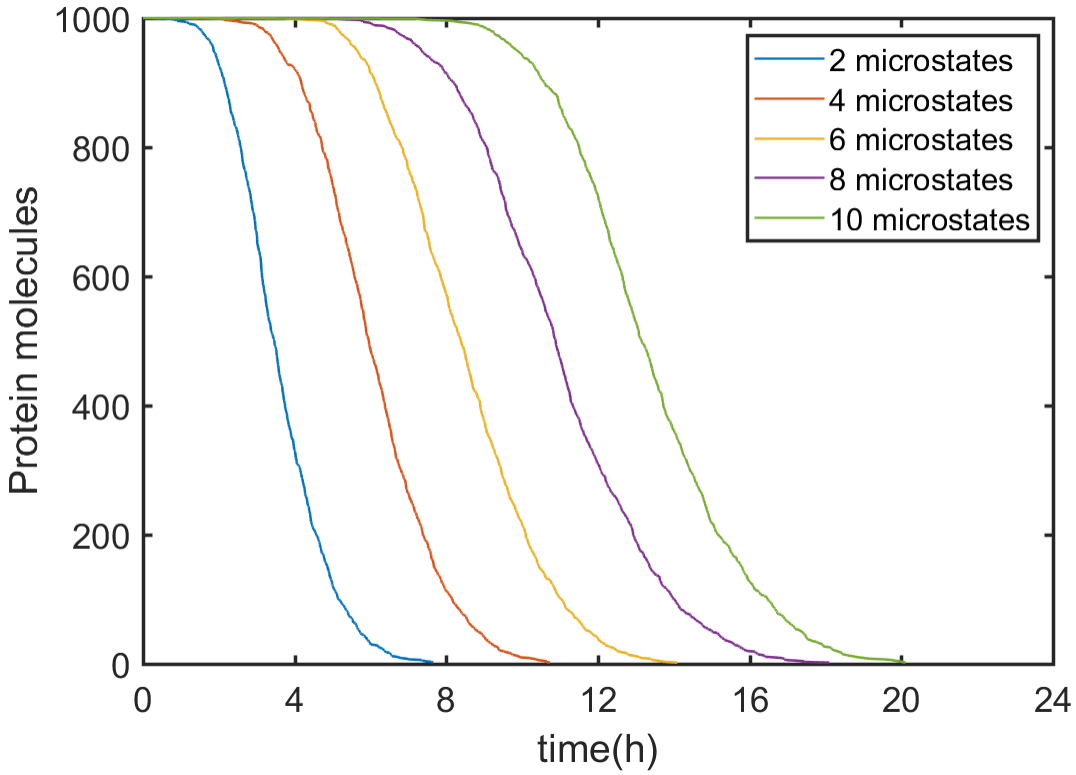

Figure 4.5: Stochastic simulations with 2 phosphorylation sites and various microstates

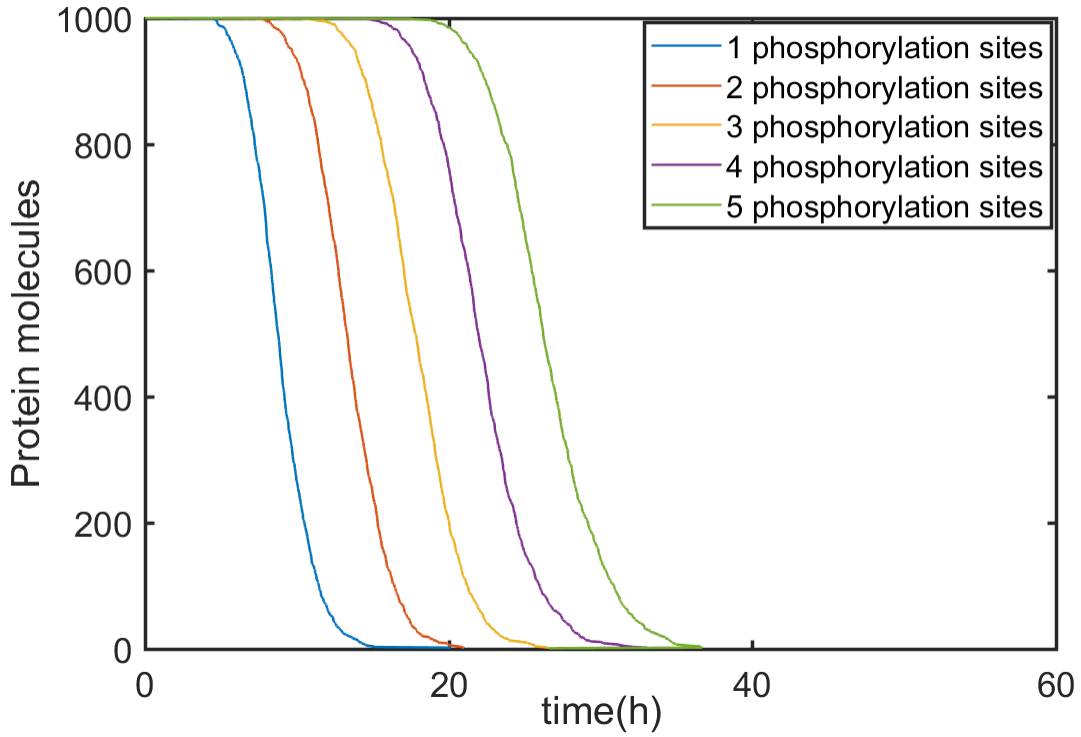

Figure 4.6: Stochastic simulations with 10 micro states and various phosphorylation sites

4.3.4 Product Inhibition

We now explore the substrate inhibition mechanism in the interval timer model where the fully phosphorylated protein can inhibit the kinase. To compare different types of inhibition scheme, we remove degradation in our model and keep track of the number of protein molecules in the unphosphorylated state.

We consider two types of product inhibition on kinases and in both cases only fully phosphorylated proteins can inhibit the kinase activities. First model utilizes a hill equation to model the inhibition mechanism:

$$K_{hill} = \frac{cP_t}{1 + \frac{(P_{tot} - P_0 - P_t)^3}{K_d}}$$

The second model assumes that kinase molecules can be sequestered by protein molecules through tight binding and the phosphorylation rate is:

$$K_{seq} = cP_t(1 - \frac{P_{tot} - P_0 - P_t}{CK_{tot}})$$

where c is the original rate for a protein molecule to phosphorylate on the next site, K_d is the dissociation constant for the hill type inhibition, P_t is the number of protein molecules with a temporary phosphate group added and P_0 are the number of proteins without a temporary phosphate group. P_{tot} is the total number of protein molecules in the system and CK_{tot} is the total number of kinase molecules in the system.

In our simulations, we find that when the product inhibition is modeled with a hill equation, the protein phosphorylation time course is longer than before but can still proceed to completion (See Figure 4.7). On the other hand, if the kinase is not abundant in the system and tightly sequestered by the fully phosphorylated protein in a one to one molar ratio, the protein phosphorylation will not proceed to completion (See Figure 4.8). When the product inhibition is down through a sequestration mechanism, the final phosphorylation level of the protein is determined

by the total concentration of the kinase.

We therefore predict that if the multisite protein phosphorylation process in mammalian circadian clocks can not proceed to completion in the presence of limited amount of kinase, the fully phosphorylated protein is more likely to interact with the kinase by a sequestration mechanism similar to that in cyanobacteria.

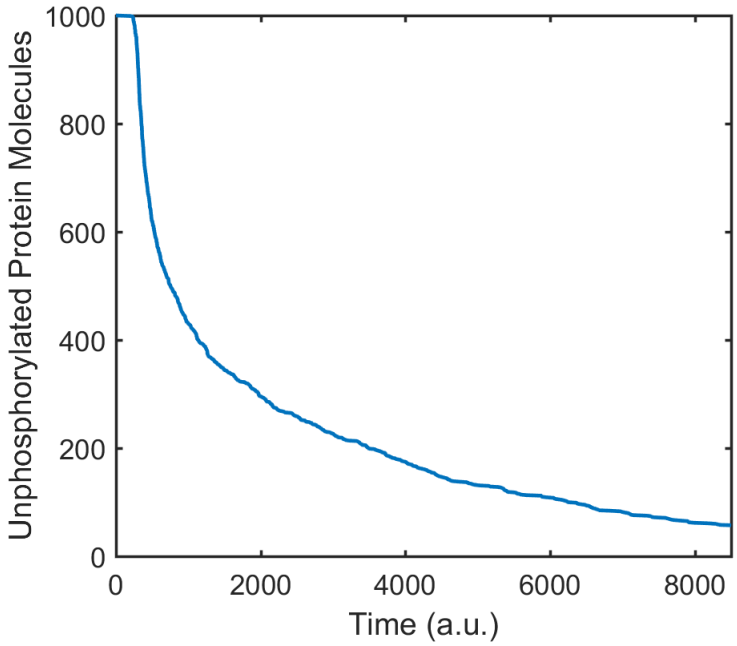

Figure 4.7: Protein phosphorylation with hill type inhibition between product and kinase.

We also find that the phosphatase activity gives rise to the initial plateau, and the length of which depends on the dephosphorylation rate (See Fig 4.10 and 4.9). The initial plateau as well as the entire phosphorylation timescale decreases when the phosphatase activity is weakened. When there is no phosphatase activity in the system, we predict that there will be no initial plateau in the protein phosphorylation process.

In Chapter III, we have established a mathematical model for the circadian clock in mammalian clock incorporating the new findings that CK1 δ/ϵ is the priming kinase. Here we investigate further the effect of product inhibition on the circadian

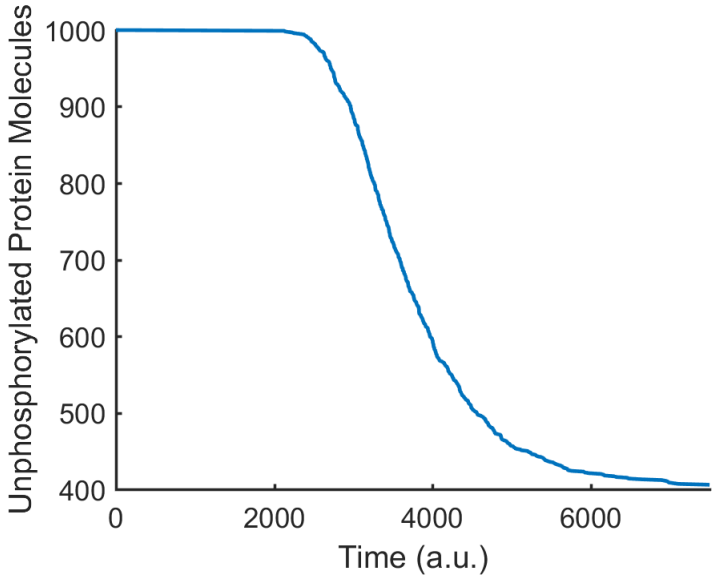

Figure 4.8: Protein phosphorylation with one to one molar binding inhibition between product and kinase.

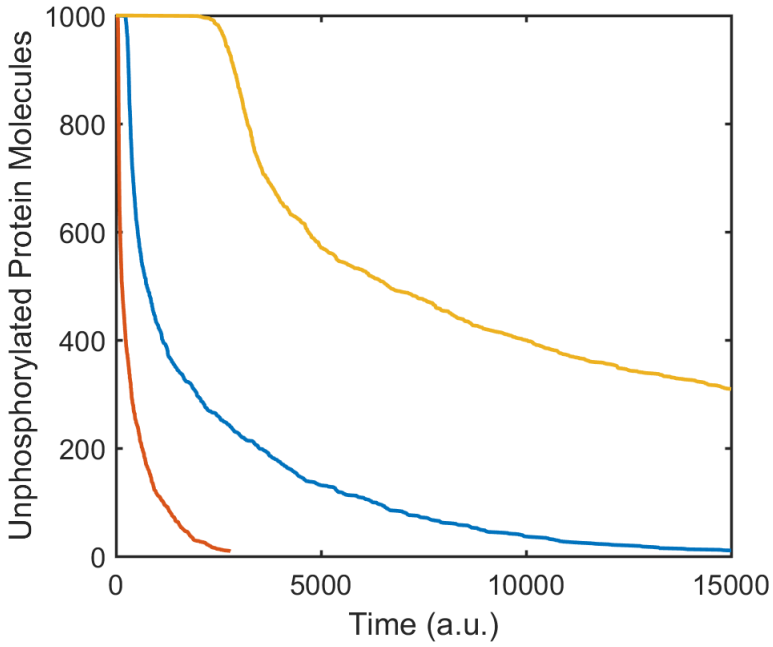

Figure 4.9: Protein phosphorylation with hill type inhibition between product and kinase. The length of initial plaeau decreases from around 2100 time units (Yellow) to 230 time units (Blue) and eventually 40 time units (Orange) as the phosphatase activity weakens.

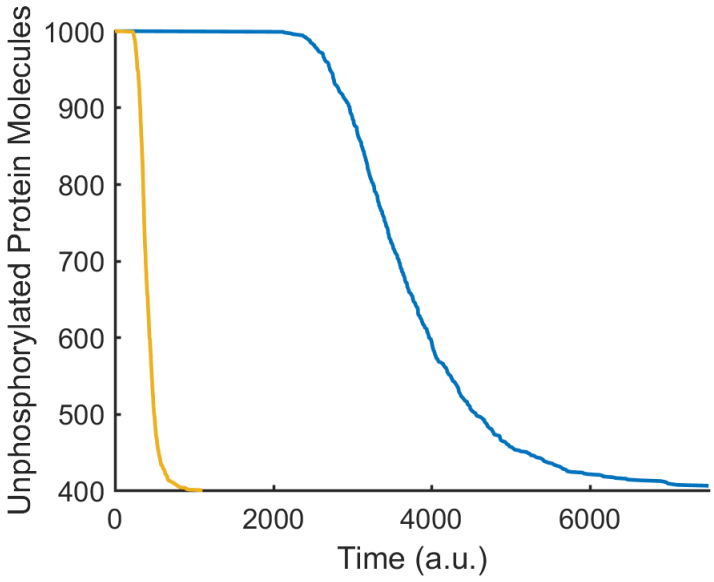

Figure 4.10: Protein phosphorylation with one to one molar binding inhibition between product and kinase. The initial plateau decreases from 2500 time units (Blue) to 250 time units (Yellow) as the phosphatase activity weakens.

rhythms with our published model in Narasimamurthy et al. (2018). In the mammalian clocks, PER2 proteins can be phosphorylated on both the β-TrCP and the FASP sites and CK1 is both the priming kinase and the downstream kinase. We modify the model for mammalian circadian clock by introducing tight binding between the kinases (CK1 δ/ϵ) and the fully phosphorylated PER2 proteins. In particular, the terms $kcf[c_4][CK_1]$ $(i = 1, 2)$ is changed to $k_{inhibition}[c_4][CK_i]$ where the value of $k_{inhibition}$ indicates the strength of product inhibition through tight binding. Detailed equations and a full description of parameters are available in the Supplement Information from Narasimamurthy et al. (2018).

In our simulations, we change the rate of $k_{inhibition}$ by various factors and simulate the model to obtain corresponding periods. We find that product inhibition may act as a rate limiting process and play a big role in controlling the period (See Figure 4.11). When we plot the length of period versus the inhibition rate, we find that the period increases along with the inhibition rate (See Figure 4.12).

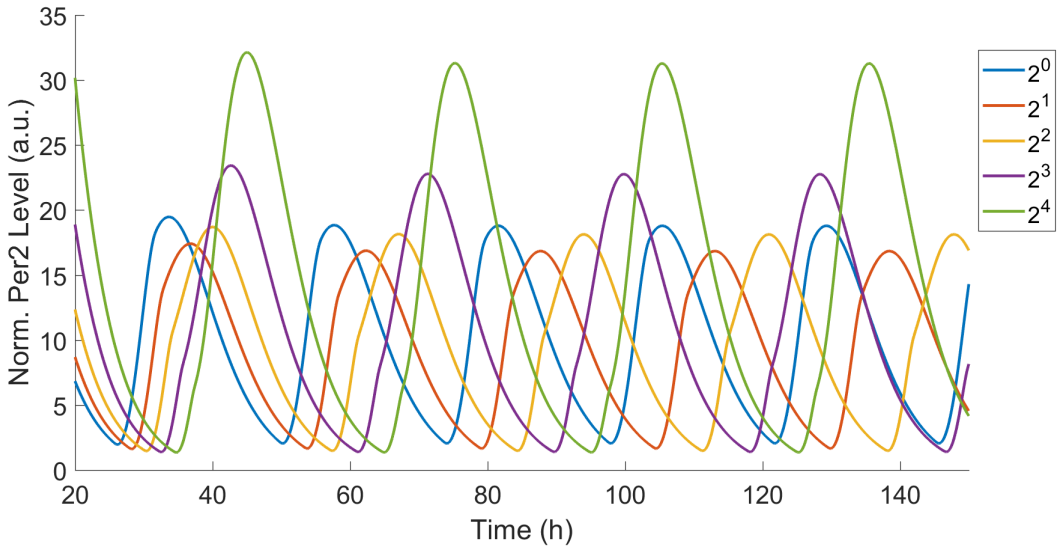

Figure 4.11: Time courses of the mammalian clock with various inhibition rate. The numbers in the legend represent the different fold changes increased from the original rate.

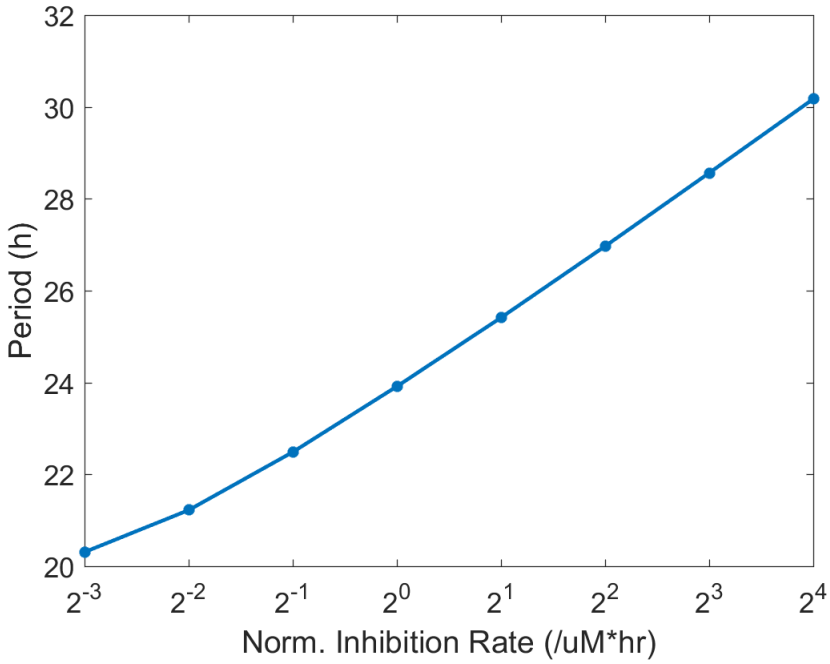

Figure 4.12: Period of oscillation increases from 20 hr to 30 hr as the product inhibition rate increases.

The results can be explained as follows: when the product inhibition rate increase, the kinase activity is weakened due to the sequestration. As a result, phophatase activities can push the equilibrium and lead to a longer phosphorylation (hence degradation) process of PER2. Since PER2 phosphorylation is a key regulator of the circadian clocks, the period also increases. In addition, the circadian rhythm can be lost when the inhibition activity is significantly decreased (See Figure 4.13). We therefore predict that this product inhibition mechanism is essential to the system.

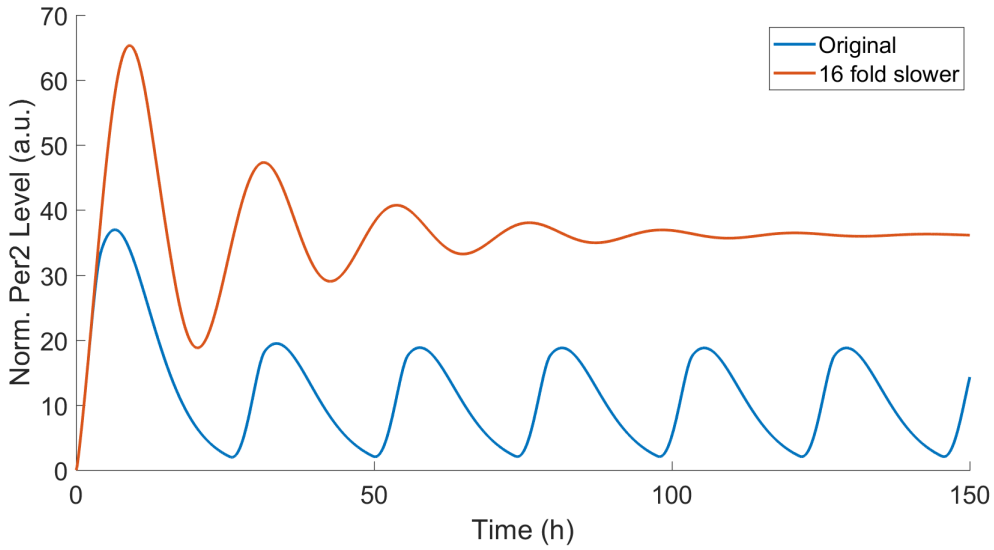

Figure 4.13: Lost of sustainable oscillation. Sustainable oscillations are lost (Orange) when the product inhibition rate is decreased by 16 fold compared to the original rate (Blue).

4.3.5 Discussion

The reason why our interval timer works is that phosphorylations are progressive but also allow for rapid phosphate group shuffling. To see this clearer, let us assume that the amount of time needed for the protein to go through all microstates is fixed. Simulations in the supplemental information under this new assumption does not affect the behavior of the resulting time course. It may seem strange to assume an

interval timer in creating an interval timer but this assumption is not necessary to build the interval timer and only used here to simplify our argument explaining the result, and the interval timer we assume has a much shorter period with respect to the main interval timer. A fixed time interval could occur due to the law of large numbers when multiple conformational changing events occur sequentially. During the time needed for the protein to proceed through all microstates, it can shuttle back to the unphosphorylated state for a Poisson number of times. The total number of visits approaches a fixed number (at least its fano factor approaches zero) as the number of dephosphorylation events increases. Although the time of each shuttling is random, the average overall is small. Thus the total time for the protein to progress from one state to the next approaches a fixed interval.

This model generates many hypotheses that can be tested. Are phosphate groups being shuttled on and off PER? Does each subsequent phosphorylation occur immediately, or do they require conformational changes to the protein? Does the sequential phosphorylation of PER take fixed amounts of time, or is it variable? Can these processes occur in individual molecules, or do they need collective behavior?

4.4 Supplement Information

We consider a single protein that goes through several phosphorylation steps before it finally gets degraded. Inspired by the Gillespie algorithm, we can model the kinetics with Markov Chain models, where each reaction corresponds to a step in the Markov Chain and we want to investigate how the number of phosphorylation sites affect the expected time to degradation under various model assumptions. This expected time can be considered as proportional to the number of steps it takes for a single molecule to proceed from initially unphosphorylated state to the degradation state.

4.4.1 FASP phosphoswitch dependent degradation

The first general model we consider in Fig.4.14 resembles the FASP phosphorylation of PER2 protein. In the diagram we denote by P_0 the unphosphorylated state, P_i the i-th phosphorylated state and $\emptyset$ the degradation state. Moreover, the forward transition rates are identical except the first step ($P_0 \to P_1$ is the only way to get away from P_0), similar with the backward transition rates, while the identity $p+q=1$ holds true.

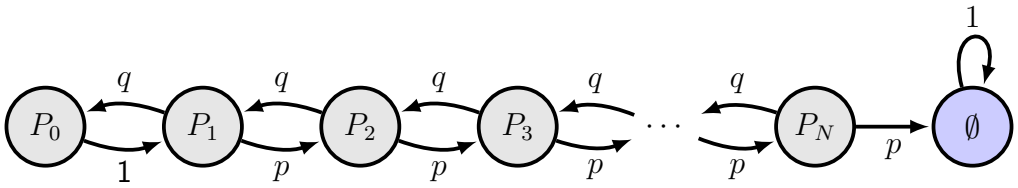

Figure 4.14: A multi-site phosphorylation model with N FASP sites

Now we rewrite the notations as follows: denote by X_n the state of the protein at time n and label the different phosphorylation states as follows:

$$X_0 \underset{q}{\overset{1}{\rightleftarrows}} X_1 \underset{q}{\overset{p}{\rightleftarrows}} X_2 \underset{q}{\overset{p}{\rightleftarrows}} \cdots \underset{q}{\overset{p}{\rightleftarrows}} X_N \overset{p}{\to} X_{N+1}$$

We want to find the expected exit time from state P_0 (labeled as 0) to the absorbing state $\emptyset$ (labeled as $N+1$) where the exit time to state y is defined as:

$$V_y = \min\{n \geq 0 : X_n = y\}$$

Here we apply the standard trick in Markov Chain and consider the following function $g(x)$ which represents the expected exit time from state $x \in \{0, 1, 2, \cdots, N, N+1\}$ to the degradation state $N+1$.

$$g(x) = \mathbb{E}_x(V_{N+1}) = \mathbb{E}(V_{N+1}|X_0 = x)$$

Conditioning on the first jump for the Markov Chain, we can derive the system of linear equations as well as the boundary conditions as follows:

$$g(0) = 1 + g(1) \tag{4.1}$$

$$g(x) = 1 + q\, g(x-1) + p\, g(x+1) \quad x = 1, 2, \cdots, N \tag{4.2}$$

$$g(N+1) = 0 \tag{4.3}$$

To solve the system, we consider two cases:

1. $p = q = \frac{1}{2}$. This is the case where the phosphorylation rate is balanced with the phosphatase rate.

   We can rewrite the equation (4.2) and find a general expression for $g(x)$:

$$\begin{aligned} g(x+1) - g(x) &= g(x) - g(x-1) - 2 \quad x = 1, 2, \cdots, N \\ &= -2x + g(1) - g(0) \\ &= -2x - 1 \\ g(x) &= g(0) + \sum_{k=0}^{x-1} (g(k+1) - g(k)) \quad x = 1, 2, \cdots, N+1 \\ &= g(0) + \sum_{k=0}^{x-1} -2k - 1 \\ &= g(0) - (x-1)x - x \\ &= -x^2 + g(0) \end{aligned}$$

   Recall again that $g(N+1) == -(N+1)^2 + g(0) = 0$ since the exit time to degradation is 0 if the protein is already degraded.

   We therefore conclude that when the forward and backward rates are balanced, the expected time to degradation grows quadratically with respect to the total

number of phosphorylation sites.

$$g(0) = (N+1)^2 \sim O(N^2)$$

2. $p \neq q \neq \frac{1}{2}$ and $p + q = 1$. This is a more general case where the forward and backward rate is not the same.

   Similar analysis leads to the following result:

$$\begin{aligned}
(p+q)g(x) &= 1 + q\ g(x-1) + p\ g(x+1) \\
g(x+1) - g(x) &= \frac{q}{p}(g(x) - g(x-1)) - \frac{1}{p} \\
&= (\frac{q}{p})^2(g(x-1) - g(x-2)) - \frac{1}{p}(1 + \frac{q}{p}) \\
&= (\frac{q}{p})^x\,(g(1) - g(0)) - \frac{1}{p}\left(1 + \frac{q}{p} + (\frac{q}{p})^2 + \cdots + (\frac{q}{p})^{x-1}\right) \\
&= (\frac{q}{p})^x\,(g(1) - g(0)) - \frac{1}{p}\frac{1 - (\frac{q}{p})^x}{1 - \frac{q}{p}} \\
&= -(\frac{q}{p})^x - \frac{1 - (\frac{q}{p})^x}{p - q}
\end{aligned}$$

We can now compute the $g(x)$:

$$\begin{aligned}
g(x) &= g(0) + \sum_{k=0}^{x-1}(g(k+1) - g(k)) \\
&= g(0) + \sum_{k=0}^{x-1}\left(-(\frac{q}{p})^k - \frac{1-(\frac{q}{p})^k}{p-q}\right) \\
&= g(0) - \frac{x}{p-q} - (1 - \frac{1}{p-q})\sum_{k=0}^{x-1}(\frac{q}{p})^k \\
&= g(0) - \frac{x}{p-q} - (1 - \frac{1}{p-q})\frac{1-\left(\frac{q}{p}\right)^x}{1-\frac{q}{p}} \\
&= g(0) - \frac{x}{p-q} + \frac{2q}{p-q}\frac{1-\left(\frac{q}{p}\right)^x}{1-\frac{q}{p}} \\
&= g(0) - \frac{x}{p-q} + 2\frac{q}{p}\frac{1-\left(\frac{q}{p}\right)^x}{(1-\frac{q}{p})^2}
\end{aligned}$$

Recall again $g(N+1) = 0$, we conclude that:

$$g(0) = \frac{N+1}{p-q} - 2\frac{q}{p}\frac{1-\left(\frac{q}{p}\right)^{N+1}}{(1-\frac{q}{p})^2}$$

The expected time to degradation from state 0 consists of a linear term and an exponential term. The overall growth pattern of the function as the number of phosphorylation sites increases

- $p > q$, let $p = \frac{k}{1+k}$, $q = \frac{1}{k+1}$, then we have $\frac{p}{q} = k > 1$. Analysis reveals

that $g(0)$ grows like a linear function since the second term is bounded:

$$\begin{aligned} g(0) &= \frac{N+1}{p-q} - 2\frac{q}{p}\frac{1-\left(\frac{q}{p}\right)^{N+1}}{(1-\frac{q}{p})^2} \\ &= \frac{k+1}{k-1}(N+1) - \frac{2}{k}\frac{1-\left(\frac{1}{k}\right)^{N+1}}{(1-\frac{1}{k})^2} \\ &= \frac{k+1}{k-1}(N+1) - \frac{2k}{(k-1)^2} + \frac{2}{(k-1)^2}\left(\frac{1}{k}\right)^N \\ &\sim O(N) \end{aligned}$$

For any given number of phosphorylation sites $N \geq 1$, we have

$$\frac{k+1}{k-1}(N+1) - \frac{2k}{(k-1)^2} \leq g(x) \leq \frac{k+1}{k-1}(N+1)$$

- $q > p$, let $q = \frac{k}{1+k}$, $p = \frac{1}{k+1}$, then we have $\frac{q}{p} = k > 1$. Analysis reveals that $g(0)$ grows like an exponential function:

$$\begin{aligned} g(0) &= \frac{N+1}{p-q} - 2\frac{q}{p}\frac{1-\left(\frac{q}{p}\right)^{N+1}}{(1-\frac{q}{p})^2} \\ &= -\frac{k+1}{k-1}(N+1) - 2k\frac{1-k^{N+1}}{(1-k)^2} \\ &= -\frac{k+1}{k-1}(N+1) + \frac{2k}{(k-1)^2}\left(k^{N+1}-1\right) \\ &= \frac{2k^2}{(k-1)^2}k^N - \frac{k+1}{k-1}(N+1) - \frac{2k}{(k-1)^2} \\ &\sim O(k^N) \end{aligned}$$

4.4.2 β-TrCP and FASP phosphorylation dependent degradation

The second model we consider here incorporates the phosphoswitch mechanism where the unphosphorylated protein P_0 can either phosphorylate on the β-TrCP site which

effectively decay rapidly, or phosphorylate on the FASP site going through similar process as in the last section, where we denote by $\emptyset_\beta$ the degradation through β-TrCP and all other states the same way as above.

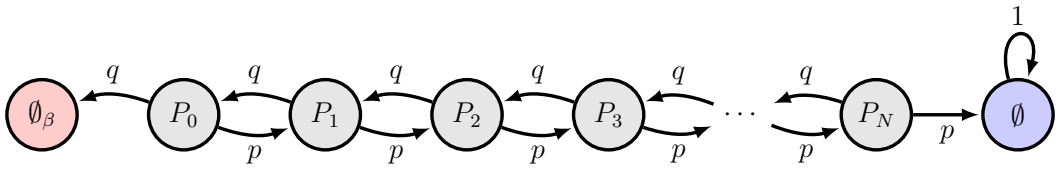

Figure 4.15: A multi-site phosphorylation model with N FASP sites and one β-TrCP site

Now we denote by X_n the state of the protein at time n and label the different phosphorylation states similarly, except that now -1 represents the degradation through β-TrCP phosphorylation:

$$X_\beta \overset{q}{\leftarrow} X_0 \underset{q}{\overset{p}{\rightleftarrows}} X_1 \underset{q}{\overset{p}{\rightleftarrows}} X_2 \underset{q}{\overset{p}{\rightleftarrows}} \cdots \underset{q}{\overset{p}{\rightleftarrows}} X_N \overset{p}{\rightarrow} X_{N+1}$$

The expected exit time to a set of states is defined as:

$$V_A = \min\{n \geq 0 : X_n \in A\}$$

Consider again the following function $g(x)$ which represents the expected exist time from state $x \in \{1, 2, \cdots, N\}$ to the set of degradation states $A = \{-1, N+1\}$.

$$g(x) = \mathbb{E}_x(V_A) = \mathbb{E}(V_A | X_0 = x)$$

The system of linear equations with boundary conditions can be written similarly as the case of a gambler's ruin problem:

$$g(-1) = 0 \tag{4.4}$$

$$g(x) = 1 + q\ g(x-1) + p\ g(x+1) \quad x = 0, 1, 2, \cdots, N \tag{4.5}$$

$$g(N+1) = 0 \tag{4.6}$$

1. When $p = q = \frac{1}{2}$ we have:

$$\begin{aligned} g(x+1) - g(x) &= g(x) - g(x-1) - 2 \quad x = 0, 1, 2, \cdots, N \\ &= -2(x+1) + g(0) - g(-1) \\ &= -2(x+1) + g(0) \\ g(x) &= g(-1) + \sum_{k=-1}^{x-1} (g(k+1) - g(k)) \quad x = 1, 2, \cdots, N+1 \\ &= \sum_{k=-1}^{x-1} (-2(k+1) + g(0)) \\ &= -(x+1)x + g(0)(x+1) \end{aligned}$$

Recall again that $g(N+1) = 0$ we have $g(0) = N+1$ and $g(x) = (x+1)(N+1-x)$. It is clear that $g(x)$ grows linearly in the number of phosphorylation sites N.

2. When $p \neq q$ $p+q=1$, we carry out similar analysis to find $g(x)$

$$
\begin{aligned}
g(x) &= 1 + q\, g(x-1) + p\, g(x+1) \quad x = 0, 1, 2, \cdots, N \\
g(x+1) - g(x) &= \frac{q}{p}(g(x) - g(x-1)) - \frac{1}{p} \\
&= (\frac{q}{p})^2 (g(x-1) - g(x-2)) - \frac{1}{p}(1 + \frac{q}{p}) \\
&= (\frac{q}{p})^{x+1} (g(0) - g(-1)) - \frac{1}{p}\left(1 + \frac{q}{p} + (\frac{q}{p})^2 + \cdots + (\frac{q}{p})^x\right) \\
&= g(0)(\frac{q}{p})^{x+1} - \frac{1}{p}\frac{1 - (\frac{q}{p})^{x+1}}{1 - \frac{q}{p}} \\
&= g(0)(\frac{q}{p})^{x+1} - \frac{1}{p-q} + \frac{(\frac{q}{p})^{x+1}}{p-q}
\end{aligned}
$$

We can now compute the $g(x)$:

$$
\begin{aligned}
g(x) &= g(-1) + \sum_{k=-1}^{x-1} (g(k+1) - g(k)) \\
&= \sum_{k=-1}^{x-1} \left(g(0)(\frac{q}{p})^{k+1} - \frac{1}{p-q} + \frac{(\frac{q}{p})^{k+1}}{p-q} \right) \\
&= -\frac{x+1}{p-q} + (g(0) + \frac{1}{p-q}) \sum_{k=-1}^{x-1} (\frac{q}{p})^{k+1} \\
&= -\frac{x+1}{p-q} + (g(0) + \frac{1}{p-q}) \frac{1 - (\frac{q}{p})^{x+1}}{1 - \frac{q}{p}}
\end{aligned}
$$

Recall again $g(N+1) = 0$, we conclude that:

$$
g(0) = \frac{N+2}{p-q} \frac{1 - \frac{q}{p}}{1 - (\frac{q}{p})^{N+2}} - \frac{1}{p-q}
$$

and generally

$$
g(x) = -\frac{x+1}{p-q} + \frac{N+2}{p-q} \frac{1 - (\frac{q}{p})^{x+1}}{1 - (\frac{q}{p})^{N+2}}
$$

Now we can analyze the growth pattern of $g(0)$ as we increase the number of phosphorylation states N.

- $p > q$, let $p = \frac{k}{1+k}$, $q = \frac{1}{k+1}$, then we have $\frac{p}{q} = k > 1$. Analysis shows that $g(0)$ grows like a linear function:

$$\begin{aligned} g(0) &= \frac{N+2}{p-q}\frac{1-\frac{q}{p}}{1-(\frac{q}{p})^{N+2}} - \frac{1}{p-q} \\ &= (N+2)\frac{k+1}{k-1}\frac{1-\frac{1}{k}}{1-(\frac{1}{k})^{N+2}} - \frac{k+1}{k-1} \\ &= (N+2)\frac{k+1}{k}\frac{1}{1-(\frac{1}{k})^{N+2}} - \frac{k+1}{k-1} \\ &\sim O(N) \end{aligned}$$

- $q > p$, let $q = \frac{k}{1+k}$, $p = \frac{1}{k+1}$, then we have $\frac{q}{p} = k > 1$. Analysis shows that $g(0)$ is approximately a constant value when the number of phosphorylation increases:

$$\begin{aligned} g(0) &= \frac{N+2}{p-q}\frac{1-\frac{q}{p}}{1-(\frac{q}{p})^{N+2}} - \frac{1}{p-q} \\ &= (N+2)\frac{k+1}{1-k}\frac{1-k}{1-k^{N+2}} - \frac{k+1}{1-k} \\ &= \frac{k+1}{k-1} - (k+1)\frac{N+2}{k^{N+2}-1} \\ &\sim O(1) \end{aligned}$$

Here is a list to summarize the two different sequential models and the different cases therein we have investigated. We can conclude that the number of phosphorylation sites can have a significant effect on the expected time to degradation.

1. When the protein only degrades through FASP phosphorylation and the phosphatase activity is **balanced** with the phosphorylation activity, we find that the expected time to degradation grows **quadratically** in the number of sites.

2. When the protein only degrades through FASP phosphorylation and the phosphatase rate is **slower** than the phosphorylation rate, the expected time to

degradation grows **linearly** in the number of sites.

3. When the protein only degrades through FASP phosphorylation and the phosphatase rate is **faster** than the phosphorylation rate,the expected time to degradation grows **exponentially** in the number of sites.

4. When the phosphoswitch mechanism is present in the system and the phosphatase activity is **balanced** with the phosphorylation activity,the expected time to degradation grows **linearly** in the number of sites.

5. When the phosphoswitch mechanism is present in the system and the phosphatase activity is **slower** than the phosphorylation activity,the expected time to degradation grows **linearly** in the number of sites.

6. When the phosphoswitch mechanism is present in the system and the phosphatase activity is **faster** than the phosphorylation activity,the expected time to degradation almost remains **constant**.

A summary is also presented in the following table:

Growth Rate	$p = q = \frac{1}{2}$	$p > q$	$p < q$
FASP only	Quadratic	Linear	Exponential
β-TrCP and FASP	Linear	Linear	Constant

Table 4.1: Growth rate of the degradation time in various cases

4.4.3 Conformational change increases time to degradation

We have established so far the expected time to degradation under various assumptions. Here we investigate further the case where forward rate is dominated by the backward rate ($p < q$) by extending the sequential multi-site phosphorylation model into a network model including intermediate conformational changes.

Instead of going through several downstream phosphorylation before degradation, the protein (in any phosphorylation state) can go through several intermediate conformational changes. In all of our models, the subscript represents phosphorylation state while the superscript represents the conformational state, e.g., P_2^1 means the protein is phosphorylated on the first 2 sites and changed its conformation from state 0 into state 1.

Recall that the expected time to degradation when $p = q = \frac{1}{2}$ grows quadratically $T = (N+1)^2 \sim O(N^2)$, while it grows exponentially $T \sim O(k^N)$ if $p < q,\ k = \frac{q}{p}$. We are interested in whether this new feature in the model serves as an extra delay element for the phosphorylation process

We start first with an extended model with three phosphorylation sites and one extra conformational change (Fig. 4.16) and find that the expected time for such a model is equivalent to one with three phosphorylation states. We also discovered that this result remain valid under different rate combinations. The key is to consider multiple states in the network as one entire state and the network model becomes equivalent to a sequential one. Similarly in Fig. 4.17, a network model with two phosphoryaltion sites and two additional micro states is equivalent to a sequential model with 4 phosphorylation sites.

Generally any network model with n phosphorylation sites and m conformational states can be shown equivalent to a sequential model with $m + n$ phosphorylation sites (Fig. 4.18)

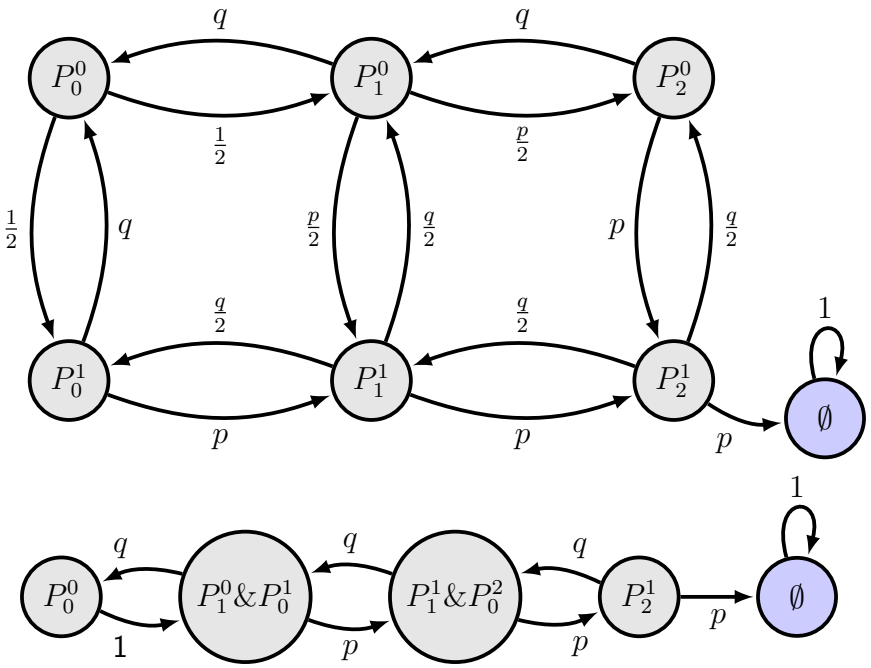

Figure 4.16: An example model for multi-site phosphorylation with two conformational states and two sites (top) and the equivalent model with 3 phosphorylation sites (bottom).

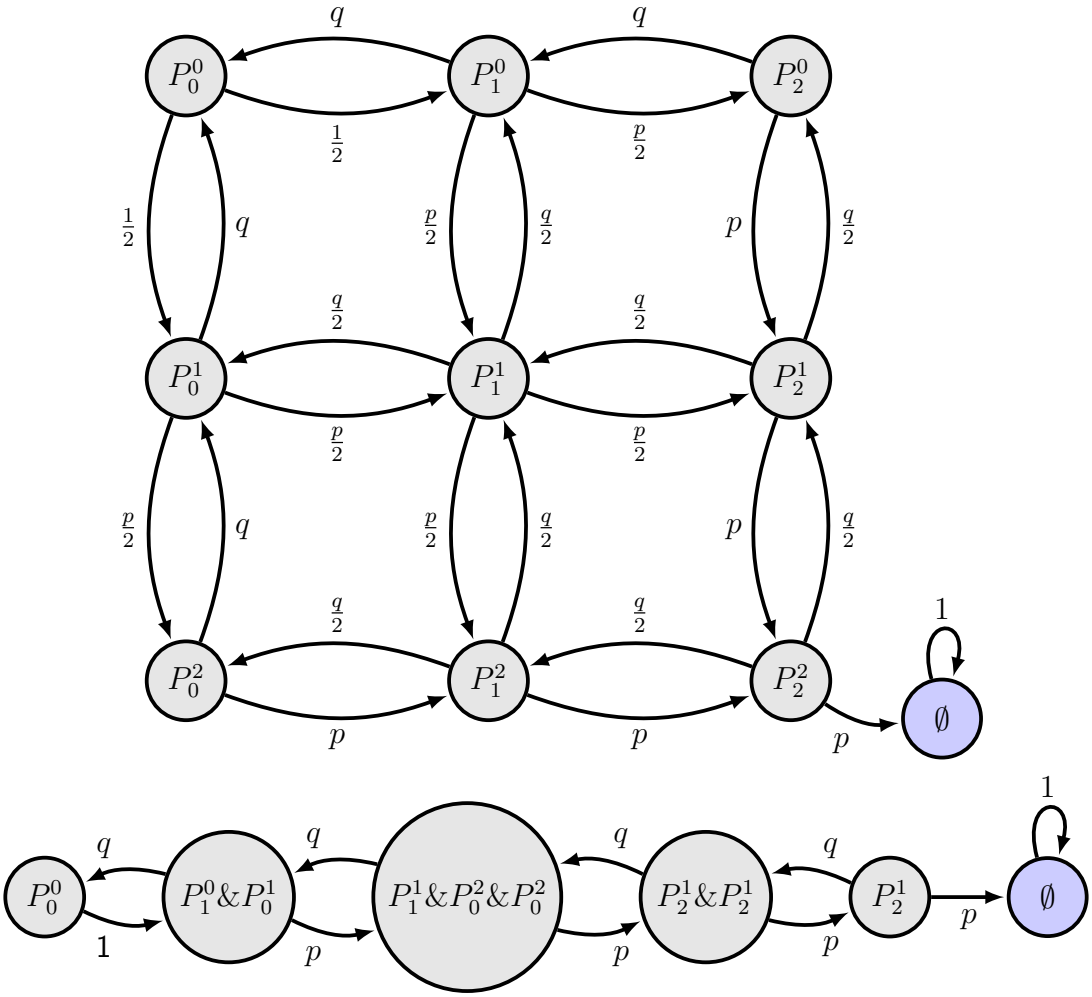

Figure 4.17: An example model for multi-site phosphorylation with three conformational states and two sites(top) and the equivalent sequential model with 4 phosphorylation sites (bottom).

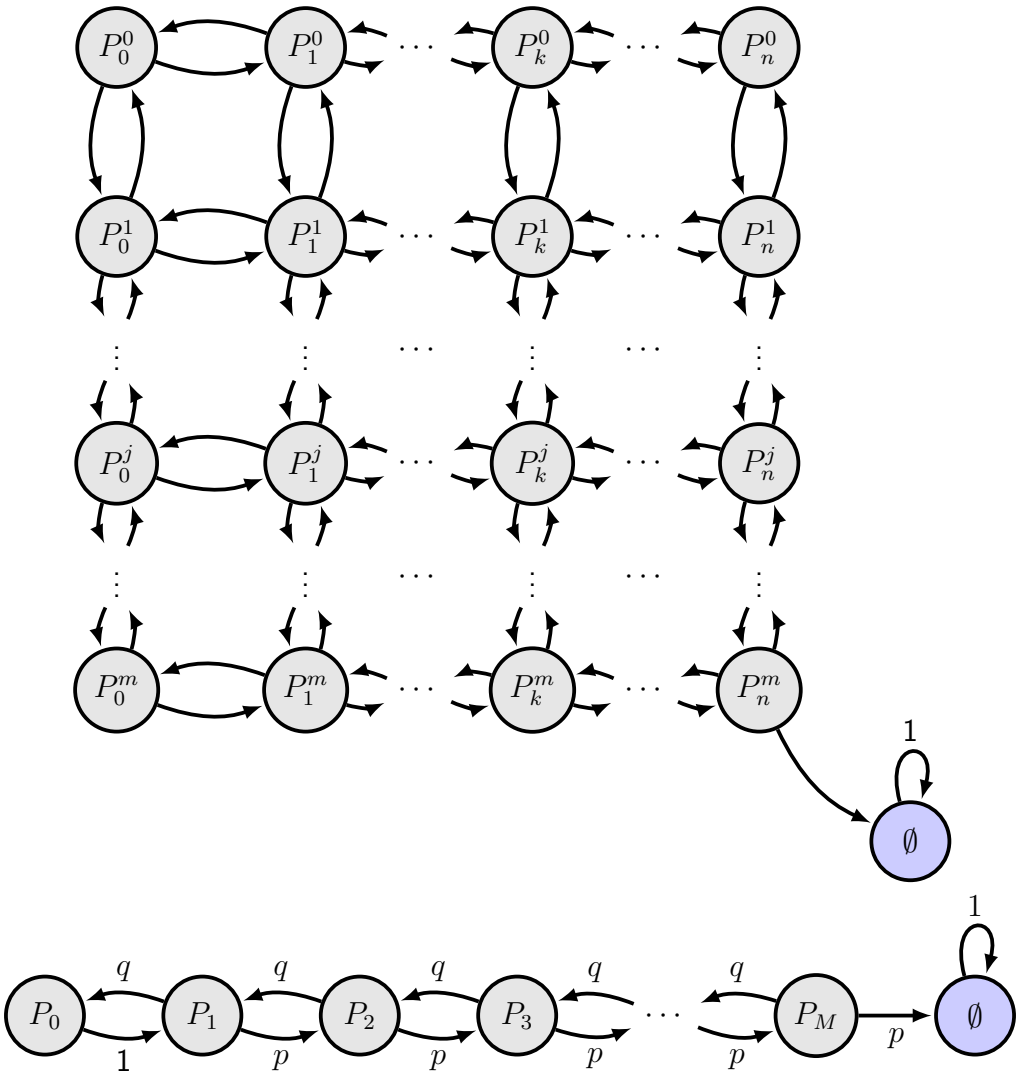

Figure 4.18: General Model with n phosphorylation sites and m conformational states. (a) An example model for multi-site phosphorylation with n phosphorylation sites and m conformational states. (b) Equivalent model with $M = m + n$ sites.

CHAPTER V

Conclusion

Circadian clocks are self-sustained biological clocks that are present in almost all organisms. This dissertation focuses on mathematical modeling of protein phosphorylation because of its central role in many circadian clocks including *Drosophila*, *Neurosphora*, mammals and even cyanobacteria. Our research goal is to investigate the connection and distinction among the various types of circadian clocks from this small yet crucial part of the biological processes.

In chapter II, we focus on the cyanobacterial clock and its connection with the mammalian clocks. Our mathematical modeling and simulation suggest that the protein sequestration mechanism is shared between cyanobacteria and mammals. Even though prokaryotes and eukaryotes are phylogenetically unrelated and different in many ways, similar dynamical principles regulating molecular timekeeping may have emerged through convergent evolution. We also predict that the transcriptional and translational feedback loop serves as a homeostatic regulator that helps maintain the balance between KaiC and KaiA proteins, thus stabilizing the post-translational oscillator. This work also raises questions about what common evolutionary pressures could yield such similar mechanisms with such dissimilar components.

In chapter III, we investigate the multi-site phosphorylation of PER2 in the mammalian circadian clocks. Our collaborators have discovered that CK1 is indeed the mammalian priming kinase responsible for phosphorylation of S659 in mPER2. A ro-

bust yet fragile design is proposed as we incorporate the experimental results. With the priming kinase being CK1 itself, our design allows the period of the circadian clock to be robust to environmental signals while being sensitive to regulatory changes in the CK1 carboxyl terminus. While a separate Nemo-like kinase has been recently identified by Chiu et al. (2011) as a priming kinase for *Drosophila* PER, our work suggests that the mPER2 phosphorylation is regulated through a completely divergent mechanism where the CK1 extreme carboxyl terminus acts as a key regulator.

In chapter IV, we study a general model of the protein sequential phosphorylation process. Sequential phosphorylation facilitated by different kinases/phosphatases can be found in *Drosophila*, *Neurosphora*, mammals, plants and even cyanobacteria. Our mathematical model proposes that the kinases and phosphatases can work together to rapidly shuttle the phosphate groups on and off the proteins. In this way, we can obtain protein degradation on timescales much longer than individual phosphorylation events. When conformational changes are incorporated into our model, we can even build an interval timer from the protein phosphorylation process. In addition, our analysis and simulations suggest that product inhibition on kinase through sequestration mechanism may act as a rate limiting step and play a significant role in controlling the period.

A direct extension of our work in chapter II would be to conduct experiments on the effect of various perturbations to the molar ratio balance among KaiABC proteins *in vivo*. Having established the connection between the cyanobacterial and mammalian circadian clocks, our future work would be to perform detailed analysis of circadian clock systems in *Drosophila*, *Neurospora* and plants. We would like to see whether similar dynamical design principles can be found among these circadian clocks despite the huge difference in their biological structure. As for future work extended from chapter III, the role of the CK1 carboxyl terminus proposed by our model can be further tested in experiments, e.g., structural analysis of the CK1 protein, *in*

vitro analysis of CK1 tail mutants and synthesized PER peptides. Finally, it will be interesting to investigate applications of our mathematical modeling from chapter IV that extend beyond the mammalian circadian clocks. To verify whether the phosphate groups are indeed shuttled on and off the PER2 proteins by integrated actions of kinases and phosphatases, one possible experiment is to measure the distribution of of PER2 proteins in different phosphorylation states by using antibody specifically to the 4th and 5th FASP phosphorylation sites. Another interesting experiment would be to introduce phosphatase inhibitors into the system and test whether the length of the plateau would decrease as our model predicts.

Bibliography

L. J. Ashmore and A. Sehgal. A fly's eye view of circadian entrainment. *Journal of biological rhythms*, 18(3):206–216, 2003.

L. Badura, T. Swanson, W. Adamowicz, J. Adams, J. Cianfrogna, K. Fisher, J. Holland, R. Kleiman, F. Nelson, L. Reynolds, et al. An inhibitor of casein kinase i induces phase delays in circadian rhythms under free-running and entrained conditions. *Journal of Pharmacology and Experimental Therapeutics*, 322(2):730–738, 2007.

C. L. Baker, A. N. Kettenbach, J. J. Loros, S. A. Gerber, and J. C. Dunlap. Quantitative proteomics reveals a dynamic interactome and phase-specific phosphorylation in the neurospora circadian clock. *Molecular cell*, 34(3):354–363, 2009.

J. Bass and J. S. Takahashi. Circadian integration of metabolism and energetics. *Science*, 330(6009):1349–1354, 2010.

D. Bell-Pedersen, V. M. Cassone, D. J. Earnest, S. S. Golden, P. E. Hardin, T. L. Thomas, and M. J. Zoran. Circadian rhythms from multiple oscillators: lessons from diverse organisms. *Nature Reviews Genetics*, 6(7):544, 2005.

P. Brazhnik and J. J. Tyson. Cell cycle control in bacteria and yeast: a case of convergent evolution? *Cell Cycle*, 5(5):522–529, 2006.

Y. Chang, S. Cohen, C. Phong, W. Myers, Y. Kim, J. Tseng, R.and Tseng, L. Zhang, J. Boyd, Y. Lee, S. Kang, S. Li, R. Britt, M. Rust, and W. Golden, S.S.and Li. A protein fold switch joins the circadian oscillator to clock output in cyanobacteria. *Science*, 349(6245):324–328, 2015. ISSN 0036-8075.

J. C. Chiu, H. W. Ko, and I. Edery. Nemo/nlk phosphorylates period to initiate a time-delay phosphorylation circuit that sets circadian clock speed. *Cell*, 145(3):357–370, 2011.

S. Clodong, U. Duhring, L. Kronk, A. Wilde, I. Axmann, H. Herzel, and M. Kollmann. Functioning and robustness of bacterial circadian clock. *Mol. Syst. Biol.*, 3:938–950, 2007.

X. Daniel, S. Sugano, and E. M. Tobin. Ck2 phosphorylation of cca1 is necessary for its circadian oscillator function in arabidopsis. *Proceedings of the National Academy of Sciences*, 101(9):3292–3297, 2004.

P. J. DeCoursey and J. R. Krulas. Behavior of scn-lesioned chipmunks in natural habitat: a pilot study. *Journal of biological rhythms*, 13(3):229–244, 1998.

J. C. Dunlap. Molecular bases for circadian clocks. *Cell*, 96(2):271–290, 1999.

J. C. Dunlap. Proteins in the neurospora circadian clockworks. *Journal of Biological Chemistry*, 281(39):28489–28493, 2006.

I. Edery, L. J. Zwiebel, M. E. Dembinska, and M. Rosbash. Temporal phosphorylation of the drosophila period protein. *Proceedings of the National Academy of Sciences*, 91 (6):2260–2264, 1994.

E. J. Eide, H. Kang, S. Crapo, M. Gallego, and D. M. Virshup. Casein kinase i in the mammalian circadian clock. In *Methods in enzymology*, volume 393, pages 408–418. Elsevier, 2005.

E. Emberly and N. Wingreen. Hourglass model for a protein-based circadian oscillator. *Phys. Rev. Lett.*, 96(3):038303, 2006.

J.-P. Etchegaray, A. Y. Elizabeth, P. Indic, R. Dallmann, and D. R. Weaver. Casein kinase 1 delta (ck1δ) regulates period length of the mouse suprachiasmatic circadian clock in vitro. *PLoS One*, 5(4):e10303, 2010.

H. Flotow, P. R. Graves, A. Wang, C. J. Fiol, R. W. Roeske, and P. J. Roach. Phosphate groups as substrate determinants for casein kinase i action. *Journal of Biological Chemistry*, 265(24):14264–14269, 1990.

D. Forger, D. Gonze, D. Virshup, and D. K. Welsh. Beyond intuitive modeling: combining biophysical models with innovative experiments to move the circadian clock field forward. *Journal of biological rhythms*, 22(3):200–210, 2007.

D. B. Forger. Signal processing in cellular clocks. *Proceedings of the National Academy of Sciences*, 108(11):4281–4285, 2011.

S. Fowler, K. Lee, H. Onouchi, A. Samach, K. Richardson, B. Morris, G. Coupland, and J. Putterill. Gigantea: a circadian clock-controlled gene that regulates photoperiodic flowering in arabidopsis and encodes a protein with several possible membrane-spanning domains. *The EMBO journal*, 18(17):4679–4688, 1999.

S. Fujiwara, L. Wang, L. Han, S.-S. Suh, P. A. Salomé, C. R. McClung, and D. E. Somers. Post-translational regulation of the arabidopsis circadian clock through selective proteolysis and phosphorylation of pseudo-response regulator proteins. *Journal of Biological Chemistry*, 283(34):23073–23083, 2008.

J.-M. Fustin, R. Kojima, K. Itoh, H.-Y. Chang, Y. Shiqi, B. Zhuang, A. Oji, S. Gibo, R. Narasimamurthy, D. Virshup, et al. Two ck1δ transcripts regulated by m6a methylation code for two antagonistic kinases in the control of the circadian clock. *Proceedings of the National Academy of Sciences*, 115(23):5980–5985, 2018.

M. Gallego and D. M. Virshup. Post-translational modifications regulate the ticking of the circadian clock. *Nature Reviews Molecular Cell Biology*, 8(2):139, 2007.

D. S. Garbe, Y. Fang, X. Zheng, M. Sowcik, R. Anjum, S. P. Gygi, and A. Sehgal. Cooperative interaction between phosphorylation sites on period maintains circadian period in drosophila. *PLoS genetics*, 9(9):e1003749, 2013.

N. Y. Garceau, Y. Liu, J. J. Loros, and J. C. Dunlap. Alternative initiation of translation and time-specific phosphorylation yield multiple forms of the essential clock protein frequency. *Cell*, 89(3):469–476, 1997.

N. R. Glossop, L. C. Lyons, and P. E. Hardin. Interlocked feedback loops within the drosophila circadian oscillator. *Science*, 286(5440):766–768, 1999.

D. Gonze. Modeling circadian clocks: from equations to oscillations. *Central European Journal of Biology*, 6(5):699, 2011.

A. Gutu and E. K. OShea. Two antagonistic clock-regulated histidine kinases time the activation of circadian gene expression. *Molecular cell*, 50(2):288–294, 2013.

P. E. Hardin, J. C. Hall, and M. Rosbash. Feedback of the drosophila period gene product on circadian cycling of its messenger rna levels. *Nature*, 343(6258):536, 1990.

E. Harms, S. Kivimäe, M. W. Young, and L. Saez. Posttranscriptional and posttranslational regulation of clock genes. *Journal of Biological Rhythms*, 19(5):361–373, 2004.

J. Hastings and .-. . Sweeney, B.M. 43(9). On the mechanism of temperature independence in a biological clock. *Proc. Natl. Acad. Sci*, 43(9):804–811, 1957.

F. Hayashi, N. Itoh, T. Uzumaki, R. Iwase, Y. Tsuchiya, H. Yamakawa, M. Morishita, K. Onai, S. Itoh, and M. Ishiura. Roles of two ATPase-motif-containing domains in cyanobacterial circadian clock protein KaiC. *J. Biol. Chem.*, 279(50):52331–52337, 2004.

C. Heintzen and Y. Liu. The neurospora crassa circadian clock. *Advances in genetics*, 58: 25–66, 2007.

M. Ishiura, S. Kutsuna, S. Aoki, H. Iwasaki, C. R. Andersson, A. Tanabe, S. S. Golden, C. H. Johnson, and T. Kondo. Expression of a gene cluster KaiABC as a circadian feedback process in cyanobacteria. *Science*, 281:1519–1523, 1998.

Y. Isojima, M. Nakajima, H. Ukai, H. Fujishima, R. G. Yamada, K.-h. Masumoto, R. Kiuchi, M. Ishida, M. Ukai-Tadenuma, Y. Minami, et al. Ckiε/δ-dependent phosphorylation is a temperature-insensitive, period-determining process in the mammalian circadian clock. *Proceedings of the National Academy of Sciences*, 106(37):15744–15749, 2009.

H. Ito, H. Kageyama, M. Mutsuda, M. Nakajima, T. Oyama, and T. Kondo. Autonomous synchronization of the circadian kaic phosphorylation rhythm. *Nature Structural and Molecular Biology*, 14(11):1084, 2007.

H. Iwasaki, T. Nishiwaki, Y. Kitayama, M. Nakajima, and K. T. KaiA-stimulated KaiC phosphorylation in circadian timing loops in cyanobacteria. *Proc. Natl. Acad. Sci*, 99: 15788–15793, 2002.

C. Jolley, K. Ode, and U. HR. A Design Principal for a Posttranslational Biochemical oscillator. *Cell Reports*, 2:938–950, 2012.

H. Kageyama, K. T., and H. Iwasaki. Circadian formation of clock protein complexes by KaiA, KaiB, KaiC, and SasA in cyanobacteria. *J. Biol. Chem*, 278:2388–2395, 2003.

H. Kageyama, T. Nishiwaki, M. Nakajima, T. Iwasaki, H.and Oyama, and T. Kondo. Cyanobacterial Circadian Pacemaker: Kai Protein Complex Dynamics in the KaiC Phosphorylation Cycle In Vitro. *Molecular Cell*, 23(2):161 – 171, 2006. ISSN 1097-2765.

J. K. Kim. Protein sequestration versus hill-type repression in circadian clock models. *IET Systems Biology*, 10(4):125–135, 2016.

J. K. Kim and D. B. Forger. A mechanism for robust circadian timekeeping via stoichiometric balance. *Mol. Syst. Biol.*, 8:630, 2012.

Y.-I. Kim, G. Dong, C. W. Carruthers, S. S. Golden, and A. LiWang. The day/night switch in kaic, a central oscillator component of the circadian clock of cyanobacteria. *Proceedings of the National Academy of Sciences*, 105(35):12825–12830, 2008.

Y. Kitayama, H. Iwasaki, T. Nishiwaki, and T. Kondo. KaiB functions as an attenuator of KaiC phosphorylation in the cyanobacterial circadian clock system. *EMBO J*, 22: 2127–2134, 2003.

B. Kloss, J. L. Price, L. Saez, J. Blau, A. Rothenfluh, C. S. Wesley, and M. W. Young. The drosophila clock gene double-time encodes a protein closely related to human casein kinase iε. *Cell*, 94(1):97–107, 1998.

R. J. Konopka and S. Benzer. Clock mutants of drosophila melanogaster. *Proceedings of the National Academy of Sciences*, 68(9):2112–2116, 1971.

P. Lakin-Thomas, S. Brody, and G. Cote. Amplitude model for the effects of mutations and temperature on period and phase resetting of the Neurospora circadian oscillator. *J. Biol. Rhythms*, 6(4):281–297, 1991.

C. Lee, J.-P. Etchegaray, F. R. Cagampang, A. S. Loudon, and S. M. Reppert. Posttranslational mechanisms regulate the mammalian circadian clock. *Cell*, 107(7):855–867, 2001.

H. Lee, R. Chen, Y. Lee, S. Yoo, and C. Lee. Essential roles of ckiδ and ckiε in the mammalian circadian clock. *Proceedings of the National Academy of Sciences*, 106 (50):21359–21364, 2009.

H.-m. Lee, R. Chen, H. Kim, J.-P. Etchegaray, D. R. Weaver, and C. Lee. The period of the circadian oscillator is primarily determined by the balance between casein kinase 1 and protein phosphatase 1. *Proceedings of the National Academy of Sciences*, page 201107178, 2011a.

Y. Lee, R. Chen, H.-m. Lee, and C. Lee. Stoichiometric relationship among clock proteins determines robustness of circadian rhythms. *Journal of Biological Chemistry*, pages jbc–M110, 2011b.

J.-A. S. Lie, J. Roessink, and K. Kjaerheim. Breast cancer and night work among norwegian nurses. *Cancer Causes & Control*, 17(1):39–44, 2006.

J. Lin, J. Chew, U. Chockanathan, and M. Rust. Mixtures of opposing phosphorylations within hexamers precisely time feedback in the cyanobacterial circadian clock. *Proc. Natl. Acad. Sci*, 111(37):E3937–E3945, 2014.

Y. Liu, J. Loros, and J. C. Dunlap. Phosphorylation of the neurospora clock protein frequency determines its degradation rate and strongly influences the period length of the circadian clock. *Proceedings of the National Academy of Sciences*, 97(1):234–239, 2000.

P. L. Lowrey, K. Shimomura, M. P. Antoch, S. Yamazaki, P. D. Zemenides, M. R. Ralph, M. Menaker, and J. S. Takahashi. Positional syntenic cloning and functional characterization of the mammalian circadian mutation tau. *Science*, 288(5465):483–491, 2000.

P. Más, W.-Y. Kim, D. E. Somers, and S. A. Kay. Targeted degradation of toc1 by ztl modulates circadian function in arabidopsis thaliana. *Nature*, 426(6966):567, 2003.

Q.-J. Meng, L. Logunova, E. S. Maywood, M. Gallego, J. Lebiecki, T. M. Brown, M. Sládek, A. S. Semikhodskii, N. R. Glossop, H. D. Piggins, et al. Setting clock speed in mammals: the ck1ϵ tau mutation in mice accelerates circadian pacemakers by selectively destabilizing period proteins. *Neuron*, 58(1):78–88, 2008.

P. Meyer, L. Saez, and M. W. Young. Per-tim interactions in living drosophila cells: an interval timer for the circadian clock. *Science*, 311(5758):226–229, 2006.

N. Naidoo, W. Song, M. Hunter-Ensor, and A. Sehgal. A role for the proteasome in the light response of the timeless clock protein. *Science*, 285(5434):1737–1741, 1999.

M. Nakajima, K. Imai, H. Ito, T. Nishiwaki, Y. Murayama, H. Iwasaki, T. Oyama, and T. Kondo. Reconstitution of circadian oscillation of cyanobacterial KaiC phosphorylation in vitro. *Science*, 308:414–415, 2005.

R. Narasimamurthy, S. R. Hunt, Y. Lu, J.-M. Fustin, H. Okamura, C. L. Partch, D. B. Forger, J. K. Kim, and D. M. Virshup. Ck1δ/ε protein kinase primes the per2 circadian

phosphoswitch. *Proceedings of the National Academy of Sciences*, page 201721076, 2018.

T. Nishiwaki and T. Kondo. Circadian Autodephosphorylation of Cyanobacterial Clock Protein KaiC Occurs via Formation of ATP as Intermediate. *J. Biol. Chem*, ;287(22): 18030–18035, 2012.

T. Nishiwaki, H. Iwasaki, M. Ishiura, and T. Kondo. Nucleotide binding and autophosphorylation of the clock protein kaic as a circadian timing process of cyanobacteria. *Proceedings of the National Academy of Sciences*, 97(1):495–499, 2000.

T. Nishiwaki, Y. Satomi, M. Nakajima, C. Lee, R. Kiyohara, H. Kageyama, and T. Kondo. Role of KaiC phosphorylation in the circadian clock system of Synechococcus elongatus PCC 7942. *Proc. Natl. Acad. Sci*, 101(38):13927–13932, 2004.

T. Nishiwaki, Y. Satomi, Y. Kitayama, K. Terauchi, R. Kiyohara, T. Takao, and T. Kondo. A sequential program of dual phosphorylation of kaic as a basis for circadian rhythm in cyanobacteria. *The EMBO Journal*, 26(17):4029–4037, 2007.

T. Nishiwaki-Ohkawa, Y. Kitayama, E. Ochiai, and T. Kondo. Exchange of adp with atp in the cii atpase domain promotes autophosphorylation of cyanobacterial clock protein kaic. *Proceedings of the National Academy of Sciences*, page 201319353, 2014.

B. Novák and J. J. Tyson. Design principles of biochemical oscillators. *Nature reviews Molecular cell biology*, 9(12):981, 2008.

Y. Ouyang, C. R. Andersson, T. Kondo, S. S. Golden, and C. H. Johnson. Resonating circadian clocks enhance fitness in cyanobacteria. *Proceedings of the National Academy of Sciences*, 95(15):8660–8664, 1998.

G. Pattanayak, G. Lambert, K. Bernat, and M. Rust. Controlling the Cyanobacterial Clock by Synthetically Rewiring Metabolism. *Cell reports*, 13(11):2362–2367, 2015.

C. Phong, J. S. Markson, C. M. Wilhoite, and M. J. Rust. Robust and tunable circadian rhythms from differentially sensitive catalytic domains. *Proceedings of the National Academy of Sciences*, 110(3):1124–1129, 2013.

J. Price, M. Dembinska, M. Young, and M. Rosbash. Suppression of period protein abundance and circadian cycling by the drosophila clock mutation timeless. *The EMBO journal*, 14(16):4044–4049, 1995.

J. L. Price, J. Blau, A. Rothenfluh, M. Abodeely, B. Kloss, and M. W. Young. double-time is a novel drosophila clock gene that regulates period protein accumulation. *Cell*, 94 (1):83–95, 1998.

C. Querfurth, A. C. Diernfellner, E. Gin, E. Malzahn, T. Höfer, and M. Brunner. Circadian conformational change of the neurospora clock protein frequency triggered by clustered hyperphosphorylation of a basic domain. *Molecular cell*, 43(5):713–722, 2011.

P. Ruoff. Temperature-compensation in biological clocks: Models and experiments. In *Function and Regulation of Cellular Systems*, pages 19–29. Springer, 2004.

M. Rust, S. Golden, and E. O'Shea. Light-Driven Changes in Energy Metabolism Directly Entrain the Cyanobacterial Circadian Oscillator. *Science*, 331(6014):220–223, 2011. ISSN 0036-8075.

M. J. Rust, J. S. Markson, W. S. Lane, D. S. Fisher, and E. K. O'Shea. Ordered Phosphorylation Governs Oscillation of a Three-Protein Circadian Clock. *Science*, 318(5851): 809–812, 2007. ISSN 0036-8075.

L. Saez and M. W. Young. Regulation of nuclear entry of the drosophila clock proteins period and timeless. *Neuron*, 17(5):911–920, 1996.

S. Sahar and P. Sassone-Corsi. Metabolism and cancer: the circadian clock connection. *Nature Reviews Cancer*, 9(12):886, 2009.

A. Sancar. The intelligent clock and the rube goldberg clock. *Nature Structural and Molecular Biology*, 15(1):23, 2008.

U. Schibler and P. Sassone-Corsi. A web of circadian pacemakers. *Cell*, 111(7):919–922, 2002.

N. P. Shanware, J. A. Hutchinson, S. H. Kim, L. Zhan, M. J. Bowler, and R. S. Tibbetts. Casein kinase 1-dependent phosphorylation of familial advanced sleep phase syndrome-associated residues controls period 2 stability. *Journal of Biological Chemistry*, 286 (14):12766–12774, 2011.

Y. Shinohara, Y. M. Koyama, M. Ukai-Tadenuma, T. Hirokawa, M. Kikuchi, R. G. Yamada, H. Ukai, H. Fujishima, T. Umehara, K. Tainaka, et al. Temperature-sensitive substrate and product binding underlie temperature-compensated phosphorylation in the clock. *Molecular cell*, 67(5):783–798, 2017a.

Y. Shinohara, Y. M. Koyama, M. Ukai-Tadenuma, T. Hirokawa, M. Kikuchi, R. G. Yamada, H. Ukai, H. Fujishima, T. Umehara, K. Tainaka, et al. Temperature-sensitive substrate and product binding underlie temperature-compensated phosphorylation in the clock. *Molecular cell*, 67(5):783–798, 2017b.

N. J. Smyllie, J. E. Chesham, R. Hamnett, E. S. Maywood, and M. H. Hastings. Temporally chimeric mice reveal flexibility of circadian period-setting in the suprachiasmatic nucleus. *Proceedings of the National Academy of Sciences*, page 201511351, 2016.

S. Sugano, C. Andronis, R. M. Green, Z.-Y. Wang, and E. M. Tobin. Protein kinase ck2 interacts with and phosphorylates the arabidopsis circadian clock-associated 1 protein. *Proceedings of the National Academy of Sciences*, 95(18):11020–11025, 1998.

S. Sugano, C. Andronis, M. S. Ong, R. M. Green, and E. M. Tobin. The protein kinase ck2 is involved in regulation of circadian rhythms in arabidopsis. *Proceedings of the National Academy of Sciences*, 96(22):12362–12366, 1999.

J. A. Swan, S. Golden, A. LiWang, and C. L. Partch. Structure, function, and mechanism of the core circadian clock in cyanobacteria. *Journal of Biological Chemistry*, pages jbc–TM117, 2018.

N. Takai, M. Nakajima, T. Oyama, R. Kito, C. Sugita, M. Sugita, T. Kondo, and H. Iwasaki. A kaic-associating sasa–rpaa two-component regulatory system as a major circadian timing mediator in cyanobacteria. *Proceedings of the National Academy of Sciences*, 103(32):12109–12114, 2006.

S.-W. Teng, S. Mukherji, J. R. Moffitt, S. De Buyl, and E. K. Oshea. Robust circadian oscillations in growing cyanobacteria require transcriptional feedback. *Science*, 340 (6133):737–740, 2013.

K. L. Toh, C. R. Jones, Y. He, E. J. Eide, W. A. Hinz, D. M. Virshup, L. J. Ptáček, and Y.-H. Fu. An hper2 phosphorylation site mutation in familial advanced sleep phase syndrome. *Science*, 291(5506):1040–1043, 2001.

J. Tomita, M. Nakajima, T. Kondo, and H. Iwasaki. No transcription-translation feedback in circadian rhythm of KaiC phosphorylation. *Science*, 307:251–254, 2005.

R. Tseng, N. F. Goularte, A. Chavan, J. Luu, S. E. Cohen, Y.-G. Chang, J. Heisler, S. Li, A. K. Michael, S. Tripathi, et al. Structural basis of the day-night transition in a bacterial circadian clock. *Science*, 355(6330):1174–1180, 2017.

J. Van Zon, D. Lubensky, P. Altena, and P. ten Wolde. An allosteric model of circadian KaiC phosphorylation. *Proc. Natl. Acad. Sci*, 104(18):7420–7425, 2007.

L. Wang, S. Fujiwara, and D. E. Somers. Prr5 regulates phosphorylation, nuclear import and subnuclear localization of toc1 in the arabidopsis circadian clock. *The EMBO journal*, 29(11):1903–1915, 2010.

Z.-Y. Wang and E. M. Tobin. Constitutive expression of the circadian clock associated 1 (cca1) gene disrupts circadian rhythms and suppresses its own expression. *Cell*, 93(7): 1207–1217, 1998.

Y. Xu, T. Mori, and C. Johnson. Circadian clock-protein expression in cyanobacteria: rhythms and phase setting. *The EMBO Journal*, 19(13):3349–3357, 2000.

Y. Xu, T. Mori, and C. Johnson. Cyanobacterial circadian clockwork: roles of KaiA, KaiB and the kaiBC promoter in regulating KaiC. *The EMBO Journal*, 22(9):2117–2126, 2003.

Y. Xu, T. Mori, R. Pattanayek, S. Pattanayek, M. Egli, and C. H. Johnson. Identification of key phosphorylation sites in the circadian clock protein kaic by crystallographic and mutagenetic analyses. *Proceedings of the National Academy of Sciences*, 101(38): 13933–13938, 2004.

Y. Xu, K. Toh, C. Jones, J.-Y. Shin, Y.-H. Fu, and L. Ptáček. Modeling of a human circadian mutation yields insights into clock regulation by per2. *Cell*, 128(1):59–70, 2007.

M. Zhou, J. Kim, G. Eng, D. Forger, and D. Virshup. A Period2 Phosphoswitch Regulates and Temperature Compensates Circadian Period. *Molecular Cell*, 60(1):77 – 88, 2015. ISSN 1097-2765.

D. Zwicker, D. K. Lubensky, and P. R. ten Wolde. Robust circadian clocks from coupled protein-modification and transcription-translation cycles. *Proc. Natl. Acad. Sci*, 107(52):22540–22545, 2010.